NAVAL POSTGRADUATE SCHOOL
Monterey, California

THESIS

ADAPTIVE CONTROL IN POSITIONING
A RIGID-FLEXIBLE ROBOT ARM

by

Constantinos Mardas

March 1988

Thesis Advisor: George J. Thaler

Approved for public release; distribution is unlimited

REPORT DOCUMENTATION PAGE

. REPORT SECURITY CLASSIFICATION UNCLASSIFIED	1b RESTRICTIVE MARKINGS
. SECURITY CLASSIFICATION AUTHORITY	3 DISTRIBUTION / AVAILABILITY OF REPORT
. DECLASSIFICATION / DOWNGRADING SCHEDULE	
PERFORMING ORGANIZATION REPORT NUMBER(S)	5 MONITORING ORGANIZATION REPORT NUMBER(S)
. NAME OF PERFORMING ORGANIZATION val Postgraduate School 6b OFFICE SYMBOL (If applicable) 62	7a NAME OF MONITORING ORGANIZATION Naval Postgraduate School
. ADDRESS (City, State, and ZIP Code) lonterey, California	7b. ADDRESS (City, State, and ZIP Code) Monterey, California
. NAME OF FUNDING / SPONSORING ORGANIZATION 8b. OFFICE SYMBOL (If applicable)	9 PROCUREMENT INSTRUMENT IDENTIFICATION NUMBER
ADDRESS (City, State, and ZIP Code)	10 SOURCE OF FUNDING NUMBERS PROGRAM ELEMENT NO. / PROJECT NO / TASK NO / WORK UNIT ACCESSION NO

. TITLE (Include Security Classification)
DAPTIVE CONTROL IN POSITIONING A RIGID-FLEXIBLE ROBOT ARM

. PERSONAL AUTHOR(S)

a. TYPE OF REPORT	13b TIME COVERED	14 DATE OF REPORT (Year, Month, Day)	15 PAGE COUNT
laster's Thesis	FROM _____ TO _____	1988 March	168

. SUPPLEMENTARY NOTATION The views expressed in this thesis are those of the author nd do not reflect the official policy or position of the Department of efense or the U.S. Government.

COSATI CODES			18 SUBJECT TERMS (Continue on reverse if necessary and identify by block number)
FIELD	GROUP	SUB-GROUP	Velocity curve following, adaptive control scheme, flexible displacement, assumed modes, hypothetical rigid motion

. ABSTRACT (Continue on reverse if necessary and identify by block number)

he feasibility of controlling a rigid-flexible, two links planar robot arm ith an adaptive computer simulation model is investigated. The velocity urve following method was used as the adaptive control scheme. The motors cting at each joint were driven by the adaptive model. The adaptive algo- ithm update the states and the gain parameter of the ideal motor used in the omputer model. This adaptation procedure was accomplished using only the easured angular position of the arm. The mathematical model for the pro- osed manipulator was derived using the Lagrangian dynamics approach. imulation results were obtained with the manipulator performing under arious conditions, by changing the load of the arm and the forces included n the environment.

. DISTRIBUTION / AVAILABILITY OF ABSTRACT ☒ UNCLASSIFIED/UNLIMITED ☐ SAME AS RPT ☐ DTIC USERS	21 ABSTRACT SECURITY CLASSIFICATION UNCLASSIFIED
a. NAME OF RESPONSIBLE INDIVIDUAL George J. Thaler	22b TELEPHONE (Include Area Code) 408-646-2134 / 22c OFFICE SYMBOL 62Tr

D FORM 1473, 84 MAR 83 APR edition may be used until exhausted
All other editions are obsolete

SECURITY CLASSIFICATION OF THIS PAGE
☆ U.S. Government Printing Office: 1986—606-243
UNCLASSIFIED

Approved for public release; distribution is unlimited.

Adaptive Control in Positioning a Rigid-Flexible Robot Arm

by

Constantinos Mardas
Lieutenant, Hellenic Navy
B.S., Hellenic Navy Academy, 1979

Submitted in partial fulfillment of the
requirements for the degrees of

MASTER OF SCIENCE IN ELECTRICAL ENGINEERING
and
ELECTRICAL ENGINEER

from the

ABSTRACT

The feasibility of controlling a rigid-flexible, two links planar robot arm with an adaptive computer simulation model is investigated. The velocity curve following method was used as the adaptive control scheme. The motors acting at each joint were driven by the adaptive model. The adaptive algorithm update the states and the gain parameter of the ideal motor used in the computer model. This adaptation procedure was accomplished using only the measured angular position of the arm. The mathematical model for the proposed manipulator was derived using the Lagrangian dynamics approach. Simulation results were obtained with the manipulator performing under various conditions, by changing the load of the arm and the forces included in the environment.

TABLE OF CONTENTS

LIST OF FIGURES

LIST OF TABLES

ACKNOWLEDGMENT

I would like to express my deepest gratitude to my Thesis Advisor, Distinguished Professor, George J. Thaler for his guidance and support in the course of this Thesis. Also I want to thank my wife Gina, whose help was very important during my studies at the Naval Postgraduate School.

I. INTRODUCTION

A. GENERAL CONCEPT

The need to improve industrial productivity has greatly motivated the implementation of a variety of forms of automation. With respect to this fact, programmable multi-functional manipulators (robots), have become increasingly important. Due to the fact that the robots will play a major role in future manufacturing systems, the need for improvement of robot's performance becomes imperative.

One of the major drawbacks of today's robots is that in general they are very slow. The speed, with which they can transfer objects from one point to another, is at many cases limited by the weight of the manipulator arm. The excessive arm weight not only hampers the rapid motion of the manipulators arm, but also increases the robot's consumption of energy and the size of the required actuators.

A flexible manipulator is free of these drawbacks, because it requires less material that results in less arm weight, less power consumption and increased maneuverability compared with the traditional (rigid-arm) manipulators. The flexible manipulator also uses smaller actuators because of the smaller power demand.

Therefore flexible arm manipulators are particularly advantageous in small lot manufacturing and also very attractive for space applications.

Manipulator arms require a reasonable accuracy in the response of the arm's end-point to the joint control system input commands. In order to achieve this accuracy most of the manipulator's arms exhibit some vibrations. These vibrations have been eliminated by increasing the rigidity of the manipulator's arm.

In the case of the flexible manipulators the above solution is unsatisfactory if their basic advantages stated above are not to be sacrificed.

It is clear that in order to realize the very attractive features of the flexible manipulator arm, extensive research has to be performed in both the areas of design and control of the system. Obviously a control system has as tasks to perform the required motion for the flexible arm of the manipulator with a reasonable accuracy in the arm's end-point position, but also to control the vibration modes of its links.

B. THESIS OBJECTIVE

The manipulator that will be used through this thesis will be a two links planar robot arm having the first link rigid and the second link flexible.

Controlling the proposed manipulator to obtain position accuracy of the end-point, fast response and control of the vibration modes of the flexible link is a very complicated problem because the dynamic motion of the manipulator is

strongly influenced by mechanical design and physical properties of the manipulator, as well as environmental effects. Coupling inertia, coriolis forces, actuator dynamics, joint friction, centripetal forces, gravity effects and mainly the vibration modes introduced due to the elastic motion of the flexible link and the coupling of the two links create an overall system that is a very nonlinear dynamic system. Because of the nonlinear dynamic model of the manipulator a robust and flexible control system is required.

The velocity curve follow technique is a powerful control scheme that was successfully used to control a single flexible arm [Ref. 1] and also for a near minimum time positioning of a planar robot arm with two rigid links [Ref. 2]. A feasibility study will be done in the application of the same technique, the velocity curve follow control scheme, for the proposed manipulator model. In order to compare the results of the proposed rigid-flexible planar robot arm, for fast and accurate response, with the results of a planar robot arm with two rigid links, the model of a rigid-rigid planar robot arm having similar parametric data and using the same adaptive control scheme will be developed and tested.

The advantages of this technique are the adaptive nature and the simplicity of the control scheme loop, that can also be implemented in a digital computer or micro-

processor with the output signals through a D/A converter used to drive the motors acting on the manipulators joints. Problems arising from modelling uncertainties, unpredictable environmental changes and noise contamination of the signals can be taken into account and solved through the adaptation procedure.

C. BASIC CONCEPTS OF THE ADAPTIVE MODEL

A very simplified block diagram of the adaptive control scheme that will be used is illustrated in Figure 1.1. In order to control the motion of the manipulator's links the adaptive control scheme receives from the actuator the position of each link. Knowing the position and previous values of the position, the digital computer calculates the velocity and updates the gain constant, the position and the velocity of the second order model, used to model the real motor in the computer, at certain time intervals. Another advantage of this control scheme, concluded from the basic implementation described above, is the elimination of a tachometer requirement.

The block named 'Curve follower', approximates the deceleration curve of an ideal motor. This curve can be obtained as an analytic expression or as a table look-up stored in the memory of the digital computer.

The 'Model-environment' block represents the dynamic equations that describe the given system. In this block are

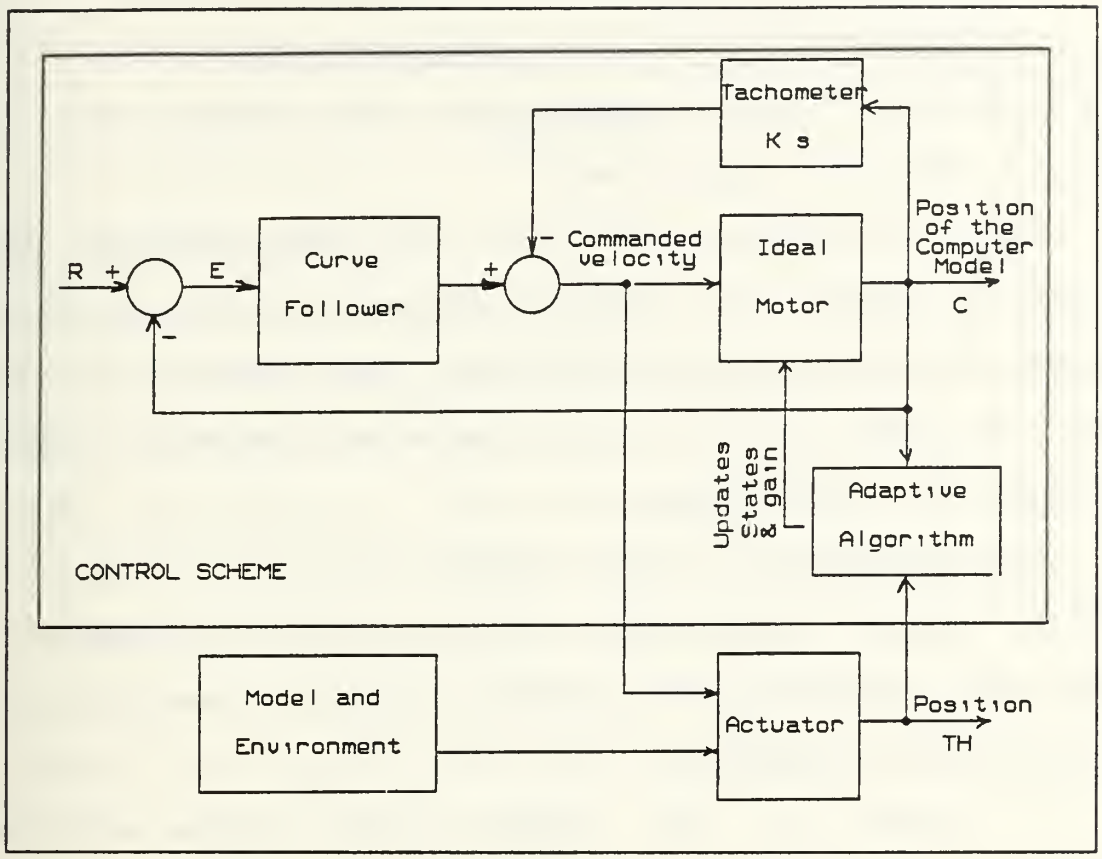

Figure 1.1 Simplified block diagram of the system.

also included gravitational torques, centripetal forces, coriolis forces, inertia of the loaded arm, forces acting on the rigid and the flexible links due to the elastic motion of the flexible beam.

The motors acting at the two joints are identical, using the same adaptive velocity curve follow control scheme. At the adaptive model both actuator and ideal motor are driven by the same velocity error input.

D. ORGANIZATION OF THE THESIS

In Chapters II and III the mathematical models for the rigid-rigid and rigid-flexible two links planar robot arm will be developed respectively.

Some preliminary studies of the models will be performed in Chapter IV, including frequency response of the systems which will help to extract, some important for the adaptive model, data from the prominent physical characteristics of the systems.

The development of the computer simulation model, that will be used in both cases, will be derived in Chapter V, where the velocity curve follow control scheme will be developed and simulated.

In Chapter VI, the velocity curve follow will be applied as the control scheme of the rigid-flexible planar robot arm, described by the model derived in Chapter III, in order to investigate if this control scheme is applicable. Simulations under different conditions (load, gravity environment) will be performed. Simulation results will be obtained under the same conditions for the rigid-rigid planar robot arm, described by the model derived in Chapter II, and the results will be compared.

In Chapter VII, the conclusions and the requirements for further studies will be given.

II. MODEL DEVELOPMENT FOR THE TWO RIGID LINKS ROBOT ARM

A. INTRODUCTION

In this chapter, a mathematical model of a planar robot arm with two rigid links will be derived by the use of Lagrangian mechanics. The planar robot arm having two rigid links was partially investigated in Ref.2. In order to compare the resulted equations of motion and the performance of the planar robot arm at two different cases, one when both links are rigid and the other when the second link is flexible, the study of the two rigid links planar robot arm will be repeated in this thesis.

Lagrange's equations will relate the torques and forces acting on the system to the position, velocity and acceleration of each link at any time. Therefore, the second order differential equations that will be derived following this Lagrangian dynamics approach will be the equations of motion, that describe the system.

B. DEVELOPMENT OF THE MODEL

The two rigid links planar robot arm is illustrated in Figure 2.1. Both joints are rotary joints and the motion will be considered to be on one plane, the xy plane. The two links having lengths l_1 and l_2, are assumed to be

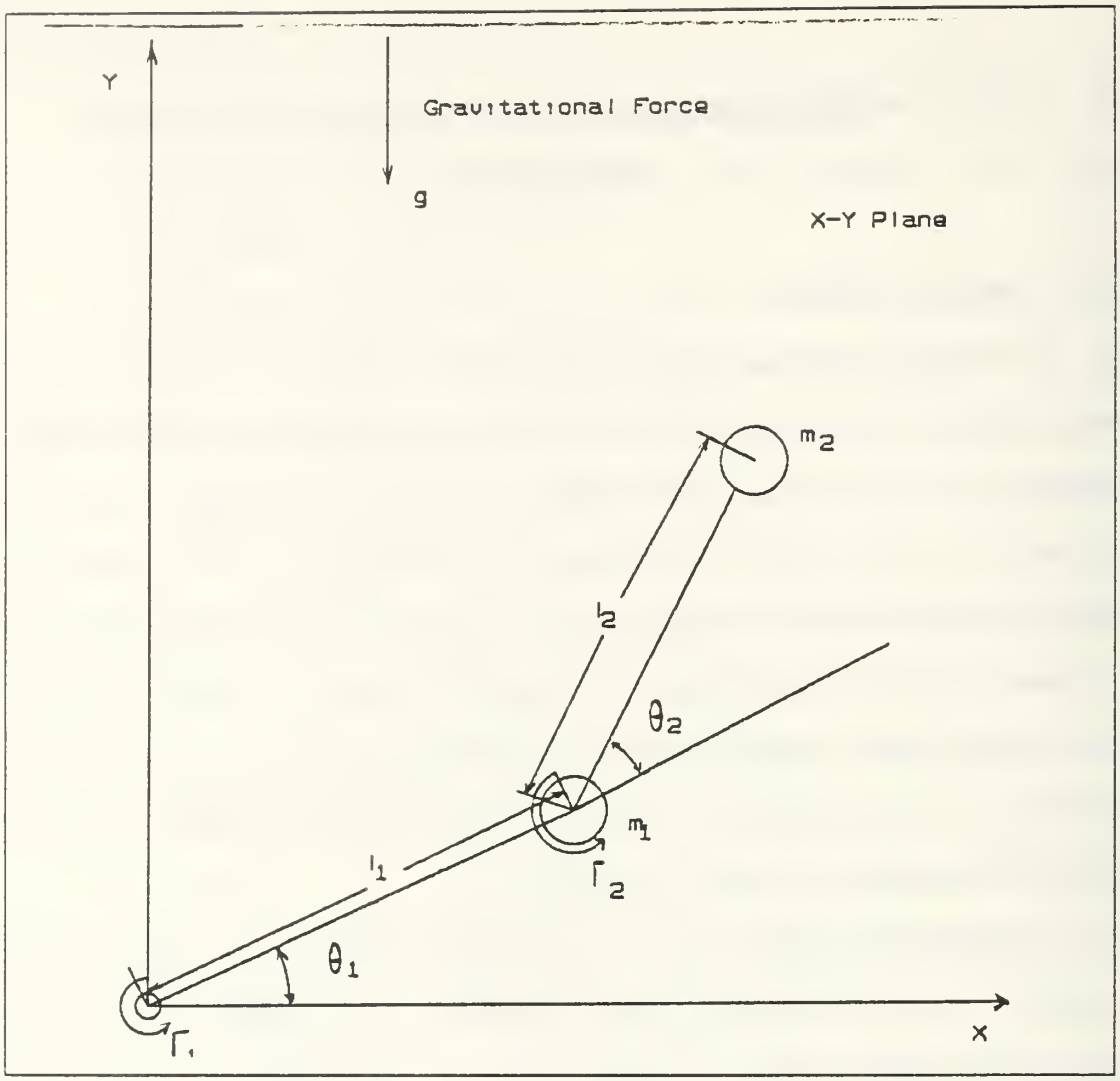

Figure 2.1 Planar robot arm with two rigid links.

massless and two equivalent masses m_1 and m_2 are lumped at the end of LINK1 and LINK2 respectively. The driving torques for the motors at each joint will be denoted as Γ_1 and Γ_2 at JOINT1 and JOINT2 respectively.

C. DERIVATION OF THE LAGRANGE'S EQUATIONS

Defining the Lagrangian function L, as L=T-V, where T and V are the kinetic and potential energies of the system,

the equations of motion that describe the system will be derived from the Lagrange's equations defined as:

$$\frac{d}{dt}\left(\frac{\delta L}{\delta \dot{q}_i}\right) - \frac{\delta L}{\delta q_i} = Q_i \qquad i = 1,2,\ldots,n \tag{2.1}$$

where:

q_i = the generalized coordinates,

Q_i = the generalized forces,

n = the number of degrees of freedom.

For that system configuration only two coordinates will be used, because the number of degrees of freedom must be equal to the number of coordinates which must be used to describe that system. Selecting the angles Θ_1 and Θ_2 to be the generalized coordinates for the system shown at Figure 2.1, the position of both arms at any instant of time, with constant lengths l_1 and l_2, will be exactly specified from these two angles. The torques $\Gamma 1$ and Γ_2 will be the generalized forces acting on that system. Derivation of the kinetic and potential energies and construction of the differential equations from the Lagrangian function L is a very lengthy approach and the detailed presentation is given in Appendix A. The pair of the second order nonlinear differential equations derived in Appendix A, will become the equations of motion that describe the system and will be used as the mathematical model at the studies of the two rigid links planar robot arm.

$$\Gamma_1 = (D_{11}+ J_1)\ddot{\theta}_1 + D_{12}\ddot{\theta}_2 + D_{122}\dot{\theta}_2^2 + D_{112}\dot{\theta}_1\dot{\theta}_2 + D_{121}\dot{\theta}_2\dot{\theta}_1 + D_1 \quad (2.2)$$

$$\Gamma_2 = (D_{22}+ J_2)\ddot{\theta}_2 + D_{21}\ddot{\theta}_1 + D_{211}\dot{\theta}_1^2 + D_2 \quad (2.3)$$

where

$D_{11} = (m_1+m_2)l_1^2 + m_2l_2^2 + 2m_2l_1l_2\cos\theta_2$

$D_{22} = m_2l_2^2$

$D_{12} = D_{21} = m_2l_2^2 + m_2l_1l_2\cos\theta_2$

$D_{112} = D_{122} = D_{121} = -D_{211} = -m_2l_1l_2\sin\theta_2$

$D_1 = (m_1+m_2)gl_1\sin\theta_1 + m_2gl_2\sin(\theta_1+\theta_2)$

$D_2 = m_2gl_2\sin(\theta_1+\theta_2)$

J_1 = the inertia of the motor at JOINT1

J_2 = the inertia of the motor at JOINT2

g = the acceleration of gravity (= 9.814 m/sec^2)

The parametric values, lengths of the links and masses at the end of each link, that will be used in this study of the two rigid links planar robot arm are given in the Table 2.1.

The D_{ii} (i=1,2) values defined in the above equations were obtained from the forces acting on each link due to acceleration and velocity of the moving robot arm. A more detailed specification for each value will be given as follows.

TABLE 2.1 PARAMETRIC DATA OF A TWO RIGID LINKS PLANAR ROBOT ARM.

$l_1 = 0.40$ m
$l_2 = 0.32$ m
$m_1 = 0.30$ kg/m/sec^2
$m_2 = 0.05$ kg/m/sec^2
$m_2 = 0.10$ kg/m/sec^2 (with load)

An acceleration of the joint i causes a torque at the same joint equal to $D_{ii}\theta_i$, therefore at this particular system D_{11} and D_{22} represent the effective inertias for the joints 1 and 2 respectively. Also an acceleration at one joint i will cause a torque at joint j of the form $D_{ij}\theta_{ij}$, and for the particular system D_{12} and D_{21} are the coupling inertias. Also a velocity at joint i will produce a centripetal force at joint j having the form $D_{jii}\theta_i$, and therefore D_{122}, D_{211} are the centripetal forces for that system (notice $D_{111}=D_{222}=0$). A combination of the form $D_{ijk}\theta_j\theta_k + D_{ikj}\theta_k\theta_j$ are the produced coriolis force acting at joint i due to the velocities at joints k and j, therefore for the two link model the coriolis forces will be represented by the coriolis acceleration coefficients D_{112}, D_{121}, D_{212} and D_{221}.

III. MODEL DEVELOPMENT FOR A PLANAR ROBOT ARM WITH TWO LINKS, THE SECOND FLEXIBLE

A. INTRODUCTION

The basic mathematical model that will be used in the computer simulations for the planar robot arm with two links, the first rigid and the second flexible, has to be derived. In order to examine its performance and to compare the simulation results with the results obtained for the planar robot arm having two rigid links, the two models have to be compatible. Therefore the mathematical model of a rigid-flexible planar robot arm, will be derived in this chapter.

B. PRIOR WORK IN THIS FIELD

From previous works and studies in the field of robotic manipulators with structural flexibility many different approaches can be used on the derivation of the different models. Book [Ref.3] applies the transfer matrix method to describe in the frequency domain the elastic bending motion of a two-link planar elastic arm and for small angular velocities. In later work Book [Ref.4] considered the linear dynamics of spatial flexible arms represented as lumped mass and spring components via 4x4 transformation matrices. Maiza-Neto [Refs.5 and 6] develops the nonlinear equations of motion in the time domain for the same problem

using Lagrangian dynamics. Usoro [Ref.7] uses the finite element/Lagrange methods coupled with the concept of a generalized inertia matrix, derived for lightweight flexible manipulators, to achieve positional and vibration control, with the mathematical background for this study presented by Mahil [Ref.8]. Schmitz [Ref.9] applies Hamilton's principle and uses boundary conditions to linearize the model of a very flexible one-link manipulator in order to describe its performance with transfer functions for the end-point position control. The latest procedure was followed by Zouzias [Ref.1] in his attempt of controlling a flexible manipulator arm with an adaptive computer simulation model.

C. DEVELOPMENT OF THE MODEL

For the sake of the comparison of the two cases, as was mentioned before, Lagrangian dynamics was decided to be used for the model development of the two links planar robot arm having the first link rigid and the second link flexible. The model of the planar robot arm, that will be used through this thesis, is illustrated in Figure 3.1. Both joints are rotary joints and the system will again assumed to have only planar motion, on the x,y plane, with relative motion of the two links due to the torques applied from the motors at each joint. The torques applied at JOINT1 and JOINT2 will again be denoted as Γ_1 and Γ_2. Both links, rigid and flexible, having lengths l_1 and l_2 respectively are assumed to be

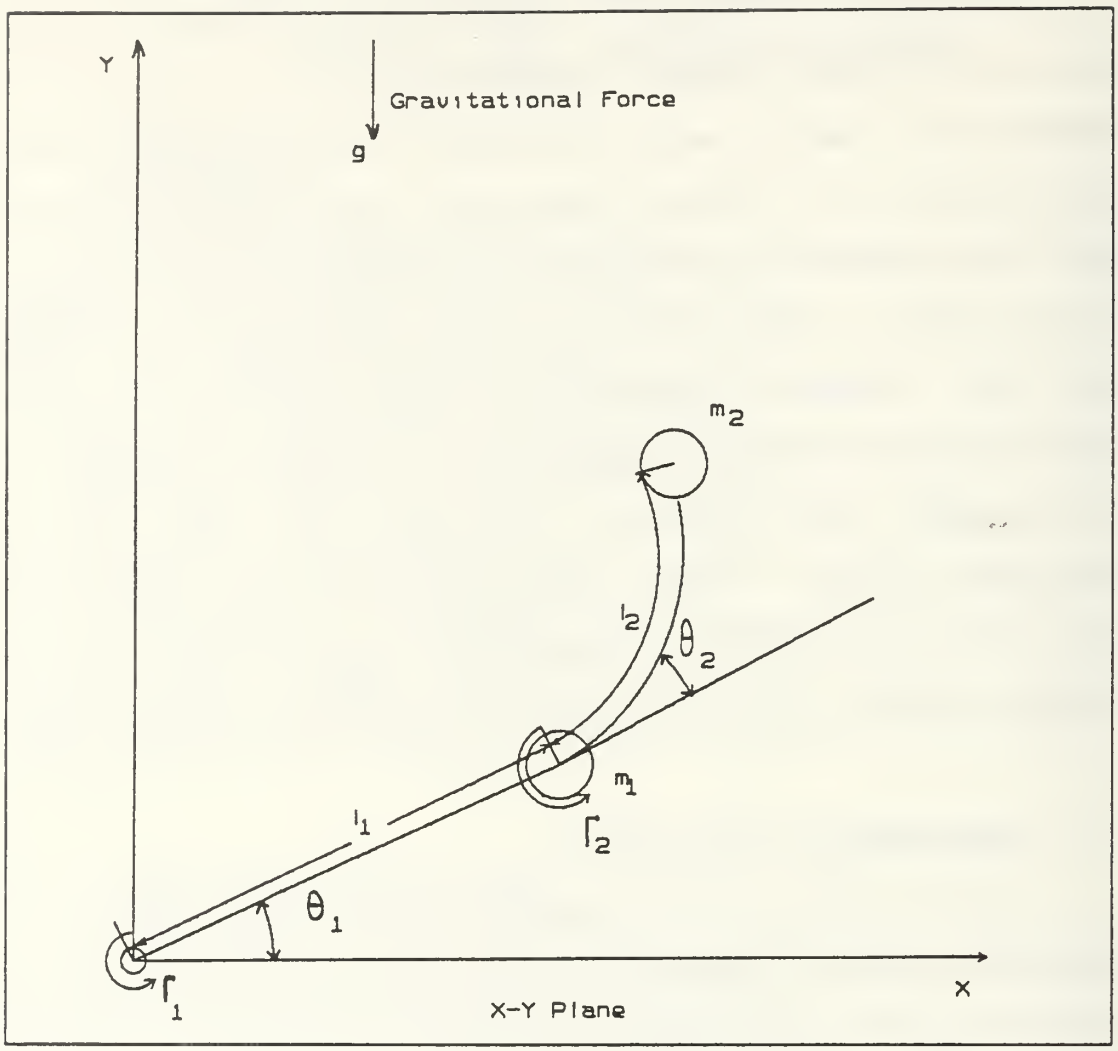

Figure 3.1 Two links (rigid-flexible) planar robot arm.

massless and two equivalent masses m_1 and m_2 are lumped at the end of each link. The discrete masses at the end of the rigid and the flexible links represent the servo motor of the flexible beam and the end-point sensor and payload.

D. DERIVATION OF THE LAGRANGE'S EQUATIONS

The model will be developed by superposing the flexible motion of the second link over the two rigid links body

motion. This approach is in favor of the finite element Lagrange method because will there result a set of second order differential equations similar to those obtained for the two rigid links planar robot arm, with additional terms due to the flexibility of the second link and the coupling effects between the rigid and the flexible link.

The coordinates for the rigid beam, first link, will be defined as in the "two rigid links arm model". For the second link, that is now a flexible beam, the coordinates will be defined as if the beam was rigid superposing in this result the flexible motion. In order to describe this flexible motion the general schematic of the model will be repeated in Figure 3.2 introducing three reference frames. These references frames can be defined as follows:

[O,X,Y] : an inertial reference frame with origin at JOINT1.

$[O,X_1,Y_1]$: a reference frame with origin at O and the X_1 axis lying on LINK1.

$[O_1,X_2,Y_2]$: a reference frame with origin at O_1 and with the X_2 axis tangent to the flexible beam at the point O_1.

The two angles can therefore be defined as follows:

Θ_1 = the angle between the axis X and X_1.

Θ_2 = the angle between the axis X_1 and X_2.

The overall motion can be understood as a motion of the hypothetical rigid system OO_1O_2 and a flexible motion of the second beam, LINK2, with respect to this moving system. The position of any point of LINK2 can be described by a

convenient definition of a set of coordinates. As indicated in Figure 3.2 any point P along the flexible beam can be specified if a new variable $u(x_2,t)$ will be defined as being the coordinate of the flexible motion with respect to the reference frame $[O_1,X_2,Y_2]$. The position (coordinates) for any point P of the flexible beam will then be given in vector notation as:

$$\vec{R}_d = [l_1\cos\theta_1 + x_2\cos(\theta_1+\theta_2) - u\sin(\theta_1+\theta_2)]\vec{\alpha}_x + [l_1\sin\theta_1 + x_2\sin(\theta_1+\theta_2) + u\cos(\theta_1+\theta_2)]\vec{\alpha}_y \quad (3.1)$$

Therefore the Cartesian coordinates of the end-point of the flexible arm can be expressed from the following equations:

$$x_2 = l_1\cos\theta_1 + l_2\cos(\theta_1+\theta_2) - u_E\sin(\theta_1+\theta_2) \quad (3.2)$$

$$y_2 = l_1\sin\theta_1 + l_2\sin(\theta_1+\theta_2) + u_E\cos(\theta_1+\theta_2) \quad (3.3)$$

where u_E is the flexible linear displacement at the end-point of the flexible beam (LINK2).

Having defined the coordinates transformation for the flexible beam, as given in the above Equations 3.2 and 3.3, Lagrange's equations can normally be derived. In order to develop a mathematical model for the proposed system the flexible displacement $u(x_2,t)$ must be given by a closed form expression.

In general for any arbitrary point of the flexible beam the corresponding flexible displacement $u(x_2,t)$ that will be superposed to the hypothetical motion of the two rigid links

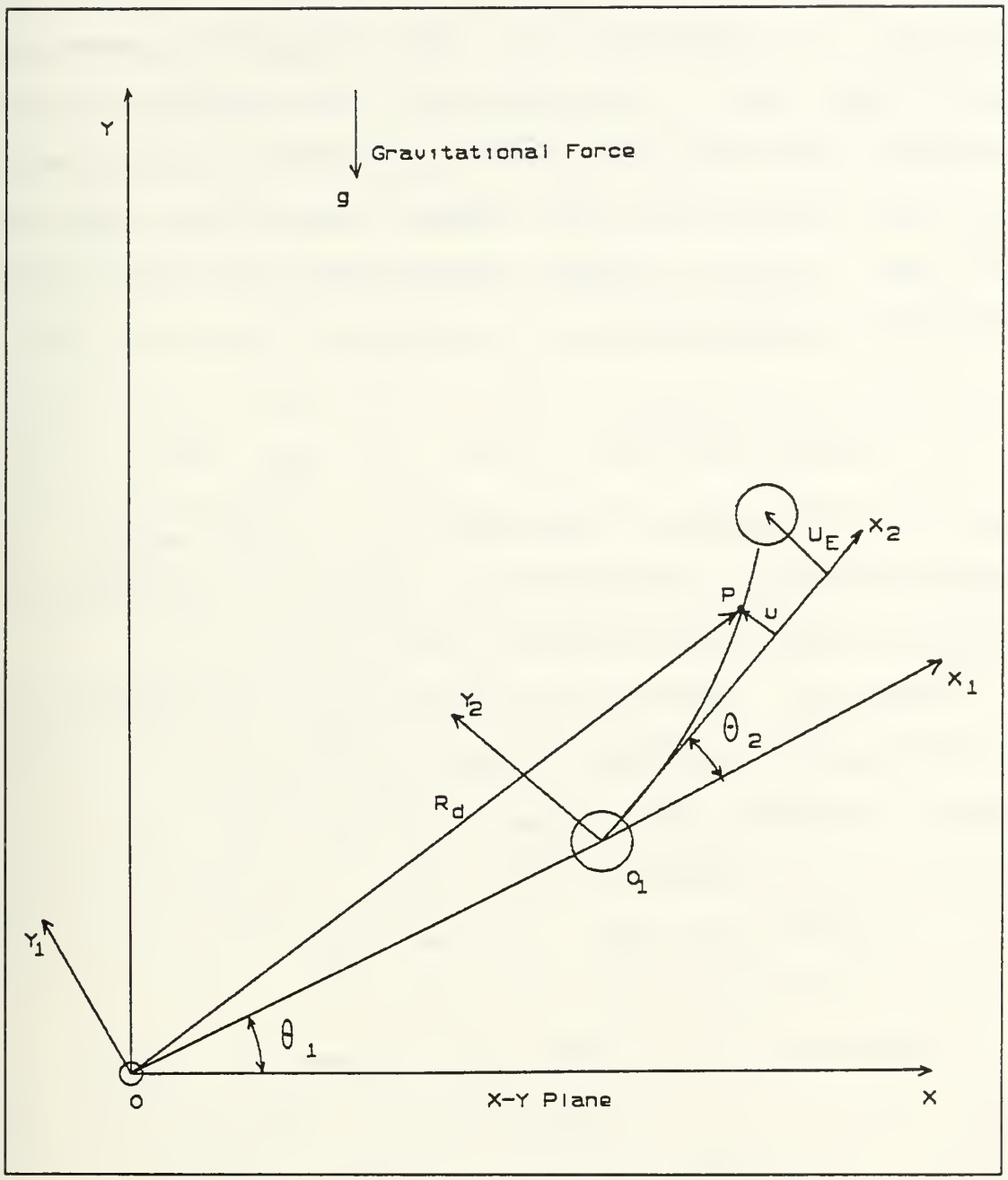

Figure 3.2 Vector position for an arbitrary point P at the flexible beam of the planar robot arm.

system can be expressed using the so called assumed-modes method. The assumed-modes method was described in detail in Ref. 10. In the case of a free vibration problem the basic idea is the assumption of a solution, in the form of a

series composed of a linear combination of admissible functions f_i multiplied by time dependent generalized coordinates $g_i(t)$. By admissible function is meant any arbitrary function of the spatial coordinates satisfying all the geometric or essential boundary conditions. Then for the case of the flexible displacement of LINK2 it is possible to assume that:

$$u = \sum_{i=1}^{n} f_i(x_2)\, g_i(t) \tag{3.4}$$

where the admissible function $f_i(x_2)$ must satisfy the geometric boundary conditions with respect to the representation of LINK2 in the reference frame $[O_1, X_2, Y_2]$.

From the above it is clear that the assumed-modes method treats a continuous system as an n-degrees of freedom system. Therefore the degrees of freedom for the overall system will be increased from 2 to n+2, and the new system will be represented with n+2 generalized coordinates that are Θ_1, Θ_2 and g_i where $i=1,2,\ldots,n$.

Increasing the number of degrees of freedom by increasing n, the estimated natural frequencies of the system will approach the true natural frequencies from above. Using a large value for n for a more accurate model of the flexible beam, the number of the generalized coordinates will also increase making the analysis of the system and the derivation of the mathematical model through Lagrange's equations a very unrealistic approach. The

system can be simplified with the assumption that the amplitudes of the higher modes for the flexible link are very small compared with the amplitudes of the first modes. Therefore, as was indicated in Ref. 5, the higher modes can be neglected and the system can be truncated with n=2, resulting in a four-degrees of freedom problem. In order to verify the stated assumption, that the modes with $n \geq 3$ can be neglected, the equations of motion are derived in Appendix B for a planar robot arm having only one flexible link by using the Lagrangian dynamics method. The elastic motion of the flexible beam that will superposed to the hypothetical rigid motion of the arm will have a flexible displacement approximated by the assumed-modes method. In Appendix B, models were developed for this flexible planar robot arm using the assumed modes with n=1,2 and 3 respectively. The resulting models were used with the adaptive control scheme (derived in Chapter V) in the simulation studies of this flexible beam. Three different DSL programs were written for these simulation studies, with the source programs given in Appendix C. The resulting phase plane and step response plots in the cases where n=1,2 and 3 are shown in Figures 3.3 to 3.8. From the analysis presented, comparing the results obtained for the different cases of n used one can observe that the step responses for n=2 (Fig. 3.8) and for n=3 (Fig. 3.8) have essentially the same duration and almost the same oscillatory characteristics. Thus it was concluded

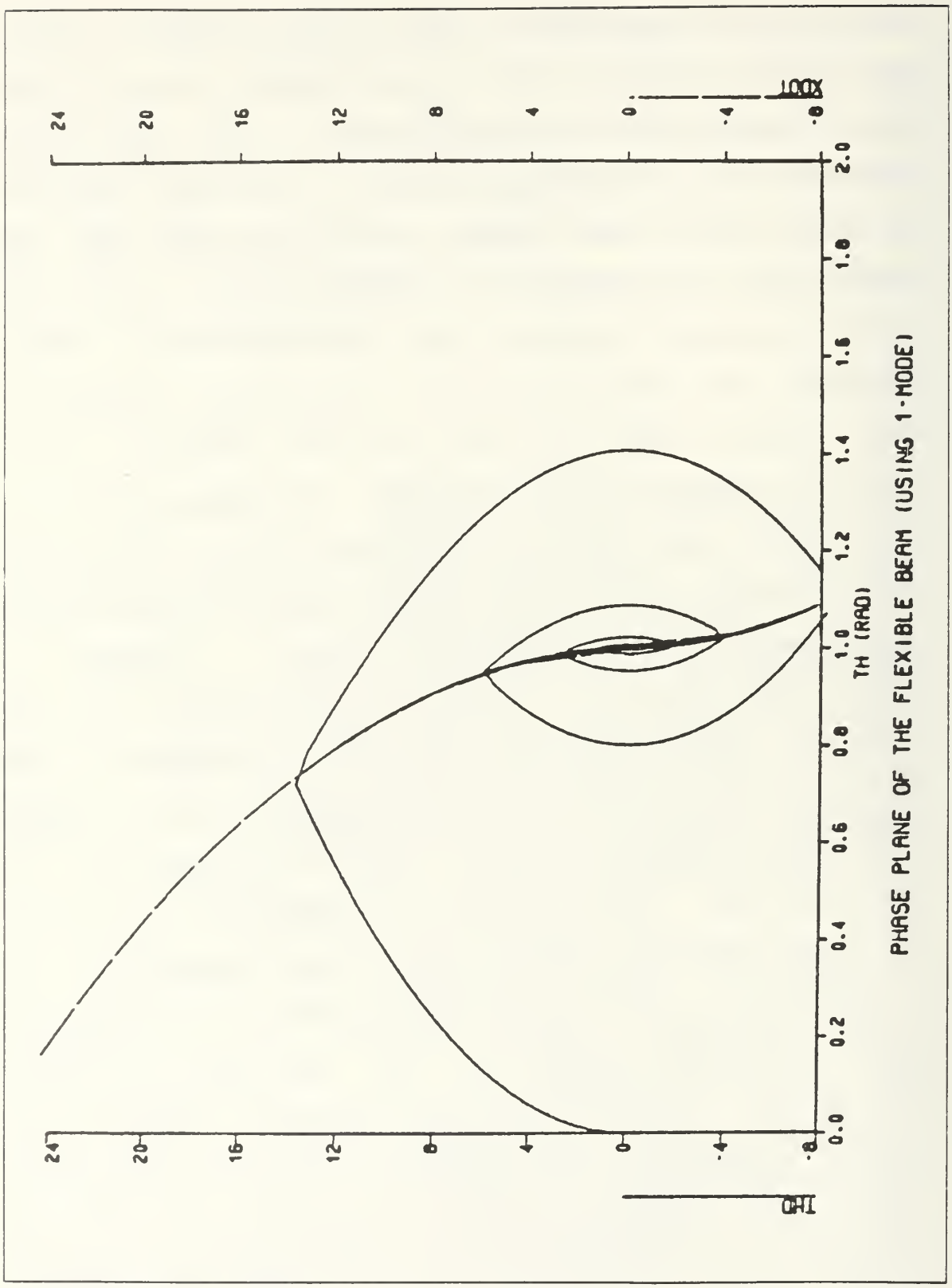

Figure 3.3 Phase plane of the flexible beam (n=1).

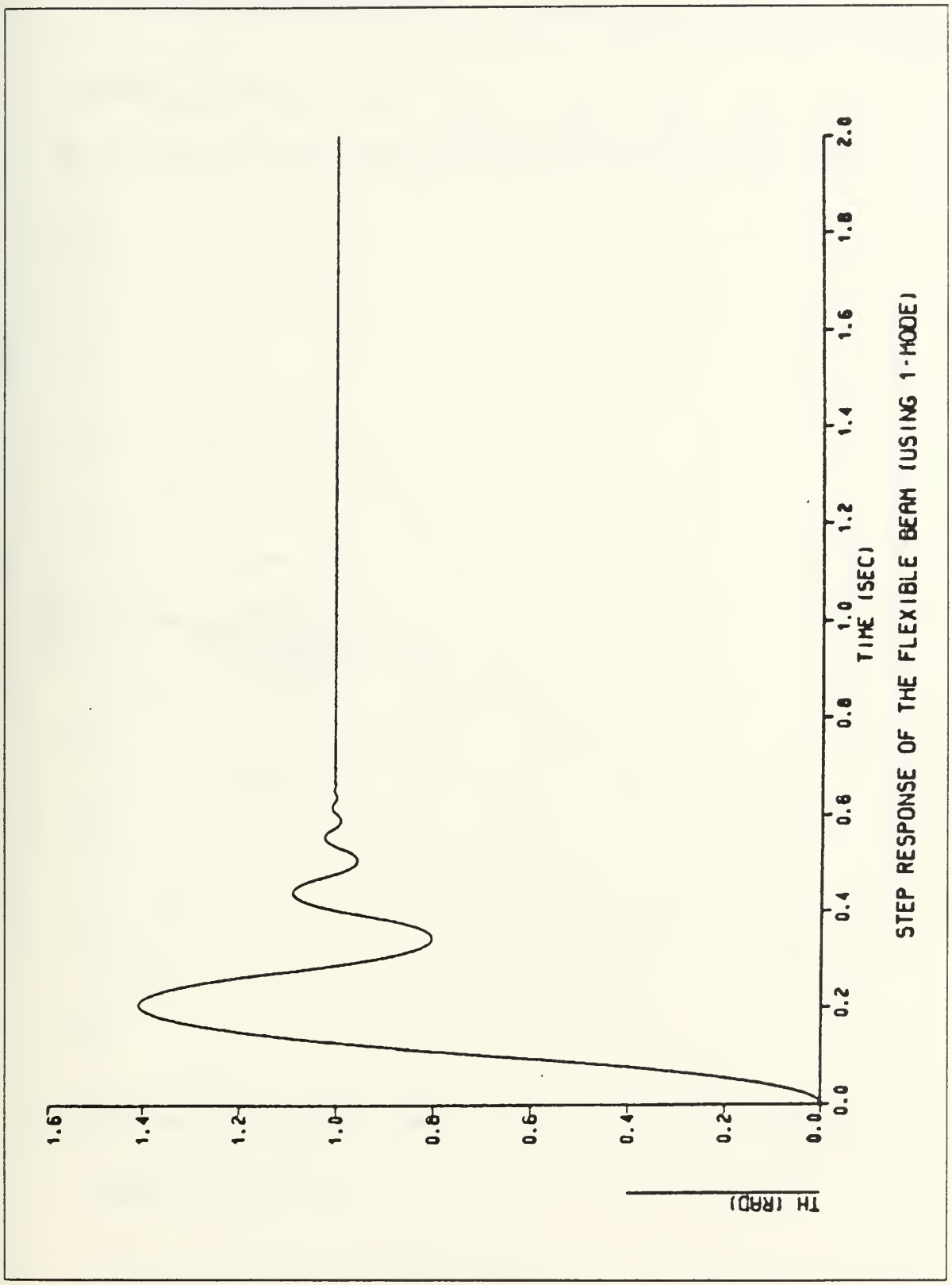

Figure 3.4 Step response of the flexible beam (n=1).

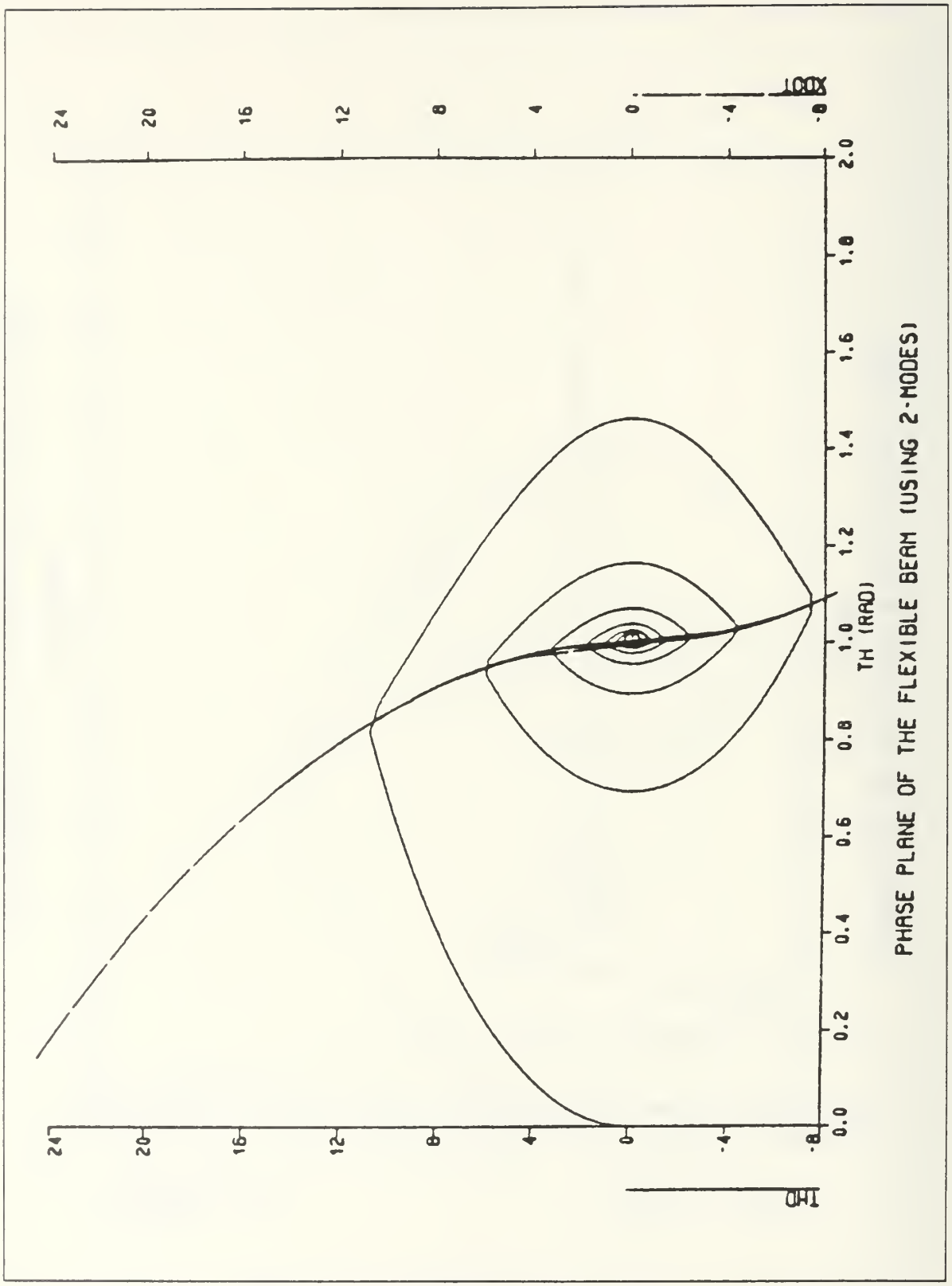

Figure 3.5 Phase plane of the flexible beam (n=2).

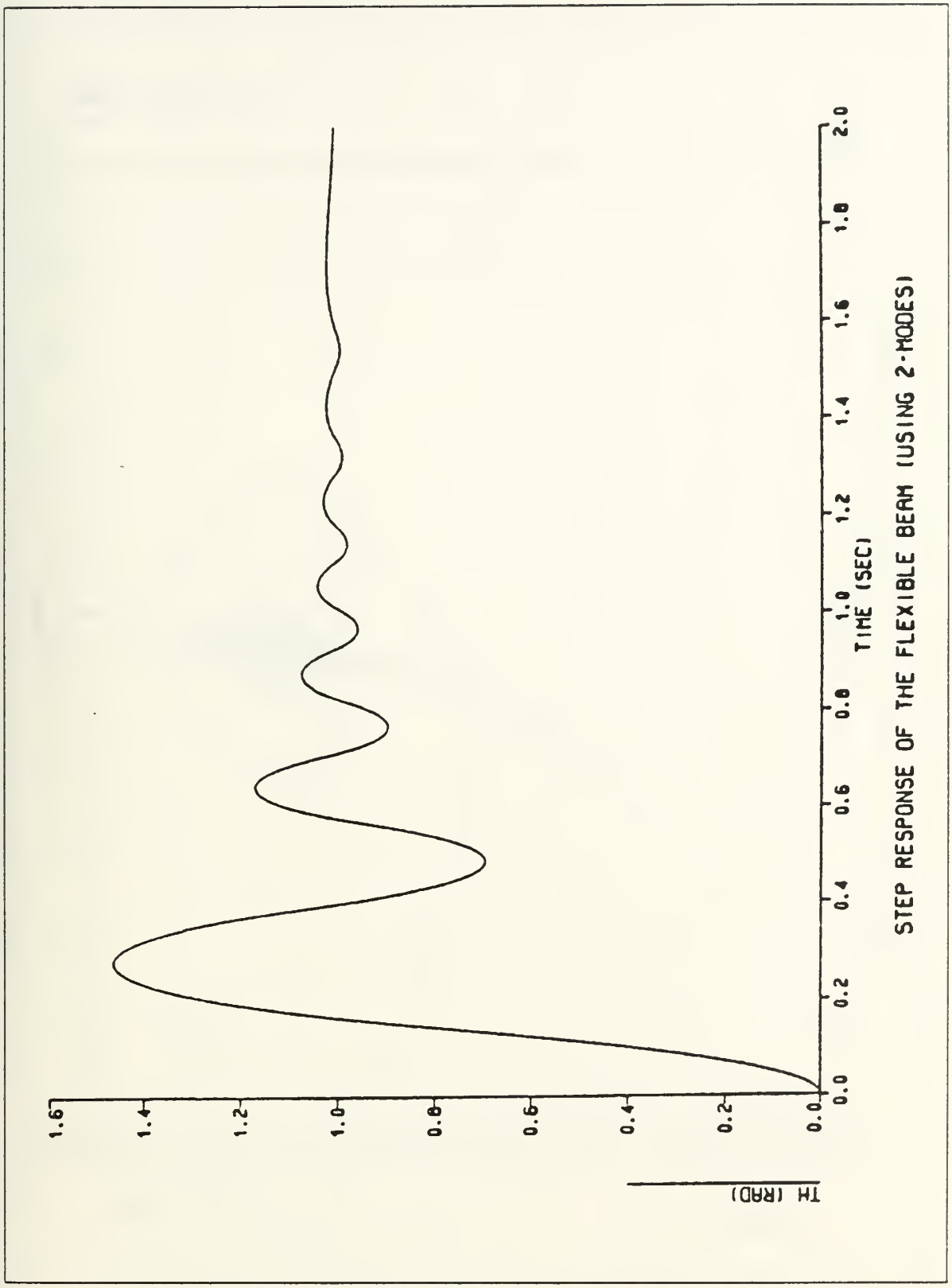

Figure 3.6 Step response of the flexible beam (n=2).

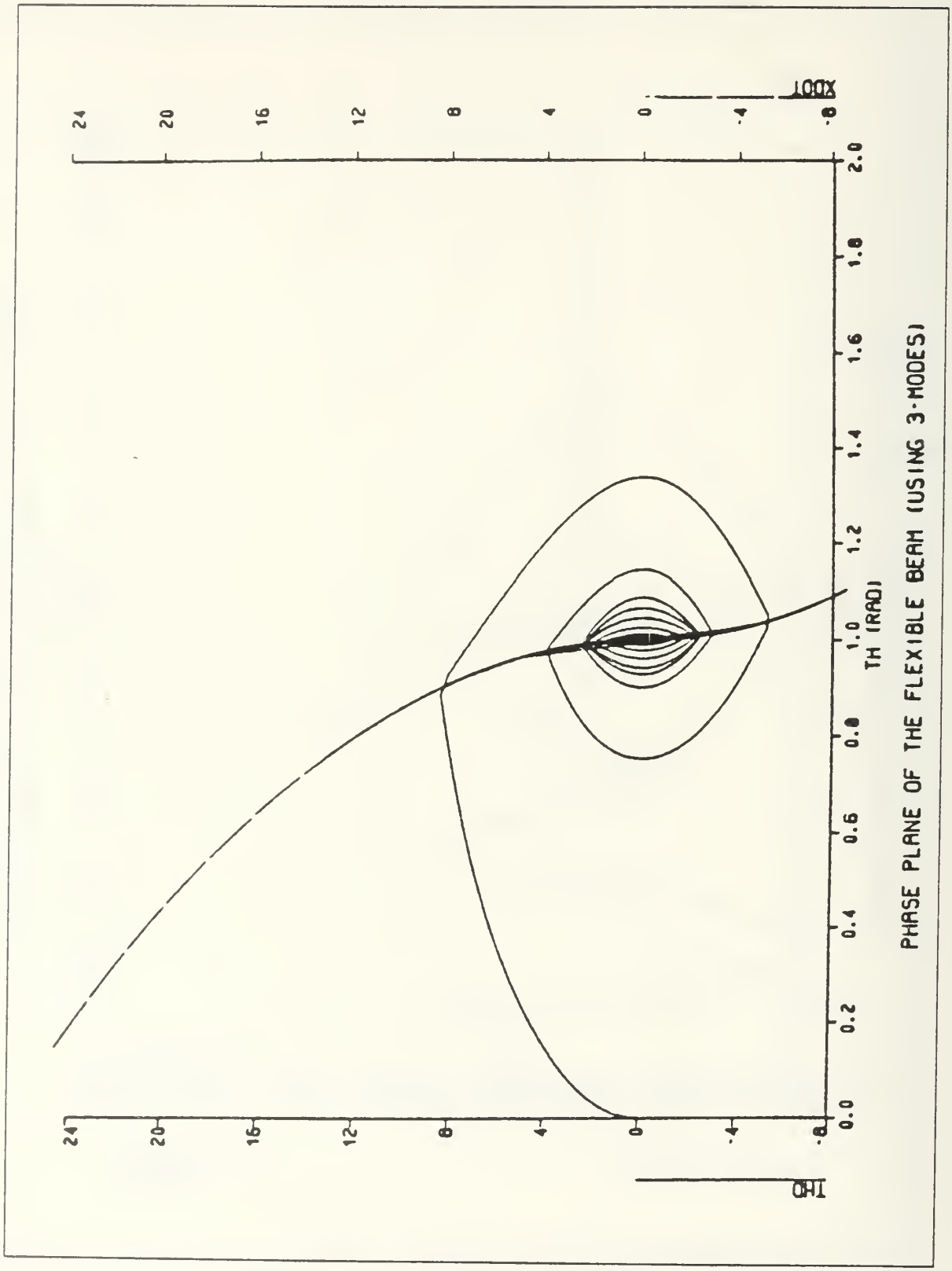

Figure 3.7 Phase plane of the flexible beam (n=3).

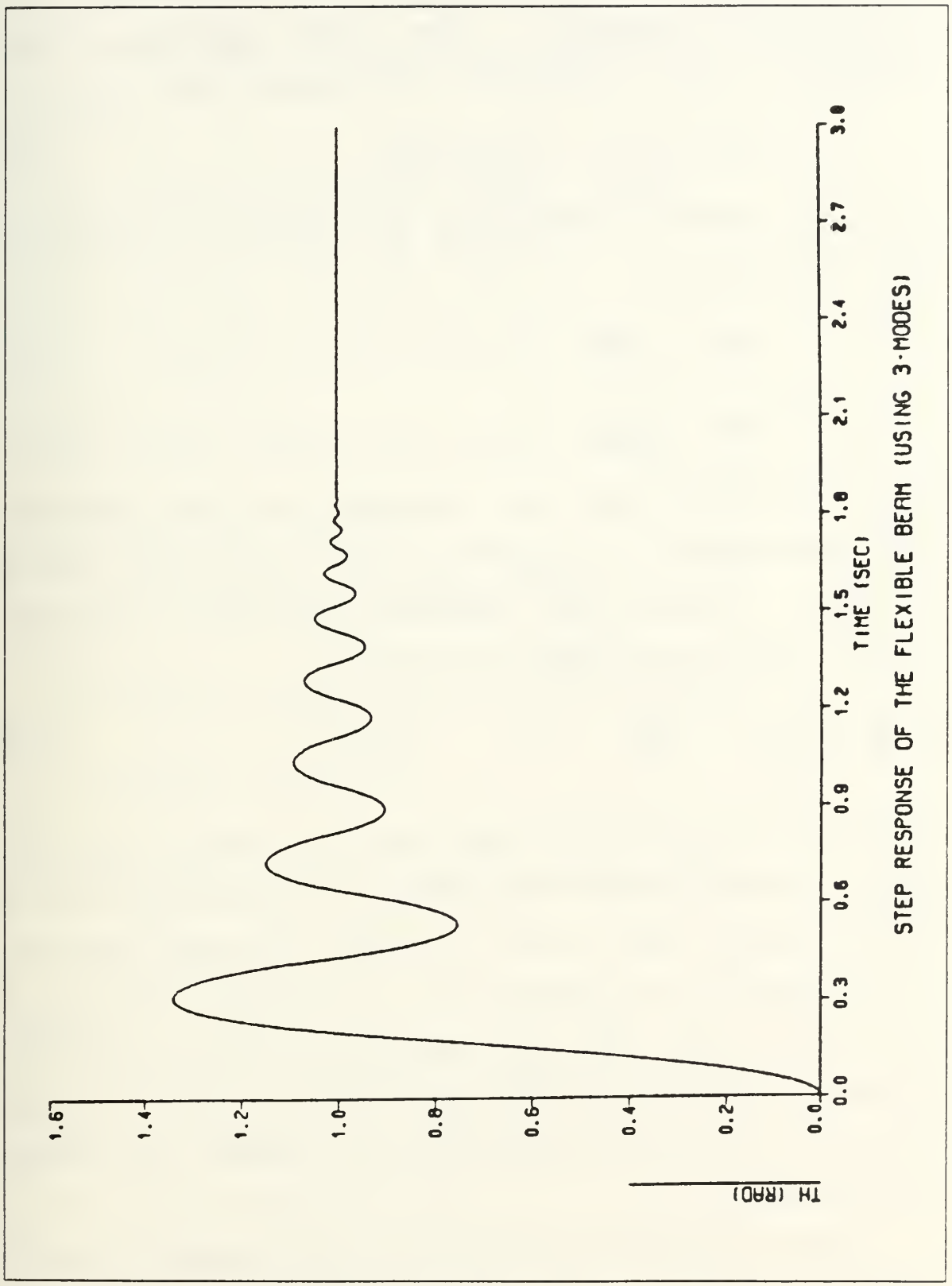

Figure 3.8 Step response of the flexible beam (n=3).

that the use of the value n=2 for the assumed-modes was a satisfactory assumption. Due to the previous analysis Equation 3.4 can be truncated obtaining the form:

$$u = f_1(x_2)\, g_1(t) + f_2(x_2)\, g_2(t) \tag{3.5}$$

with the flexible displacement and velocity at the end of the LINK2 given as:

$$u_E = f_{1E} g_1 + f_{2E} g_2 \tag{3.6}$$

$$\dot{u}_E = f_{1E} \dot{g}_1 + f_{2E} \dot{g}_2 \tag{3.7}$$

From that point the derivation of the Lagrange's equations becomes a solvable but also lengthy and tedious problem. Forming the Lagrangian function L, from the general form of the Lagrange's equation

$$\frac{d}{dt}\left(\frac{\delta L}{\delta \dot{q}_i}\right) - \frac{\delta L}{\delta q_i} = Q_i \qquad i=1,2,3,4 \tag{3.8}$$

a set of four nonlinear second order differential equations can be derived, where the generalized coordinates will be given as $q_1=\Theta_1$, $q_2=\Theta_2$, $q_3=g_1$ and $q_4=g_2$. From the definition of the generalized coordinates for the proposed system it is possible to show that the generalized forces obtain the values $Q_1=\Gamma_1$, $Q_2=\Gamma_2$ and $Q_3=Q_4=0$, where Γ_1 and Γ_2 are the torques applied to the motors at JOINT1 and JOINT2 respectively.

With the complete derivation of the Lagrange's equations given in Appendix D, the final form of the differential

equations that describe the system and that will be used as the basic model through that thesis will be given as follows:

$$\Gamma_1 = (D_{111}+J_1)\ddot{\theta}_1 + D_{122}\ddot{\theta}_2 + D_{133}\ddot{g}_1 + D_{144}\ddot{g}_2 + D_{112}\dot{\theta}_1\dot{\theta}_2 + D_{113}\dot{\theta}_1\dot{g}_1 + D_{114}\dot{\theta}_1\dot{g}_2 + D_{1222}\dot{\theta}_2^2 + D_{123}\dot{\theta}_2\dot{g}_1 + D_{124}\dot{\theta}_2\dot{g}_2 + D_1 \tag{3.9}$$

$$\Gamma_2 = D_{211}\ddot{\theta}_1 + (D_{222}+J_2)\ddot{\theta}_2 + D_{233}\ddot{g}_1 + D_{244}\ddot{g}_2 + D_{213}\dot{\theta}_1\dot{g}_1 + D_{214}\dot{\theta}_1\dot{g}_2 + D_{223}\dot{\theta}_2\dot{g}_1 + D_{224}\dot{\theta}_2\dot{g}_2 + D_{2111}\dot{\theta}_1^2 + D_2 \tag{3.10}$$

$$0 = D_{311}\ddot{\theta}_1 + D_{322}\ddot{\theta}_2 + D_{333}\ddot{g}_1 + D_{344}\ddot{g}_2 + D_{312}\dot{\theta}_1\dot{\theta}_2 + D_{3111}\dot{\theta}_1^2 + D_{3222}\dot{\theta}_2^2 + D_3 \tag{3.11}$$

$$0 = D_{411}\ddot{\theta}_1 + D_{422}\ddot{\theta}_2 + D_{433}\ddot{g}_1 + D_{444}\ddot{g}_2 + D_{412}\dot{\theta}_1\dot{\theta}_2 + D_{4111}\dot{\theta}_1^2 + D_{4222}\dot{\theta}_2^2 + D_4 \tag{3.12}$$

where

$$D_{111} = D_{122}+(m_1+m_2)l_1^2+m_2l_1l_2\cos\theta_2-m_2l_1\sin\theta_2U_E$$

$$D_{122} = m_2l_2^2+m_2U_E^2+m_2l_1l_2\cos\theta_2-m_2l_1\sin\theta_2U_E$$

$$D_{133} = m_2l_1\cos\theta_2f_{1E}+m_2l_2f_{1E}$$

$$D_{144} = m_2l_1\cos\theta_2f_{2E}+m_2l_2f_{2E}$$

$$D_{112} = -2m_2l_1(\cos\Theta_2 U_E + l_2\sin\Theta_2)$$

$$D_{113} = 2m_2f_{1E}(U_E - l_1\sin\Theta_2)$$

$$D_{114} = 2m_2f_{2E}(U_E - l_1\sin\Theta_2)$$

$$D_{1222} = -m_2l_1(l_2\sin\Theta_2 + \cos\Theta_2 U_E)$$

$$D_{123} = D_{113}$$

$$D_{124} = D_{114}$$

$$D_1 = [(m_1+m_2)l_1\cos\Theta_1 + m_2l_2\cos(\Theta_1+\Theta_2) - m_2U_E\sin(\Theta_1+\Theta_2)]g$$

$$D_{211} = D_{122}$$

$$D_{222} = m_2l_2^2 + m_2U_E^2$$

$$D_{213} = D_{223} = 2m_2f_{1E}U_E$$

$$D_{214} = D_{224} = 2m_2f_{2E}U_E$$

$$D_{233} = m_2l_2f_{1E}$$

$$D_{224} = m_2l_2f_{2E}$$

$$D_{2111} = m_2l_1l_2\sin\Theta_2 + m_2l_1\cos\Theta_2 U_E$$

$$D_2 = [m_2l_2\cos(\Theta_1+\Theta_2) - m_2U_E\sin(\Theta_1+\Theta_2)]g$$

$$D_{311} = m_2f_1(l_1\cos\Theta_2 + l_2)$$

$$D_{322} = m_2l_2f_{1E}$$

$$D_{333} = m_2f_{1E}^2$$

$$D_{344} = m_2f_{1E}f_{2E}$$

$$D_{312} = -2m_2f_{1E}U_E$$

$$D_{3222} = -m_2f_{1E}U_E$$

$$D_{3111} = D_{3222} + m_2 l_1 f_{1E} \sin\theta_2$$

$$D_3 = g m_2 f_{1E} \cos(\theta_1+\theta_2) - KW_1 g_1$$

$$D_{422} = m_2 l_2 f_{2E}$$

$$D_{411} = D_{422} + m_2 l_1 f_{2E} \cos\theta_2$$

$$D_{433} = D_{344}$$

$$D_{444} = m_2 f_{2E}^2$$

$$D_{412} = -2 m_2 f_{2E} U_E$$

$$D_{4222} = -m_2 f_{2E} U_E$$

$$D_{4111} = D_{4222} + m_2 l_1 f_{2E} \sin\theta_2$$

$$D_4 = g m_2 f_{2E} \cos(\theta_1+\theta_2) - KW_2 g_2$$

$$KW_1 = EI \int_0^{l_2} \ddot{f}_1(x) \; \ddot{f}_1(x) \, dx$$

$$KW_2 = EI \int_0^{l_2} \ddot{f}_2(x) \; \ddot{f}_2(x) \, dx$$

J_1 = the inertia of the motor at JOINT 1

J_2 = the inertia of the motor at JOINT 2

g = the acceleration of gravity (= 9.814 m/sec^2)

$U_E = f_{1E} g_1 + f_{2E} g_2$ = the end-point displacement

E is the Young's modulus, and I is the second moment of area of the beam cross section.

The admissible functions f_i (i=1,2) are assumed to be the eigenfunctions of a clamped-free beam. According to Ref.11 the restrictions for the geometric boundary conditi-

ons will be satisfied because of the orthogonality of these functions:

$$\int_0^1 f_r(x)\ f_s(x)dx = \int_0^1 \ddot{f}_r(x)\ \ddot{f}_s(x)dx = \begin{cases} 0 , & r\neq s \\ 1 , & r=s \end{cases} \qquad (3.13)$$

with

$$f_r(x) = \cosh(\mu_r x)-\cos(\mu_r x)-\sigma_r[\sinh(\mu_r x)-\sin(\mu_r x)] \qquad (3.14)$$

where, r is the mode of vibration.

$$\sigma_r = \frac{\sinh(\mu_r x)-\sin(\mu_r x)}{\cosh(\mu_r x)+\cos(\mu_r x)} \qquad (3.15)$$

with sinh and cosh to be the hyperbolic sine and cosine functions respectively, given as:

$$\sinh(x) = \frac{e^x - e^{-x}}{2} \qquad (3.16)$$

$$\cosh(x) = \frac{e^x + e^{-x}}{2} \qquad (3.17)$$

Because the model takes into account only two modes for the vibration of the flexible beam, the superscript r will obtain the values 1 and 2. The values for μ_r and σ_r, at the end-point of the flexible beam where x = l, will then be as given in Table 3.1.

TABLE 3.1 CHARACTERISTIC VALUES FOR A CLAMPED-FREE BEAM.

r	$\Omega_r = \mu_r l$	σ_r
1	1.8751	0.7341
2	4.6941	1.0185

Because of the orthogonality identity of the assumed-modes the flexible component of the potential energy will be evaluated as follows:

$$KW_r = \frac{EI}{\pi} \Omega_r^4 \qquad r=1,2 \qquad (3.18)$$

with EI the beam stiffness, π the density per unit length and Ω_r the flexible value given above for the r^{th} mode. Therefore the values of the flexible components KW_i (i=1,2) of the potential energy can be computed, and they will be given in Table 3.2.

TABLE 3.2 PARAMETERS FOR THE ELASTIC COMPONENTS OF THE POTENTIAL ENERGY.

r	KW_r
1	0.00124
2	0.0433

The other parametric values, lengths of the links and discrete masses that are lumped at the end of each link, that will be used in this thesis for the study of the two links planar robot arm (with the first link rigid and the second flexible) are given in Table 3.3.

The D_{ii} (i=1,2,3,4) values defined in the above equations were obtained from the forces acting on each link due to acceleration and velocity of the moving robot arm as was done in the case of the two rigid links planar robot arm. Additional terms are due to the forces introduced by

the flexible motions of the second link and the coupling forces acting on the system.

TABLE 3.3 PARAMETRIC DATA OF A RIGID-FLEXIBLE PLANAR ROBOT ARM.

$l_1 = 0.40$ m
$l_2 = 0.32$ m
$m_1 = 0.30$ kg/m/sec^2
$m_2 = 0.03$ kg/m/sec^2
$m_2 = 0.10$ kg/m/sec^2 (with load)

IV. PRELIMINARY STUDIES USING THE COMPUTER SIMULATION MODEL

A. INTRODUCTION

The second order models derived in Chapters II and III for the rigid-rigid and rigid-flexible planar robot arms respectively will become the mathematical models for this case. Each arm will be driven, open loop, by a servo motor. The servo motors have to follow a predetermined curve until the desired position is reached. In order to achieve this the states of the second order model have to be adapted such that the computer model mimics the position and the velocity of the actual servo motor with equivalent gain constants.

For the sake of the analysis identical servo motors are used independently at each joint to provide the proper torques for the required movements.

B. SERVO MOTOR SELECTION

From Ref. 12 the equivalent transfer function of a servo motor can be expressed as:

$$\frac{\Theta(s)}{V(s)} = \frac{1/K_v}{s\left(s\frac{JR}{K_vK_t}+1\right)\left(s\frac{L}{R}+1\right)} \tag{4.1}$$

with the parameters Θ, V, K_v, K_t, J, R and L obtained from the data of the specific motor to be used. For the purpose of this thesis a permanent magnet motor drive currently used in industrial robots was selected. The parametric data for this motor obtained from Ref. 13 are listed in Table 4.1.

TABLE 4.1 PARAMETRIC DATA FOR THE JOINT SERVO MOTOR.

Torque constant	K_t:	10.37	gr-m/amp
Motor inertia	J_m:	0.024	gr-m-sec^2/rad
Damping coefficient	B_m:	0.031	gr-m-sec/rad
Back-emf constant	K_v:	0.1012	V-sec/rad
Armature inductance	L :	0.0001	H
Terminal resistance	R :	0.91	Ω

Adding a large inertia to represent the arm of the robot to the motor inertia given above the mechanical pole of the motor becomes very small. Since R/L represents a large number the electrical pole of the motor becomes large with no significant effect on the response of the servo motor and can be neglected. Therefore the transfer function of the servo motor can be approximated as:

$$\frac{\Theta(s)}{V(s)} = \frac{K_m}{s^2} \qquad (4.2)$$

where the value of K_m will be computed from the preliminary studies of the arm-motor systems given below.

C. ANALYSIS OF THE ARM-MOTOR SYSTEMS

1. Rigid-rigid planar robot arm

The inertia of each arm will be given from D_{11} and D_{22}, as they are defined in Chapter II, for the first and

the second link respectively. Evaluating the expressions of D_{11} and D_{22} from the parametric data given in Table 2.1 and adding the result to the inertia of the servo motor used at each joint (in this particular case the motor inertia J_m is the same for both joints), the effective joint inertias can be evaluated. Knowing the effective joint inertias at each joint the exact transfer function for each motor will be calculated. The inertia of the first arm is also a function of the angle Θ_2 of the second link, solving for the case $\Theta_2=0^\circ$ the effective joint inertias become:

$J_1 = D_{11}+J_{m1} = 65.92+0.024 = 65.944$ gr-m-sec^2/rad, and

$J_2 = D_2 +J_{m2} = 5.12+0.024 = 5.144$ gr-m-sec^2/rad.

Substituting the effective inertias calculated above and the parametric data for the servo motor, given in Table 4.1, into the Equation 4.1 the transfer functions for the two servo motors will be obtained as follows:

$$G_1(s) = \frac{9.88}{s\ (s/9100 +1)\ (s/0.016 +1)} \quad \text{rad/volt} \qquad (4.3)$$

$$G_2(s) = \frac{9.88}{s\ (s/9100 +1)\ (s/0.204 +1)} \quad \text{rad/volt} \qquad (4.4)$$

The open loop Bode plots for the servo motors acting at each joint were obtained using the software package 'CONTROLS' with the resulted plots are shown in Figures 4.1 and 4.2. From the Bode plots it can be observed that the gain curves of both servo motors have a slope of -40 db/dec and their gain crossover frequencies are $\Omega_1=0.402$ and $\Omega_2=1.43$ rad/sec

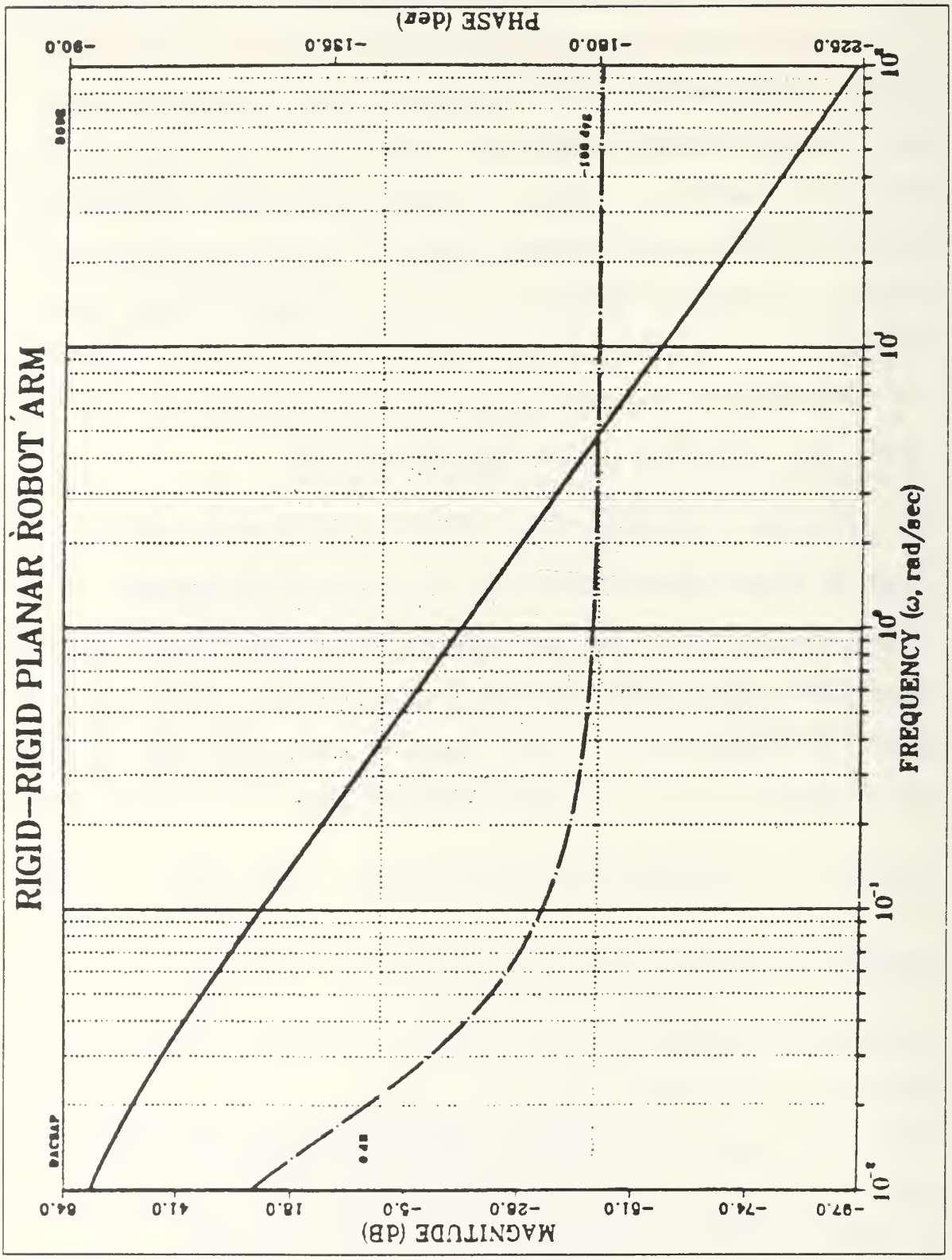

Figure 4.1 Open loop Bode plot of the servo motor at JOINT1 (rigid-rigid, case).

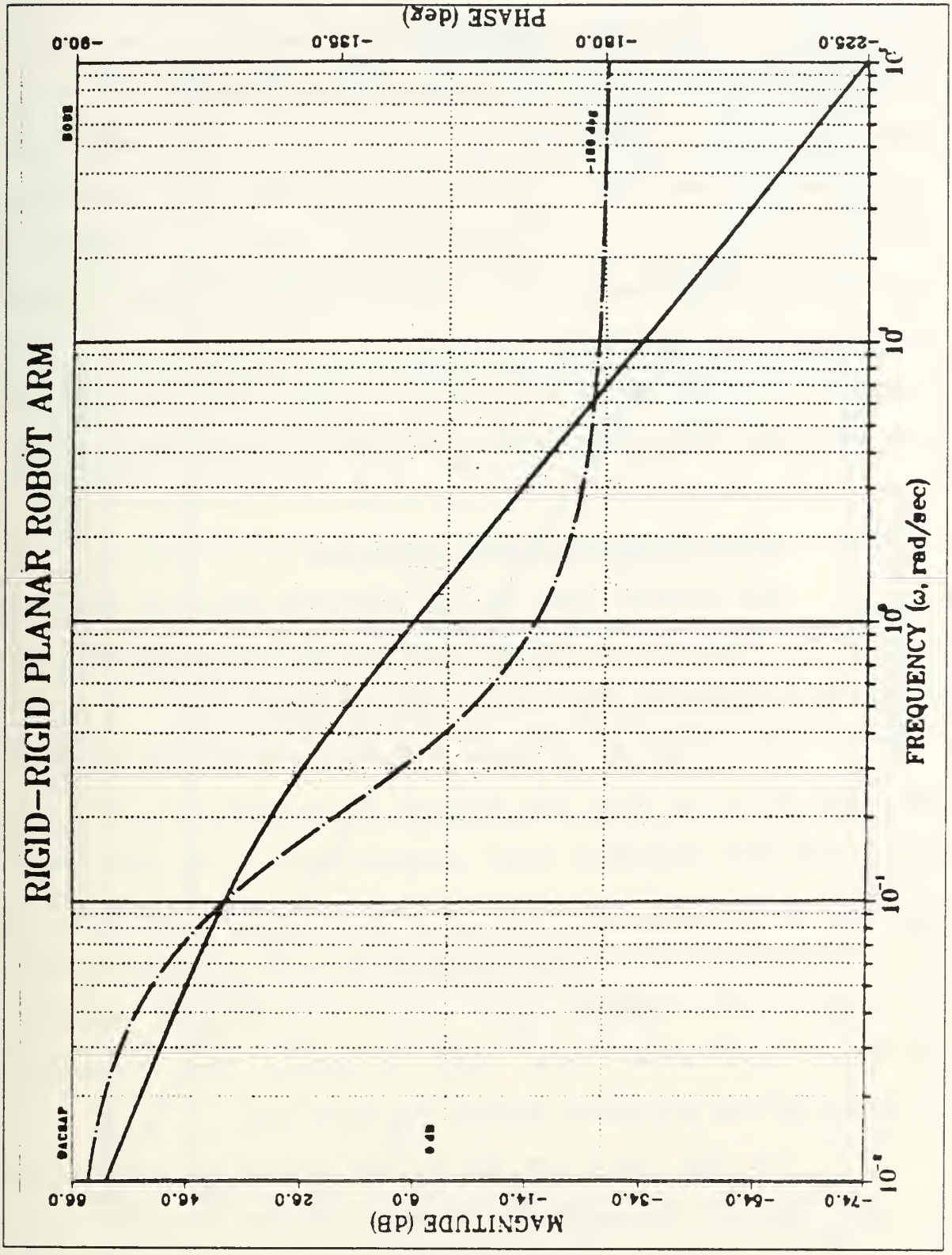

Figure 4.2 Open loop Bode plot of the servo motor at JOINT2 (rigid-rigid, case).

respectively. These results indicate that the electrical pole can be neglected and the approximation of an ideal motor, with its transfer function given as Equation 4.2, is valid for both systems. In order to have the same gain crossover frequency for the ideal motor, the error coefficient Km must have the value $Km_i = \Omega_i^2$ (i=1,2). Therefore the error coefficients for the second-order ideal motors have the values Km_1=0.162 and Km_2=2.045 respectively. The frequency responses of the ideal motors using the error coefficients calculated above are given in Figures 4.3 and 4.4.

2. Rigid-flexible planar robot arm

The general idea of the previous analysis for the case of a rigid-rigid planar robot arm is not affected by changing the second link to be a flexible one.

The inertia of each arm will now be given from D_{111} and D_{222}, as they are defined in Chapter III, for the rigid and the flexible link respectively. In this case evaluation of D_{111} and D_{222} is not so simple because in their expressions are also involved terms due to the elastic motion of the flexible arm. To overcome that problem different approaches were used to obtain the frequency response of the arm-motor system for each arm.

For the rigid arm due to the nature of the system and observing the quantities involved in the expression of the inertia of the arm, D_{111}, the "flexible" terms can be

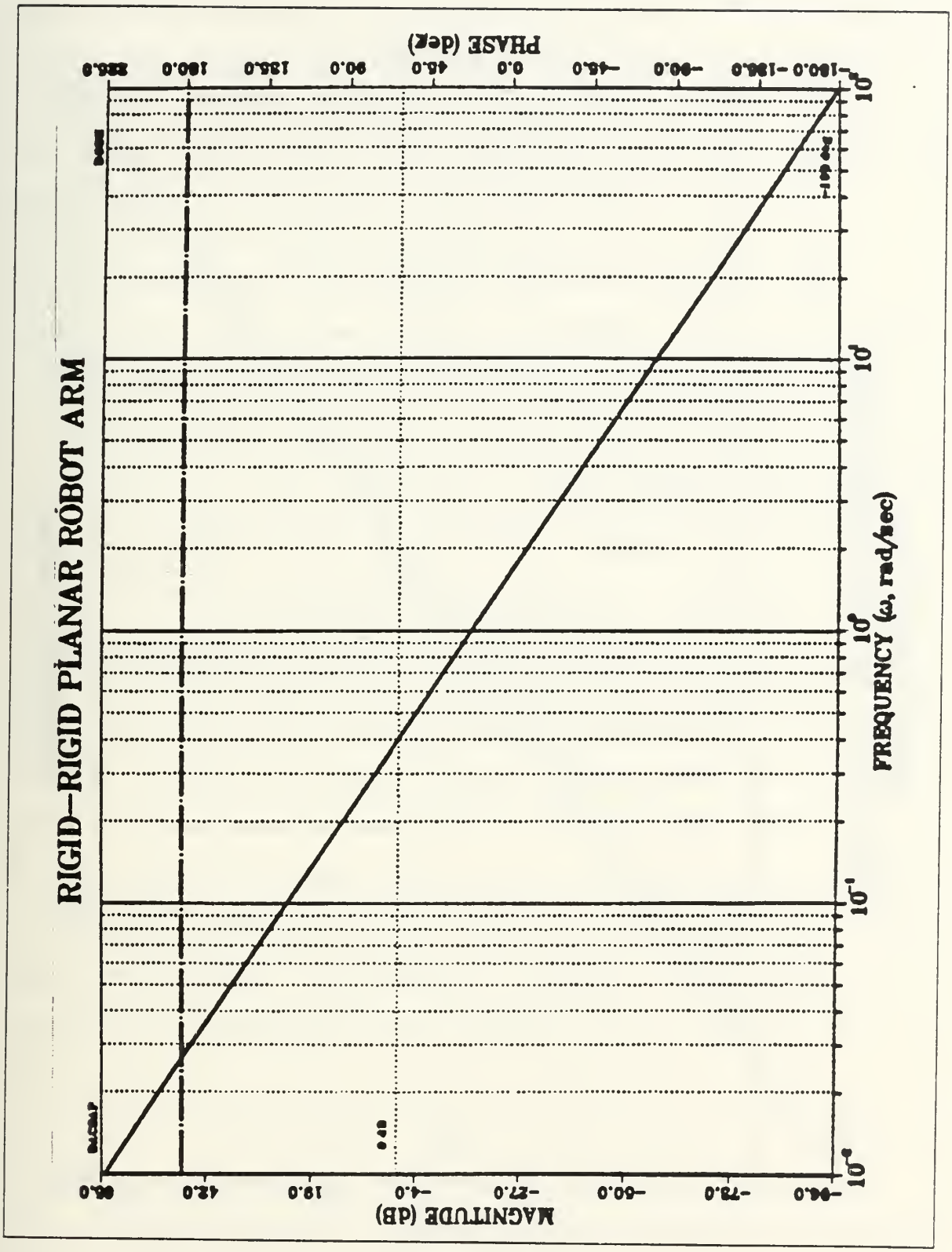

Figure 4.3 Open loop Bode plot for the ideal motor Km_1/s^2 (rigid-rigid, case).

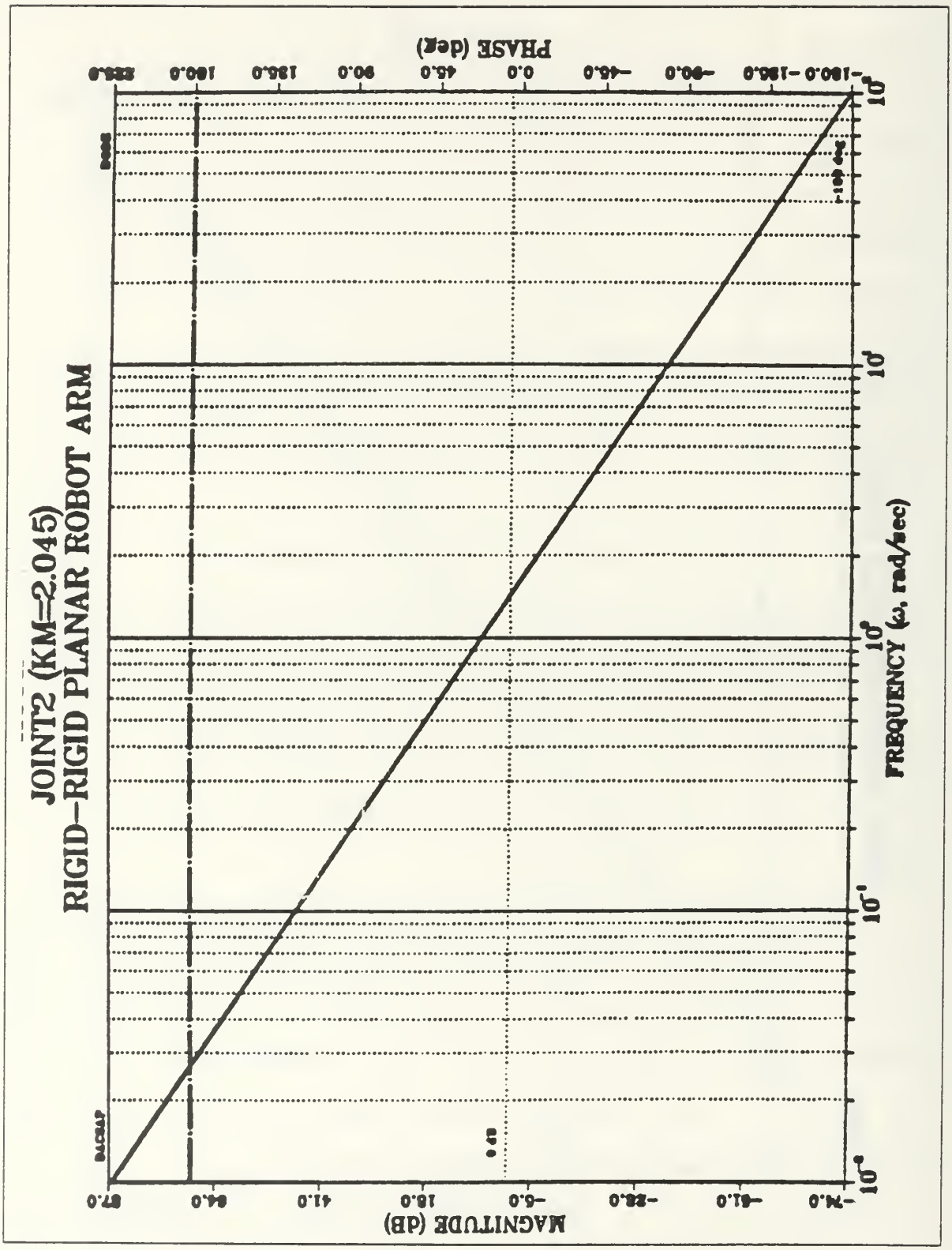

Figure 4.4 Open loop Bode plot for the ideal motor Km_2/s^2 (rigid-rigid, case).

neglected. Therefore the inertia of the arm can be computed using the parametric data given at Table 3.3 in Chapter III. With $\Theta_2=0^\circ$ again, and adding the result to the inertia of the servo motor, Jm_1, the effective joint inertia can be evaluated:

$$Jf_1 = D_{111}+J_{m1} = 58.75+0.024 = 58.774 \quad \text{gr-m-sec}^2/\text{rad}$$

Knowing the effective inertia at JOINT1 the exact transfer of the motor will be calculated. Substituting the effective inertia and the parametric data for the servo motor (given in Table 4.1) into Equation 4.1 the transfer function for the servo motor acting at JOINT1 is obtained as follows:

$$Gf_1(s) = \frac{9.88}{s\ (s/9100+1)\ (s/0.018+1)} \quad \text{rad/volt} \qquad (4.5)$$

The open loop Bode plot for this servo motor was obtained and the resulteing plot is given in Figure 4.5. The gain curve of the servo motor again has a slope of -40 db/dec with gain crossover frequency at $\Omega f_1=0.431$ rad/sec. In order that the ideal motor have the same gain crossover frequency, the error coefficient Km_{f1} must have the value $Km_{f1}=\Omega f_1{}^2=0.185$. The frequency response of the ideal motor using the calculated error coefficient is given in Figure 4.6.

In the case of the flexible arm the "flexible" terms are significant and they cannot be neglected. A satisfactory approach in terms of the frequency response is to uncouple the flexible arm from the rigid arm. With the

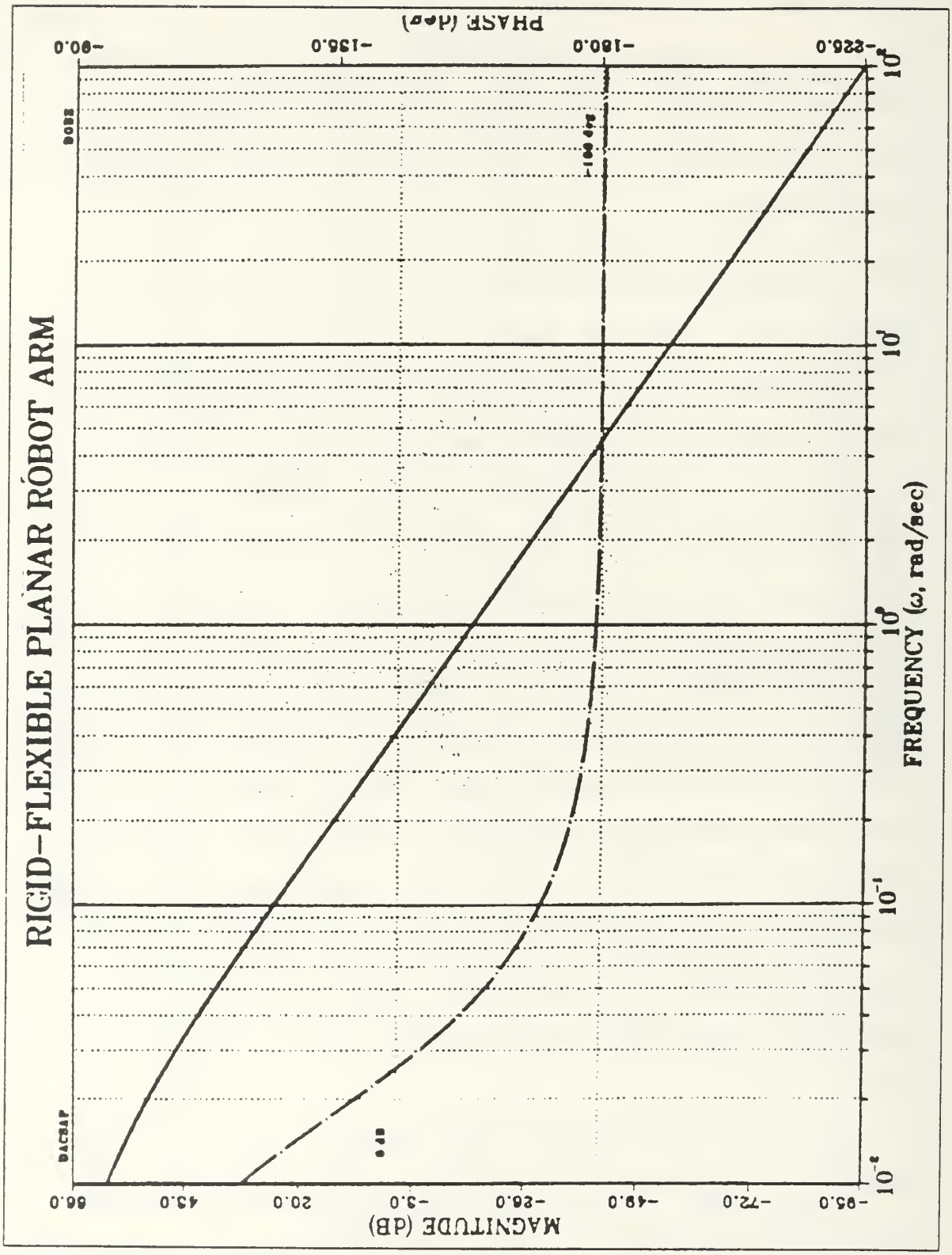

Figure 4.5 Open loop Bode plot of the servo motor at JOINT1 (rigid-flexible, case).

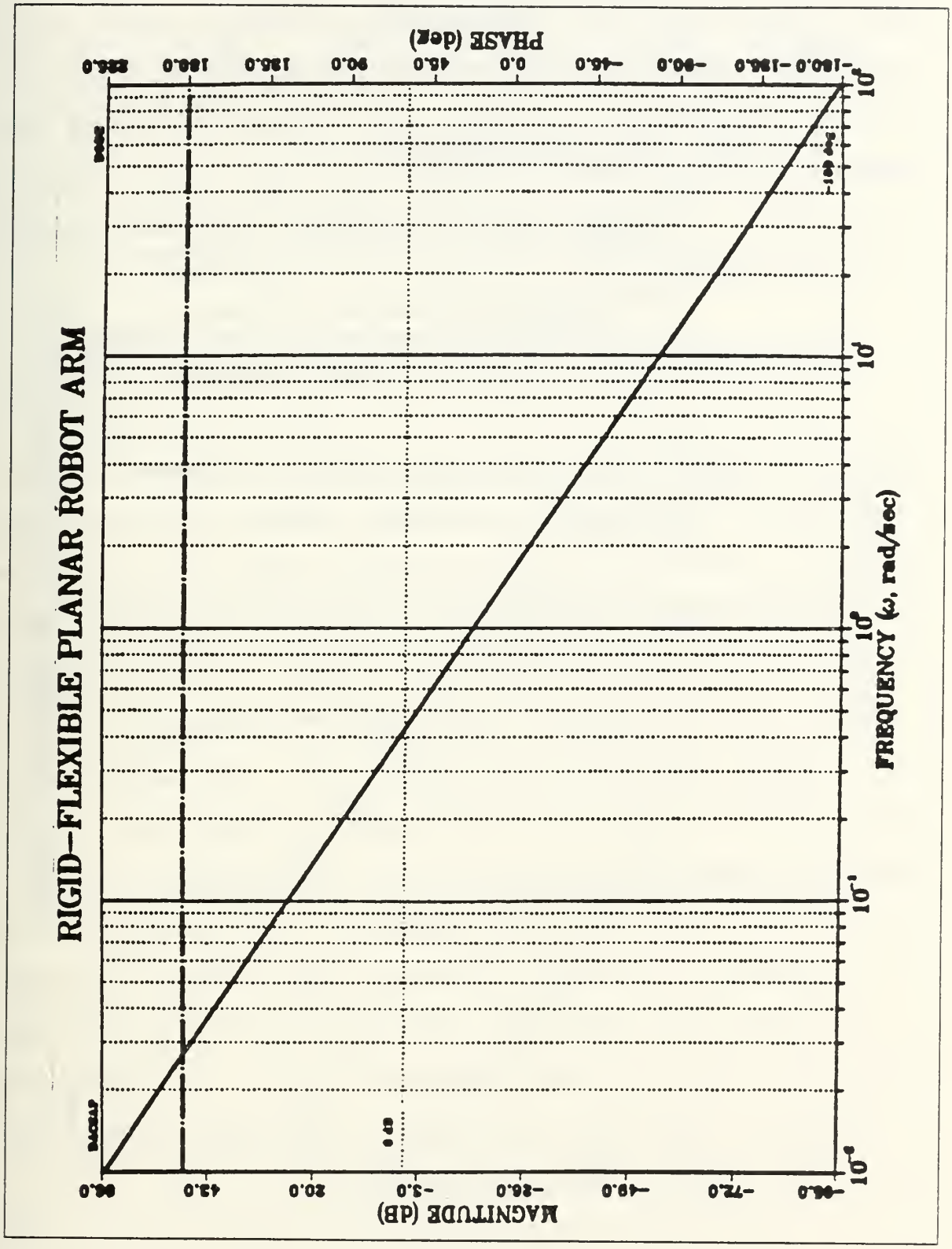

Figure 4.6 Open loop Bode plot of the ideal motor Km_1/s^2 (rigid-flexible, case).

flexible arm uncoupled, the transfer function given in Ref.1 can be used after appropriate scaling to represent the flexible beam with the parametric values of mass, length and strength used in this study. The transfer function that describes the system, flexible arm and motor, can be obtained by combining the two transfer functions and its final form is:

$$Gf_2(s) = \frac{585130\ (s+1\pm j30)(s+3.2\pm j170)(s+9.1\pm j462)}{s(s+0.3)(s+9100)(s+1.8\pm j120)(s+4\pm j215)(s+7.3\pm j481)} \quad (4.6)$$

The open loop Bode plot was obtained for the transfer function of the flexible arm-motor system, with the plot given in Figure 4.7. One can observe that the gain curve has a slope that is approximately -40 db/dec, and the gain crossover frequency is Ωf_2=1.52 rad/sec. In the frequency response are also shown three resonant frequencies due to the elastic motion of the flexible arm. The magnitude at the resonant frequencies is decreasing in amplitude with the first resonance occurring at about 120 rad/sec. For the case of the ideal motor the response at high frequencies can be neglected. In order to have the ideal motor's response at the same gain crossover frequency the error coefficient Km_{f2} must have the value $Km_{f2}=\Omega f_1{}^2=2.34$. The frequency response of the ideal motor using the error coefficient calculated above is shown in Figure 4.8.

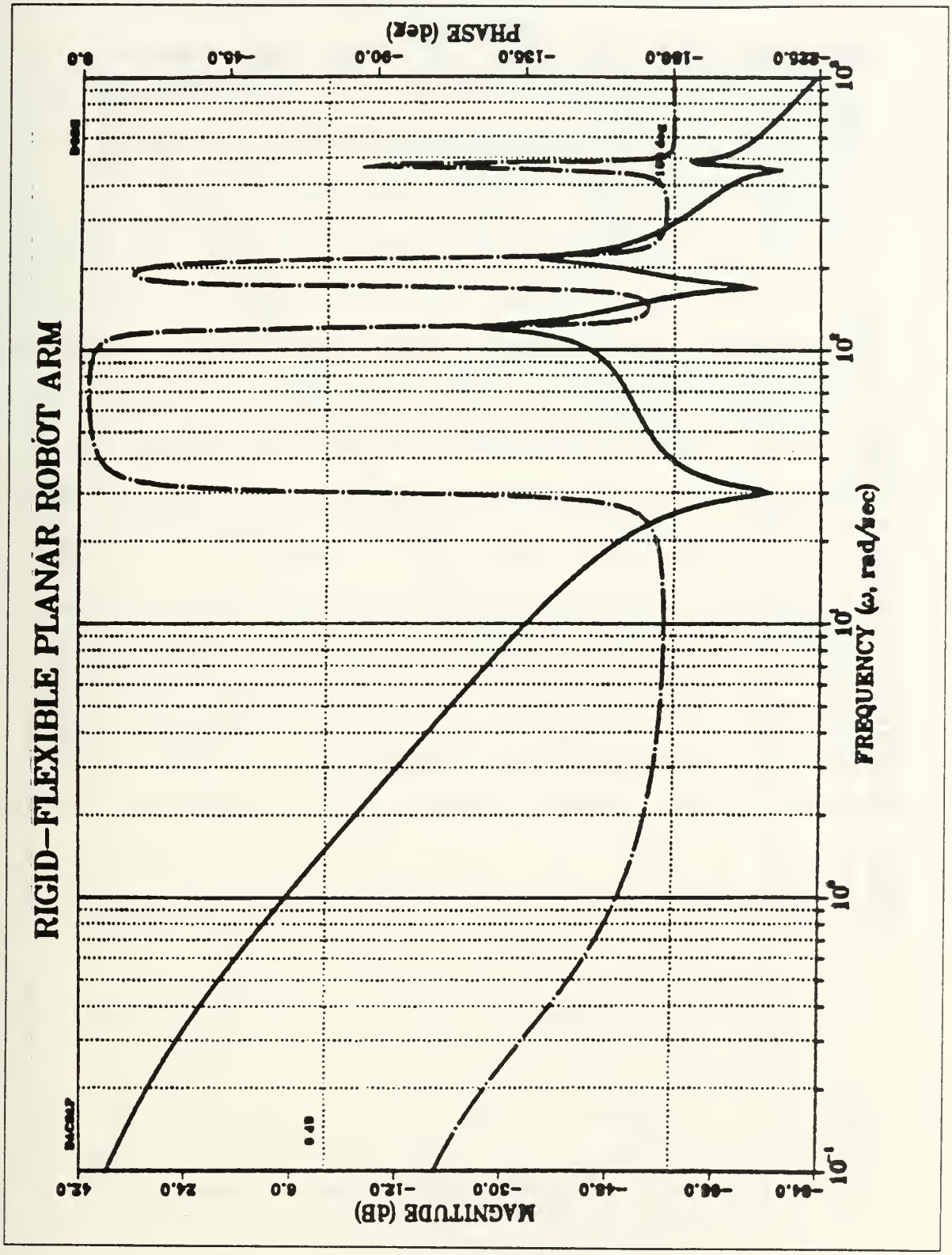

Figure 4.7 Open loop Bode plot of the arm-motor at JOINT2 (rigid-flexible, case).

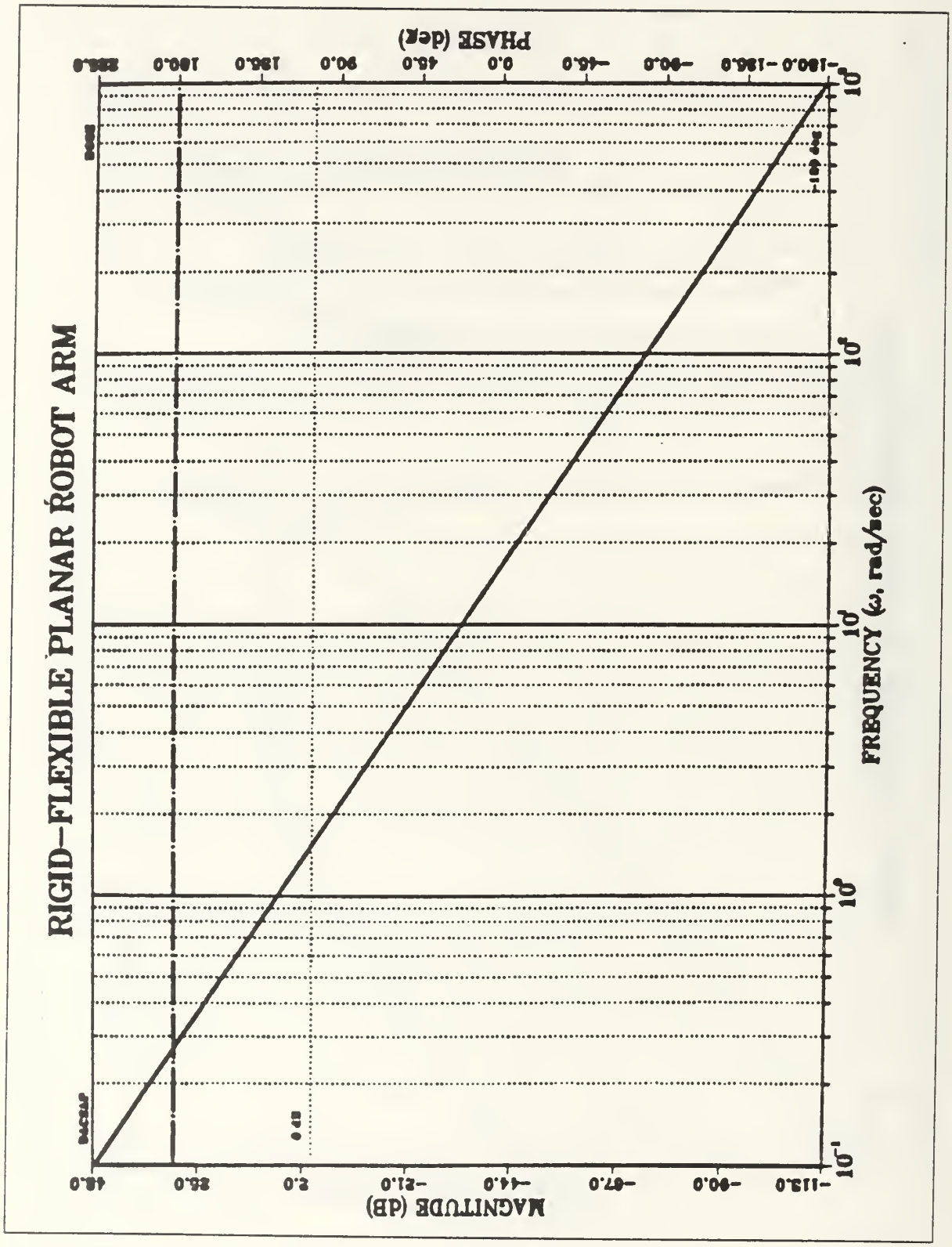

Figure 4.8 Open loop Bode plot of the ideal motor Km_2/s^2 (rigid-flexible, case).

V. VELOCITY CURVE FOLLOWER CONTROL SCHEME

A. BACKGROUND

A commonly used modification of a bang-bang controller is the "curve following" servo [Ref.14]. The "curve following" control scheme usually involves three modes of operation in following a step position command. There are an initial full acceleration mode, a curve following mode and a terminal linear servo mode. The nice feature of this control scheme is that the amplifiers used are intentionally being driven into saturation resulting in fast response and taking full advantage of the available power in the motor, which is being driven with full forward or full reverse power. This is the main advantage compared to linear controllers where saturation of the amplifiers must be avoided because it renders the controller ineffective. Other advantages of this control scheme are its implementation on a digital machine and the adaptive capabilities which were discussed at the introduction in Chapter I.

B. DESCRIPTION OF THE VELOCITY CURVE FOLLOW SYSTEM

The velocity curve following control scheme is illustrated in Figure 5.1. The control scheme that will be used has two modes of operation in following a step input command. It can be shown that the commanded input does not have to be a step. Actually any input command (of arbitrary

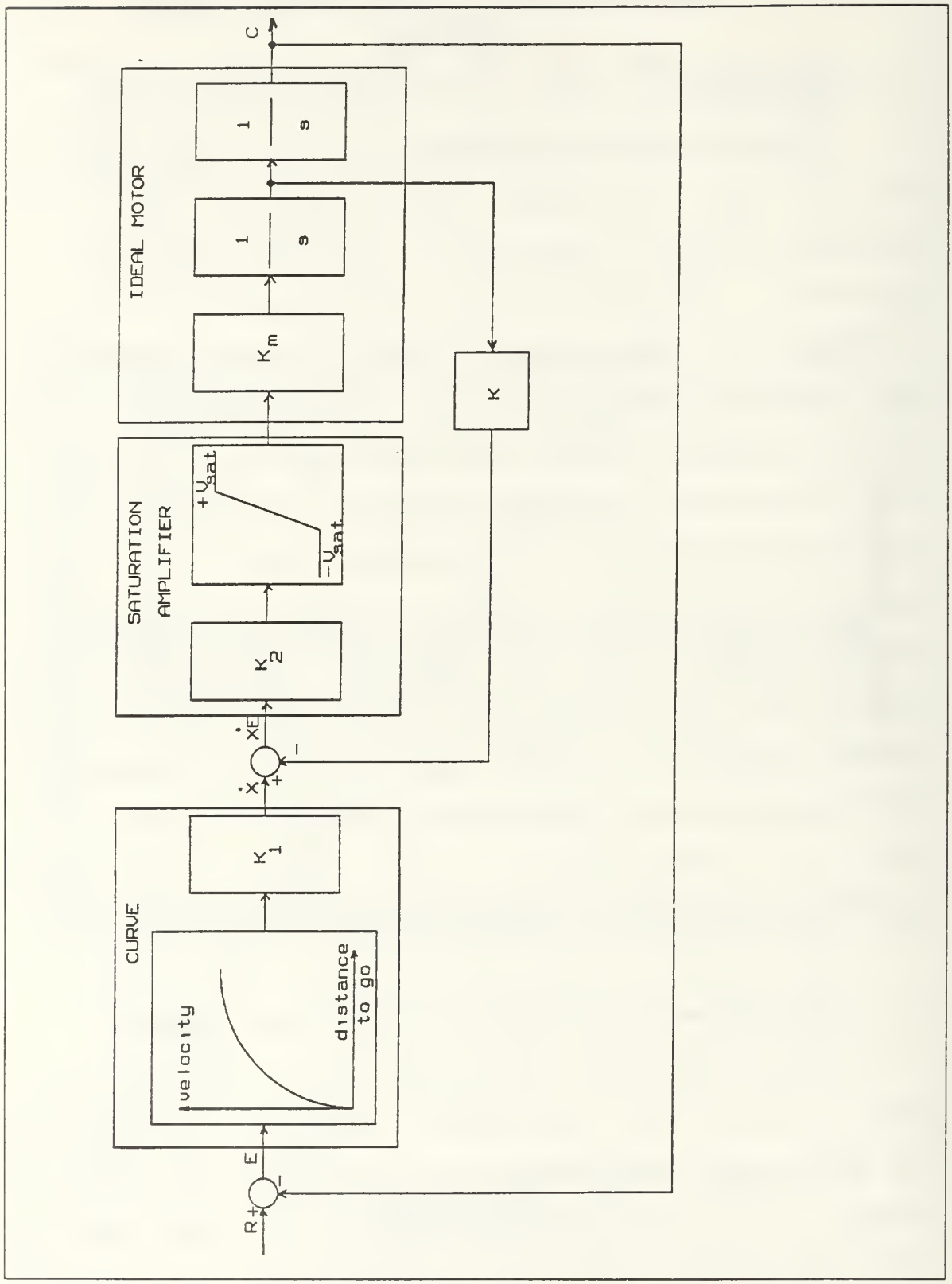

Figure 5.1 The velocity curve follow system.

shape) can be used with the proposed control scheme.

Initially the system gets into full acceleration until the designed curve is reached, at which point the system follows the curve. The velocity curve follow control scheme is therefore a nonlinear control scheme and practically it is a modification of a bang-bang controller.

When an input is applied to the system, the resulting error signal, E, will enter the curve as the "distance to go" producing as output the corresponding velocity ordinate of the curve, $\dot{X}$. This velocity $\dot{X}$, becomes the input of the velocity loop. The "Saturation Amplifier", saturates and a full forward signal is applied to the motor. As the position error signal decreases, the output from the curve is reduced and the velocity feedback signal, $K\dot{C}$, increases until the velocity error, $\dot{X}E$, becomes zero. Zero velocity error means that the acceleration trajectory crosses the designed curve. From that point the velocity error reverses sign, causing the input voltage to the motor to reverse, and the system decelerates following the curve down until it reaches the final position.

C. DESIGN OF THE CURVE

The curve used in any curve follow control scheme must have a shape that fits the requirements for the specific system and the application of that system.

For the purpose of this study the curve will have a

parabolic shape. The equations describing this curve can be derived from the equations of the ideal motor as follows:

$$\ddot{C} = K_m V_{sat} \tag{5.1}$$

$$\dot{C} = \int \ddot{C}\, dt = K_m V_{sat} t + \dot{C}(0) \tag{5.2}$$

$$C = \int \dot{C}\, dt = \frac{1}{2} K_m V_{sat} t^2 + \dot{C}(0)t + C(0) \tag{5.3}$$

Solving Equation 5.2 for t and substituting its expression into Equation 5.3, after some algebraic manipulations and with the initial conditions $C(0)=0$ and $\dot{C}(0)=0$, the following equation is obtained:

$$C = \frac{1}{2} \frac{\dot{C}^2}{K_m V_{sat}} \tag{5.4}$$

For deceleration of the system from initial conditions, with the input $R=0$, then:

$$C = -E \tag{5.5}$$

$$\dot{C} = -\dot{E} \tag{5.6}$$

Combining Equations 5.4, 5.5 and 5.6, finally:

$$\dot{X} = A \sqrt{E} \tag{5.7}$$

where

$$A = \sqrt{2K_m V_{sat}}$$

$$\dot{X} = \dot{E}$$

Therefore the output of the curve that represents the commanded velocity can be generated at any instant of time from the multiplication of the square root of the position error by the defined constant factor A. This constant factor will be initially calculated from the specific parameters K_m and V_{sat} and its value stored in the memory of a digital computer. The gain constant of the second order model, K_m, is determined by the actuator parameters and the effective inertia seen by the actuator and is updated through the adaptive algorithm. The initial values for these gain constants have been derived in Chapter IV for two different cases of a planar robot arm with two links, the rigid-rigid and the rigid-flexible.

The saturation limits, V_{sat}, of the amplifier are determined by the available servo motor parameters, the mechanical design of the arm of the manipulator and the working conditions. The gain parameter K_2 must have a relatively large value in order to saturate the amplifier even for small commanded velocity signals.

The gain parameter K_1, used to reshape the curve as a weight factor of the commanded velocity signal, and the feedback gain K will be used in the velocity curve follow model in order to give best system performance and suitable results for each specific problem. The calculations of the values of K and K_1 will be based on the simulation results.

D. SIMULATION STUDIES OF THE CONTROL SCHEME MODEL

To demonstrate the good performance of the basic model, shown in Figure 5.1, and the ability of the velocity curve follow control scheme to follow the designed curve, the model was simulated using DSL/VS. The DSL/VS simulation program is listed in Appendix E.

The basic model was simulated with different values corresponding to each link of the planar robot arm, for both cases the rigid-rigid and the rigid-flexible. The resulted four sets of parameters are given in Table 5.1.

TABLE 5.1 RESULTED PARAMETERS FROM THE SIMULATION STUDY OF THE BASIC MODEL.

	Rigid-Rigid	Rigid-Flexible
LINK 1	K_m = 0.162 rad/V V_{sat} = ±300 V	K_m = 2.045 rad/V V_{sat} = ±150 V
LINK 2	K_m = 0.185 rad/V V_{sat} = ±300 V	K_m = 2.340 rad/V V_{sat} = ±150 V

To guarantee the saturation of the amplifier the value K_2=10,000 was chosen to be used at the simulation studies for all the different cases.

From the simulation studies the appropriate gain values were obtained using trial and error. The best value for the

feedback gain, in all cases, was found to be K=1. For the constant weight factor K_1, the values 0.8 and 1 gave the best system performance when used with the parameters corresponding to the first and the second link respectively.

Simulating the basic model for a commanded input R=1 rad by using the calculated parametric values of the rigid-rigid planar robot arm, the step response and the phase plane trajectories are given in Figures 5.2 and 5.3. Using the parametric values (extracted from the rigid-flexible planar robot arm) the corresponding plots are given in Figures 5.4 and 5.5.

From the phase plane, where the trajectories of the angular velocity C and of the commanded velocity X versus the angular position C are given, one can observe that the angular velocity increases with constant acceleration until the curve is reached. From that point the angular velocity follows the designed curve until the desired position is reached. Reaching the final position the system stops with no oscillations.

The step responses demonstrate good performance of this basic model with fast response and with no overshoots, even for this relatively large commanded input signal.

E. THE ADAPTIVE MODEL

The block diagram of the adaptive model that will be used in controlling the two links planar robot arm (at both

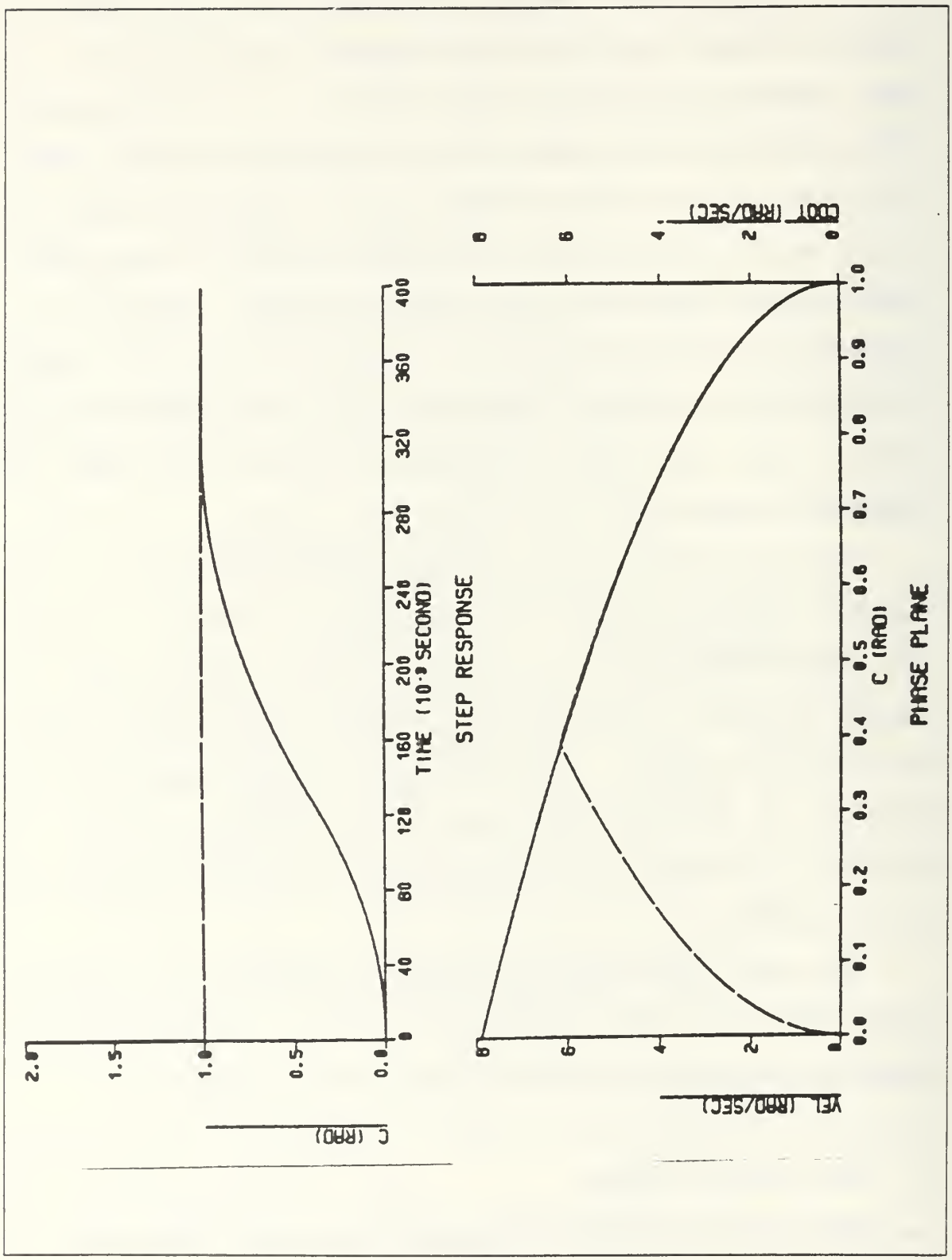

Figure 5.2 Basic model using data corresponding to LINK1 (rigid-rigid case).

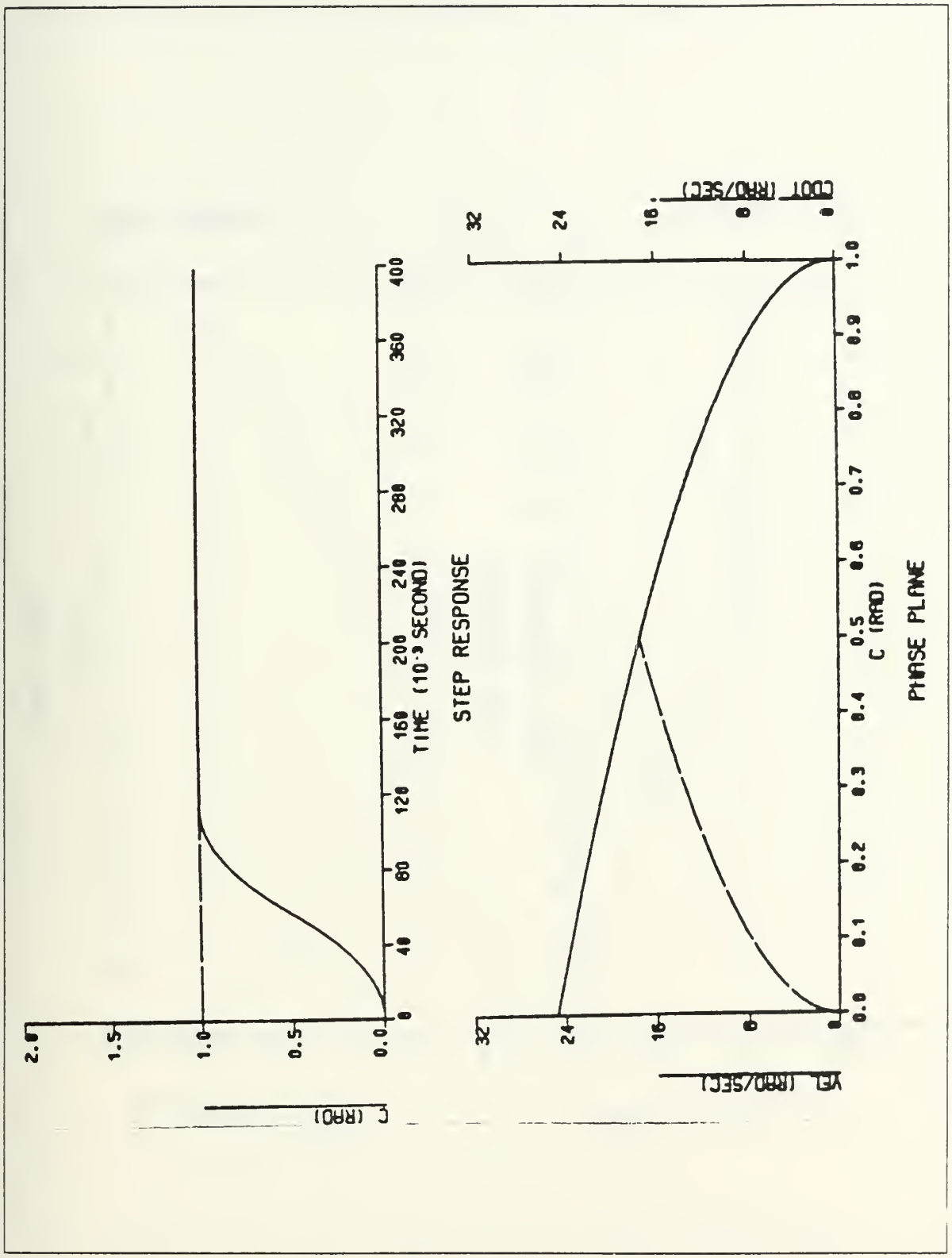

Figure 5.3 Basic model using data corresponding to LINK2 (rigid-rigid case).

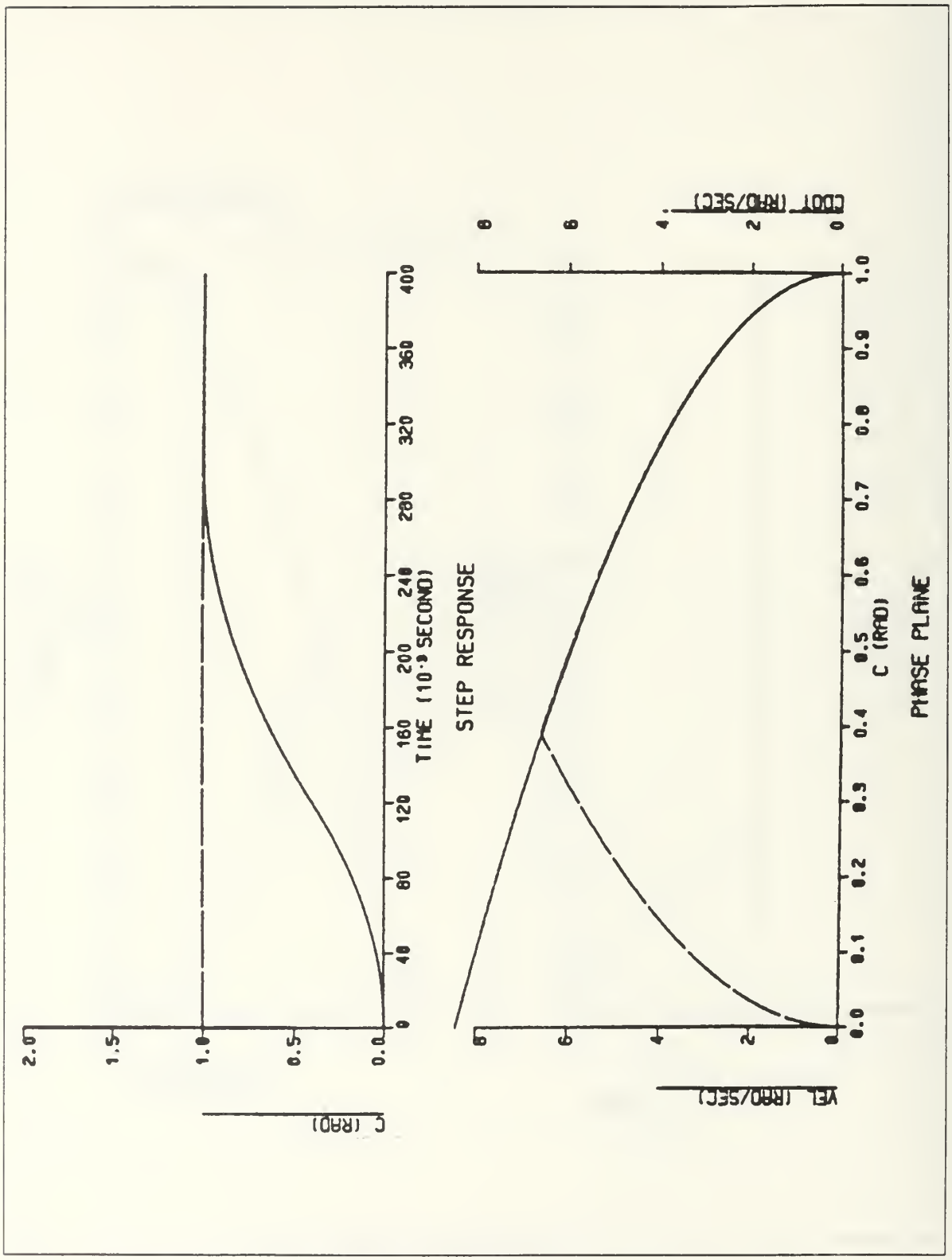

Figure 5.4 Basic model using data corresponding to LINK1 (rigid-flexible case).

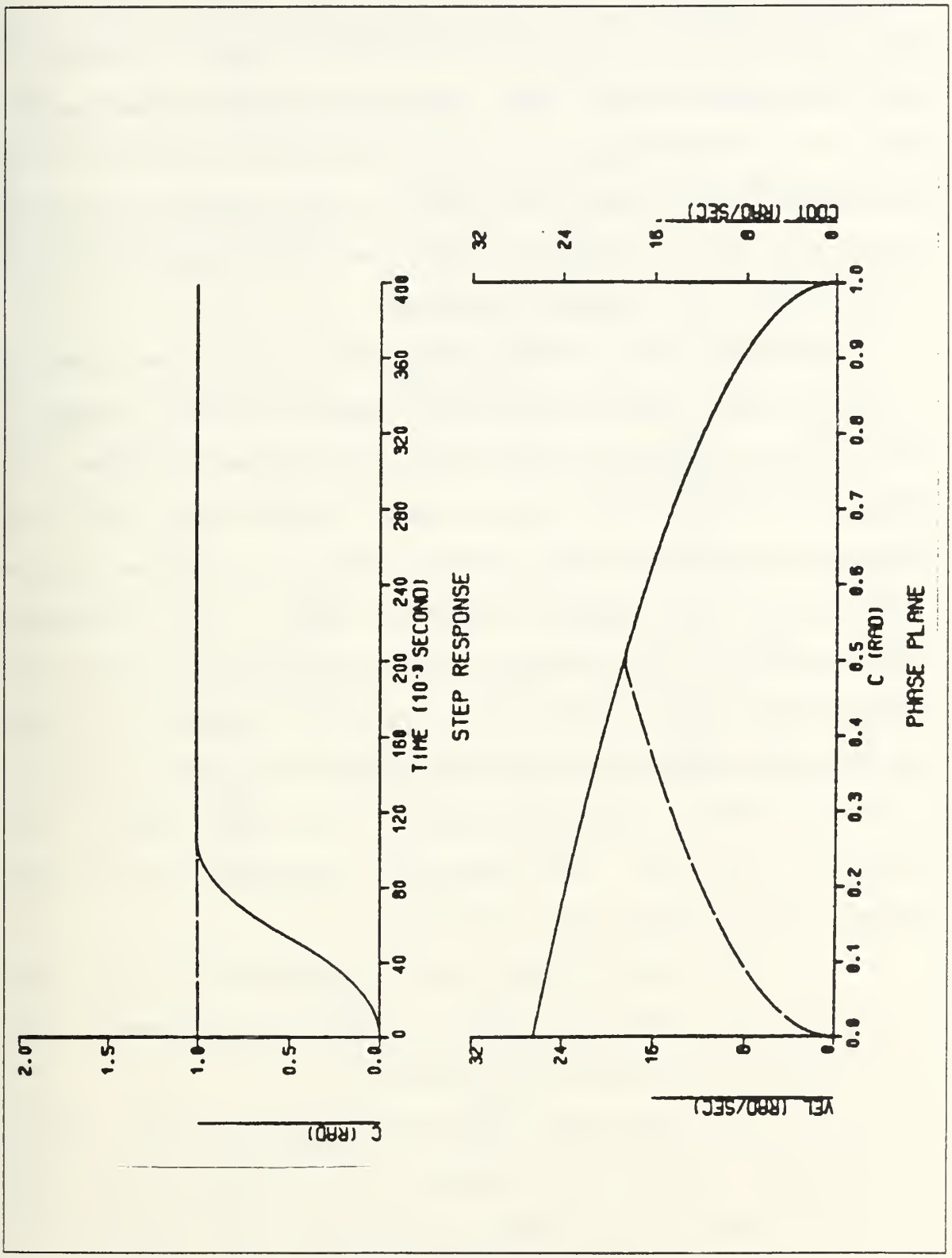

Figure 5.5 Basic model using data corresponding to LINK2 (rigid-flexible case).

cases) is illustrated in Figure 5.6. The output signal from the saturating amplifier of the adaptive model is common to both the second order ideal motor and to the actual system that is a combination of the real motor and the arm of the manipulator. Therefore the control scheme forces the actual system to follow the second order model of the ideal motor which in turn is adaptive in nature.

The angle, TH, of the manipulator's arm is measured at specified time intervals and the resulting value is used in the adaptive algorithm to update the states and the gain constant of the second order model. Figure 5.6 shows that the entire control scheme and the adaptive algorithm can be implemented in a digital computer and the only hardware requirement for the proposed system will be the device that measures the angle of the arm. The gain constant K_m of the second order model has to be adjustable in order to account for the inertia reflected back to the joint due to the motion of the arm. The adaptation algorithm for K_m must satisfy the following two conditions:

1) The calculations must be accurate to allow the states of the second order model to approximate the trajectory of the actual system.

2) The required calculations must be kept simple because K_m must be updated in minimum time and the algorithm has to be easily programmed in a computer.

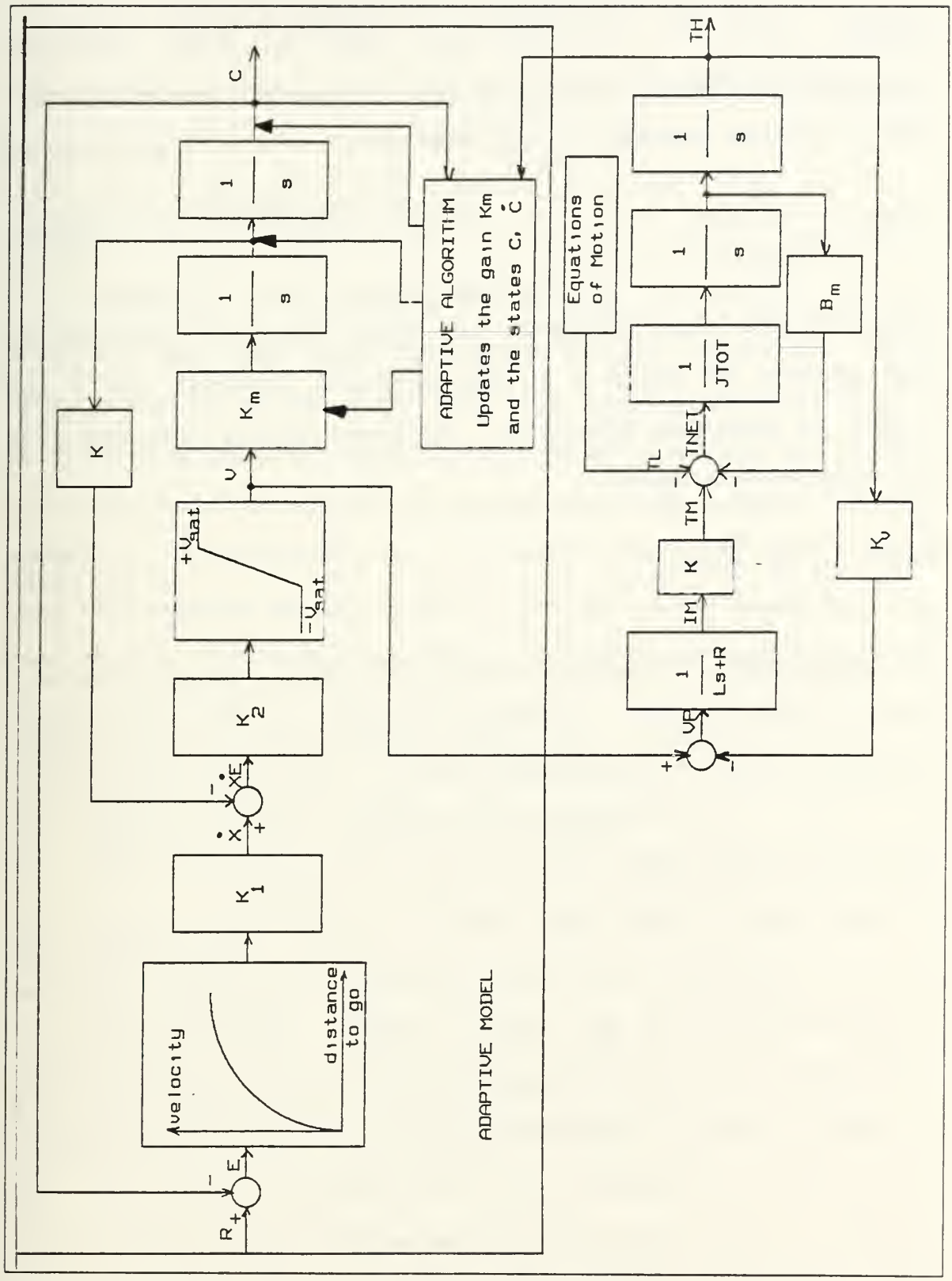

Figure 5.6 Block diagram of the adaptive model.

The method described in Ref 15 satisfies the above stated conditions and will be used in this analysis. Solving Equation 5.3 for K_m, with zero initial conditions, the following expression was obtained:

$$K_m = \frac{2C}{V_{sat}\ t^2} \tag{5.8}$$

For discrete time intervals the time t will be replaced by the product NT where T is the sampling interval and N the number of sampling intervals. By also letting C=TH Equation 5.8 obtains the form:

$$K_m = \frac{2\ TH}{V_{sat}\ (NT)^2} \tag{5.9}$$

Equation 5.9 for K_m is valid only for constant acceleration of the system. Therefore the gain K_m will be updated during the full acceleration mode and until the velocity of the actual motor reaches the velocity curve. During the curve following mode K_m will remain unchanged.

To update the states of the second order model the adaptive algorithm requires the angular position and the angular velocity of the actual system. The actual angular velocity of the system cannot be used and therefore must be estimated from the measured angular position of the system. Therefore the estimation of the angular velocity will be obtained as the derivative of the sampled angular position, that in discrete representation is:

$$\dot{TH}(N) = \frac{2[TH(N)-TH(N-1)]}{T} - \dot{TH}(N-1) \qquad (5.10)$$

where $\dot{TH}(N-1)$ is the last estimation of the angular velocity given from:

$$\dot{TH}(N-1) = \frac{TH(N)- TH(N-2)}{2T} \qquad (5.11)$$

Equation 5.10 requires the storage of the last angular position and the last estimated angular velocity. From Equation 5.11 it is clear that the angular velocity can be estimated after two samples of angular position are taken. Equation 5.10 is not self correcting if the system switches from full acceleration to the curve following mode, until two new samples of the angular position are taken after the switching. To eliminate this problem, the switching time has to be detected and the value of the velocity of the second order model at that time must be stored as $\dot{TH}(N-1)$, in order to be used at the next calculation.

The storage of the data and the required calculations as given in Equations 5.10 and 5.11, and also the required checks can be easily programmed in a microprocessor.

This adaptive model will be used through the end of this thesis at the simulations of the two links planar robot arm, for both the rigid-rigid and the rigid-flexible cases.

VI. SIMULATION OF THE ADAPTIVE MODEL

A. INTRODUCTION

In this Chapter simulation results will be obtained for the two cases, the rigid-rigid and the rigid-flexible, of a two links planar robot arm. The proposed velocity curve follow adaptive control scheme will be investigated for the case of the rigid-flexible two links planar robot arm in order to examine how well it can correspond to the control requirements of the model. The simulation results of each model will be examined in order to obtain the corresponding performance. Finally the performance of the two different models will be compared as well as the equations of motion derived for each model, as given in Chapters II and III respectively.

B. COMPARISON OF THE EQUATIONS OF MOTION

The equations of motion that describe the two models were given as Equations 2.2 and 2.3 in Chapter II for the case of the two rigid links, and as Equations 3.9 - 3.12 in Chapter III for the case of the rigid-flexible two links planar robot arm.

Comparing the two sets of equations one can observe that the second order differential equations obtained by evaluating Lagrange's equation with respect to the generalized coordinates θ_1 and θ_2, are exactly the same for both

cases except that some additional terms are included in the first two equations of motion for the rigid-flexible planar robot arm due to the flexibility of the second link. The number of additional terms is proportional to the number of assumed-modes used to express the elastic motion of the flexible beam. The other terms are identical because they represent the same rigid motion with the elastic motion superimposed this rigid motion, for the case of the rigid-flexible planar robot arm.

In the case of the rigid-flexible planar robot arm n additional second order differential equations will be obtained, by evaluating Lagrange's equation for n generalized coordinates g_i (i=1,2,...,n), in order to model the elastic displacement of the flexible link using n assumed-modes.

C. PLANNING THE SIMULATION STUDIES

The sample motion used to investigate the performance of the two links planar robot arm is depicted in Figure 6.1. The same sample motion was used for both, rigid-rigid and rigid-flexible, combinations of the two links planar robot arm. This sample motion was decided in order to remove as many of the nonlinearities as possible and to investigate the system behavior for possible overloading conditions.

A step input with amplitude 1.0 rad was used to drive the two motors acting on JOINT1 and JOINT2 respectively.

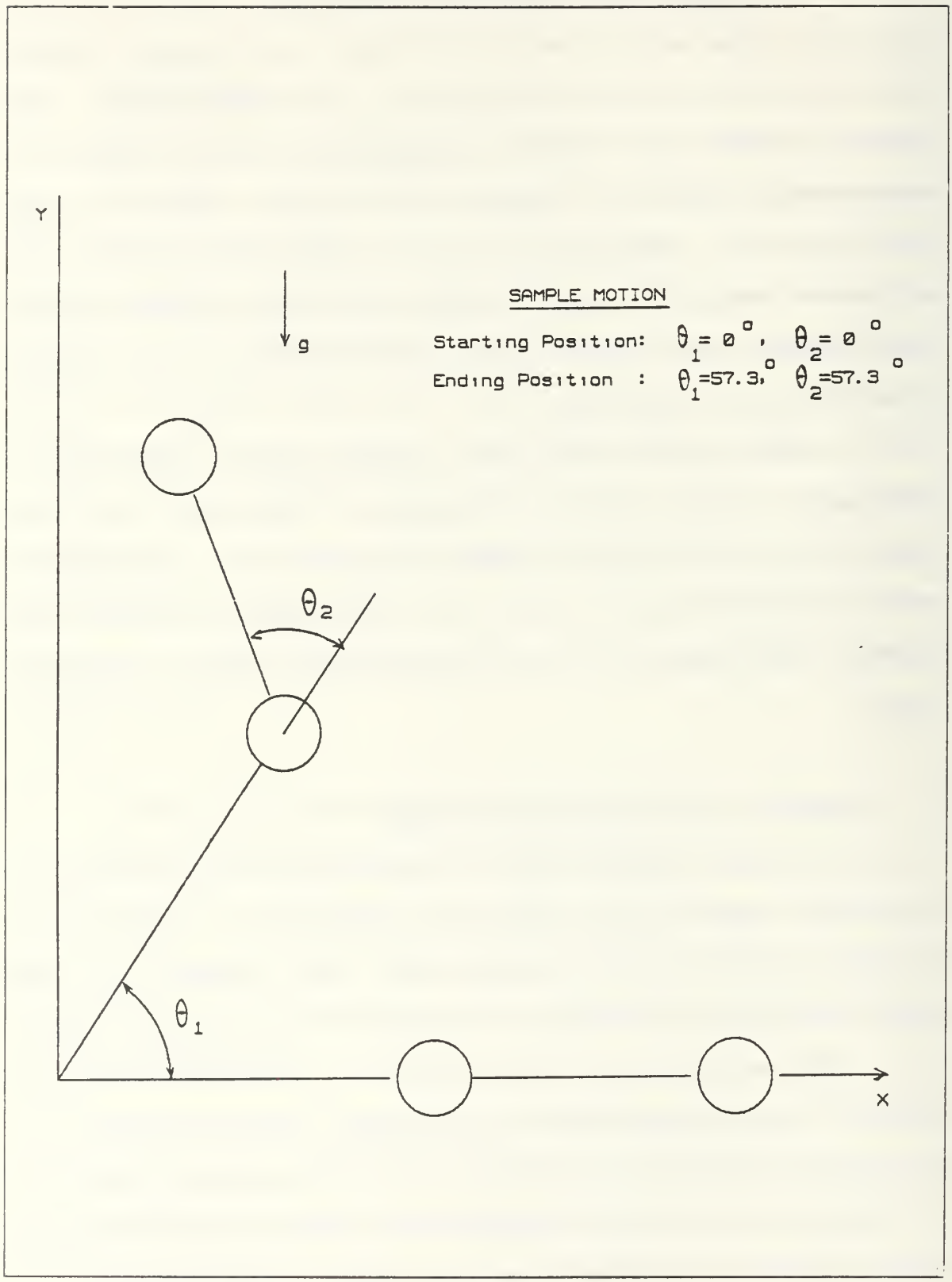

Figure 6.1 Sample motion of the planar robot arm.

In order to have a more complete understanding of the system's performance the sample motion of the two links planar robot arm in the simulation studies will considered with and without load in both gravitational and gravity-free environments. The case where the sample motion will be completed in two successive steps, by first moving only the first link and, when its final position is reached, then moving the second link, will be also investigated in the simulation studies.

First, a complete set of simulation results will be obtained for the case of the two rigid links planar robot arm, with the phase plane and the step response plots given for the two generalized coordinates θ_1 and θ_2 corresponding to the angular position of LINK1 and LINK2 respectively.

Similar studies will investigate the performance of the rigid-flexible planar robot arm, with plots giving the end-point displacement as well as the phase plane and the step response plots for each of the two angles θ_1 and θ_2 of the hypothetical rigid motion.

D. SIMULATION OF THE RIGID-RIGID PLANAR ROBOT ARM.

The simulation results for the two rigid links planar robot arm are given in Figures 6.2 - 6.13.

Figures 6.2 and 6.3 are the phase plane and the step response respectively of the unloaded arm in a gravitational environment. Considering a load, equal to the mass of the

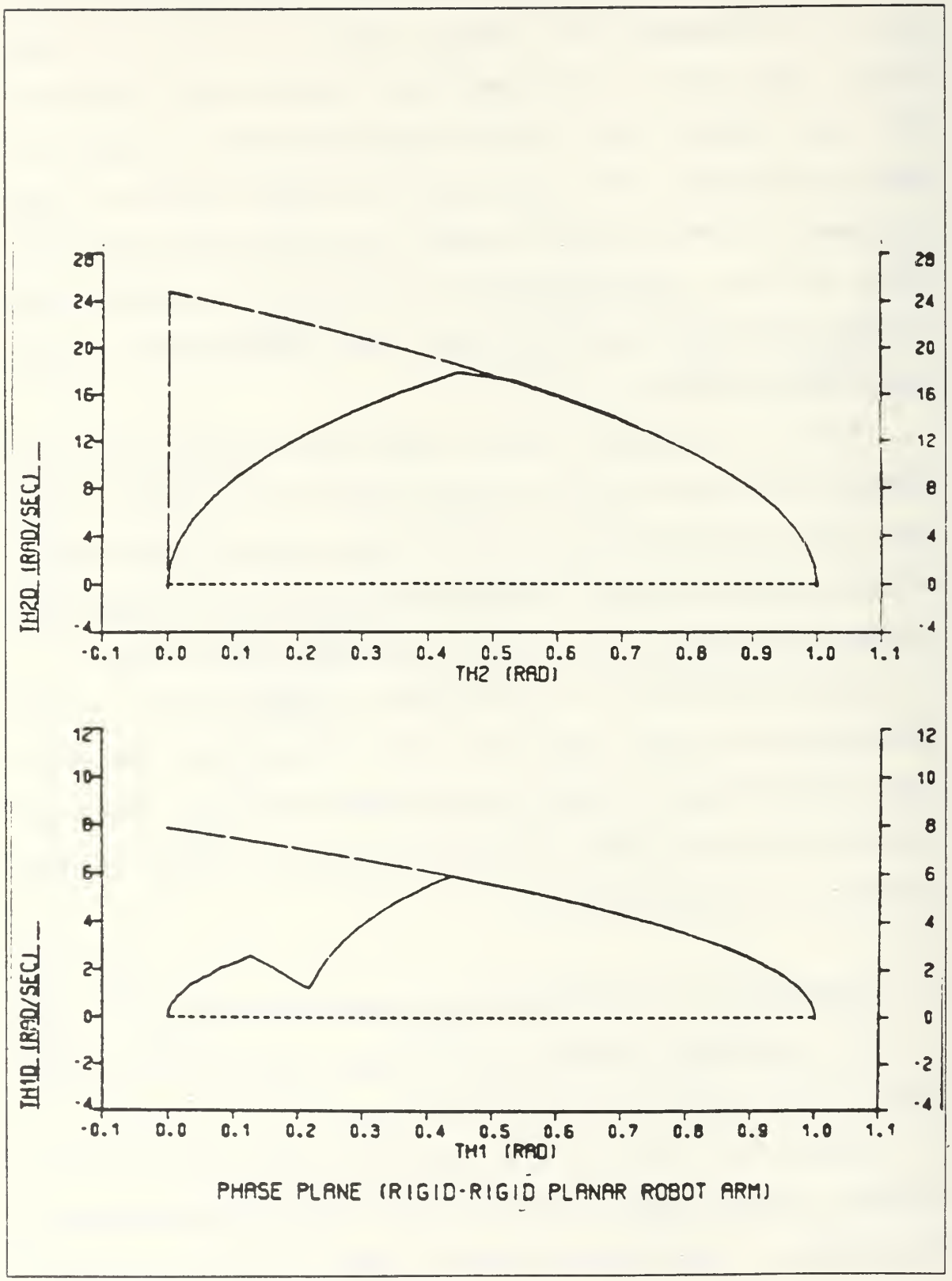

Figure 6.2 Rigid-rigid planar robot arm, Phase plane.

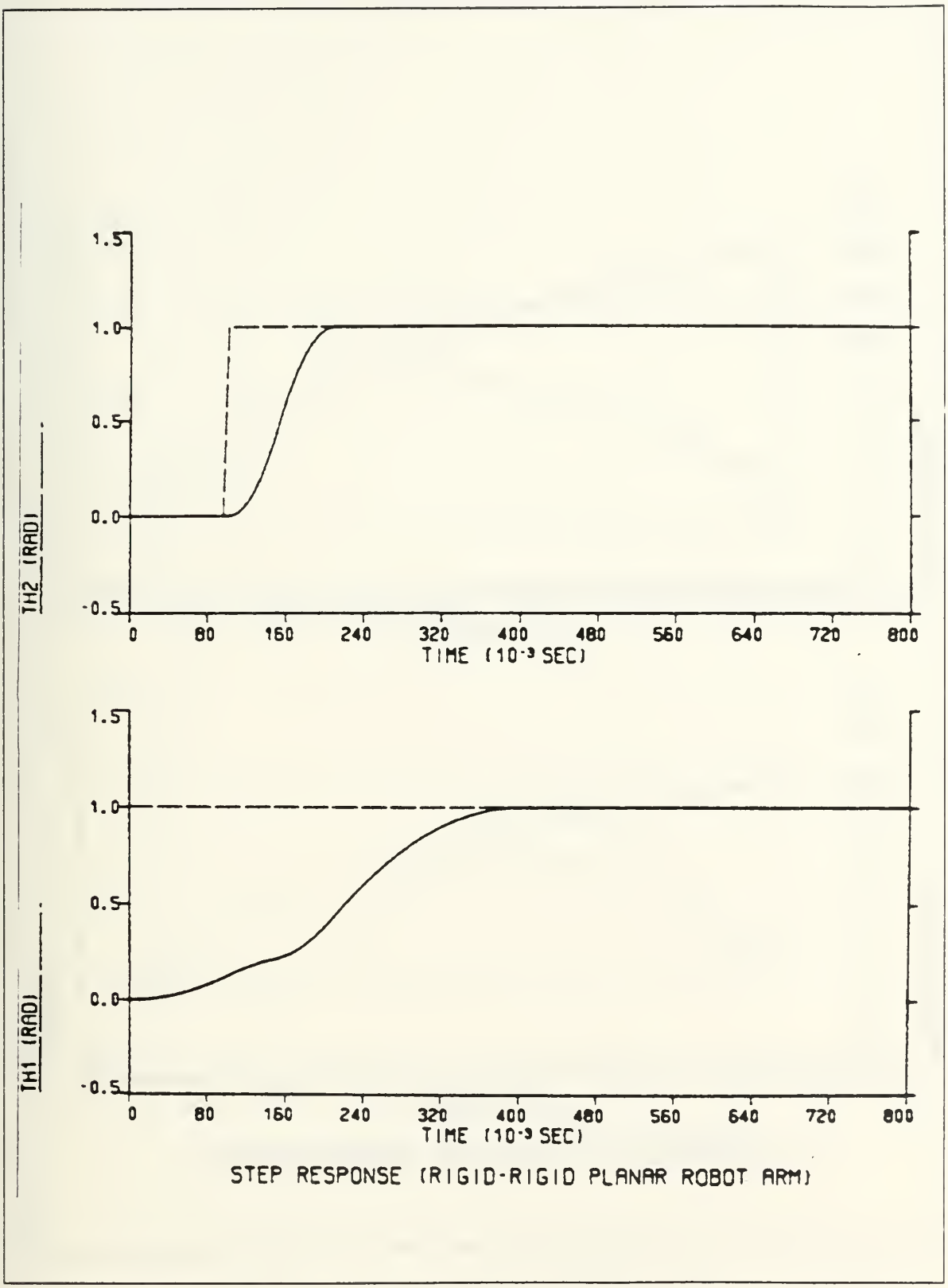

Figure 6.3 Rigid-rigid planar robot arm, Step response.

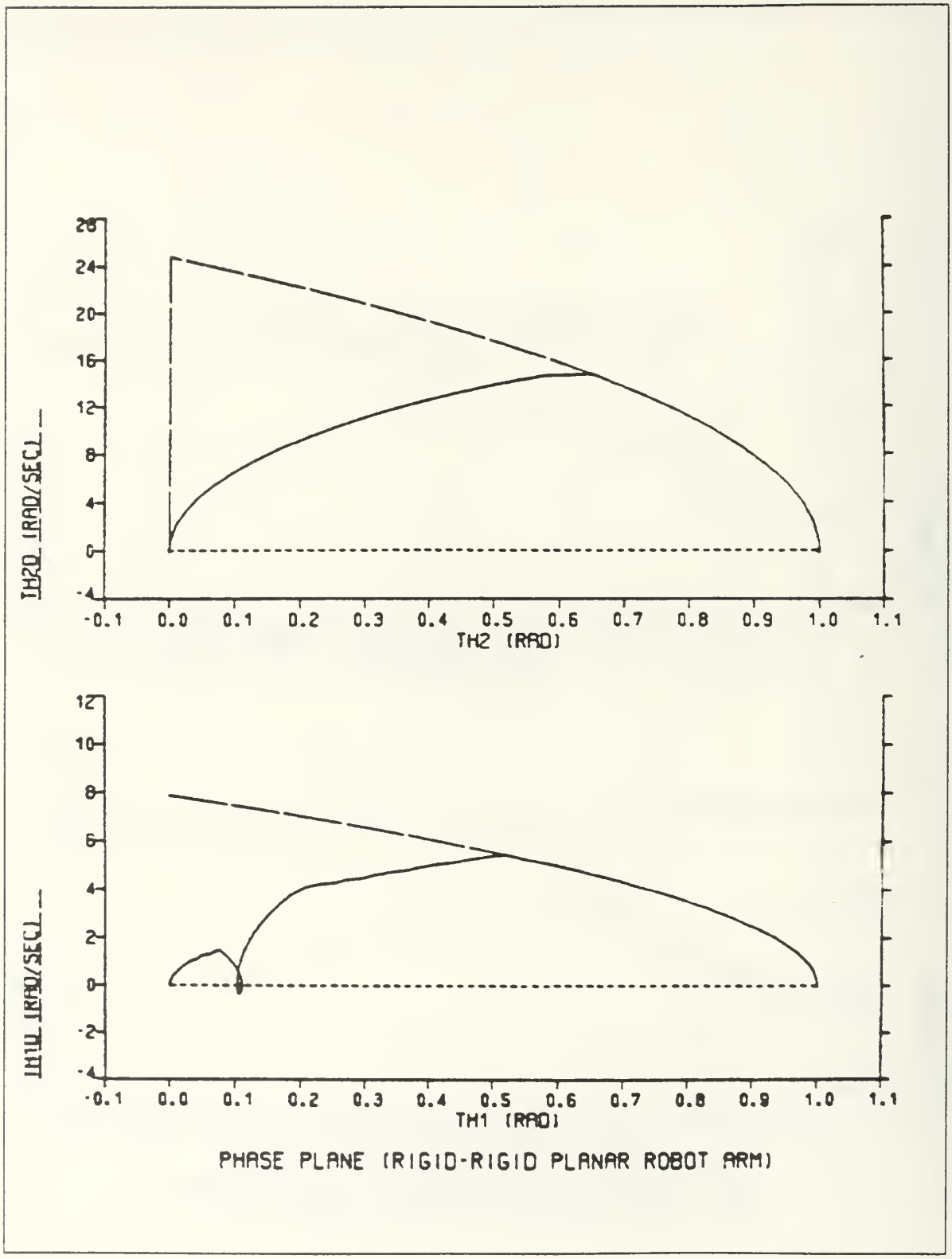

Figure 6.4 Rigid-rigid planar robot arm, Phase plane (arm loaded).

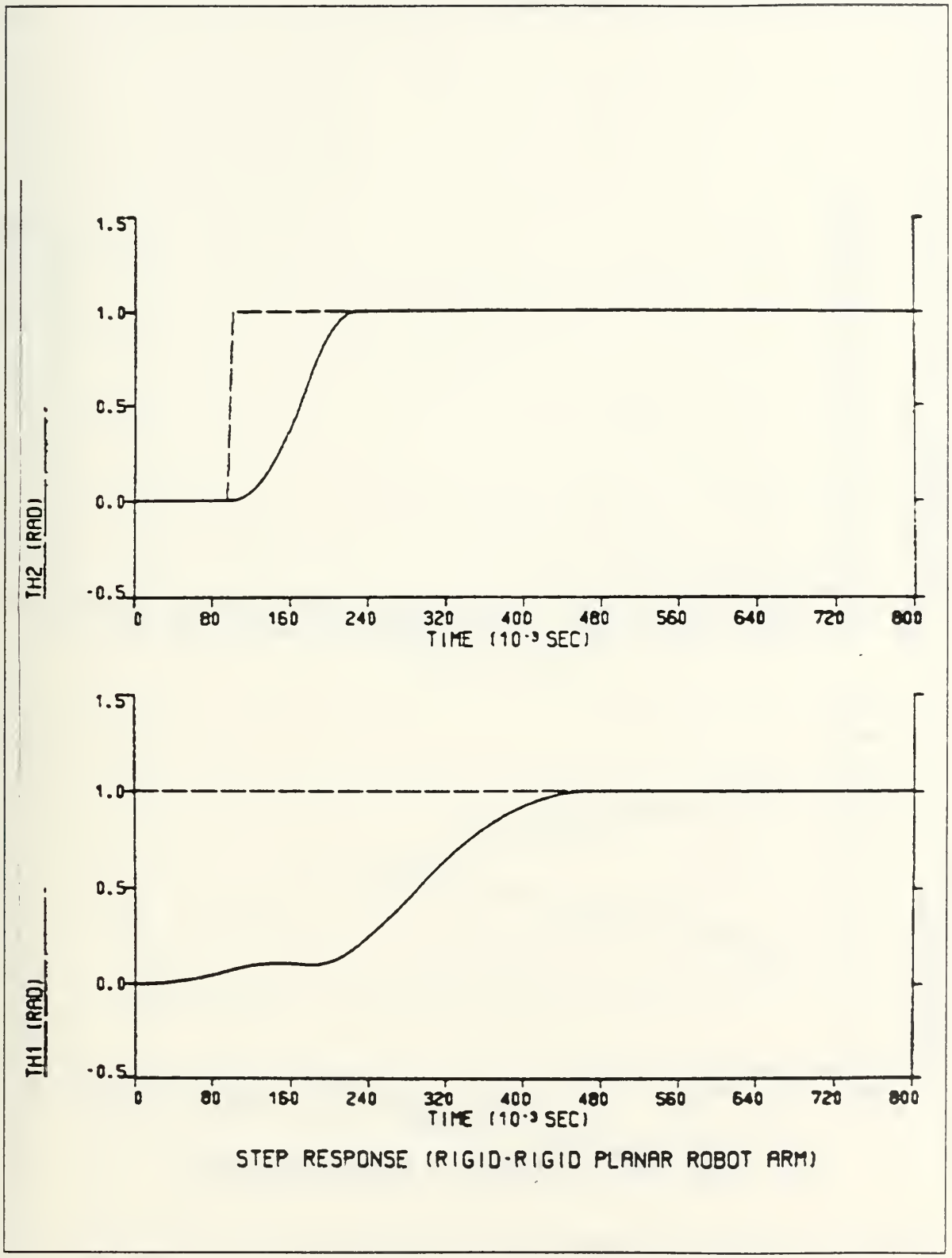

Figure 6.5 Rigid-rigid planar robot arm, Step response (arm loaded).

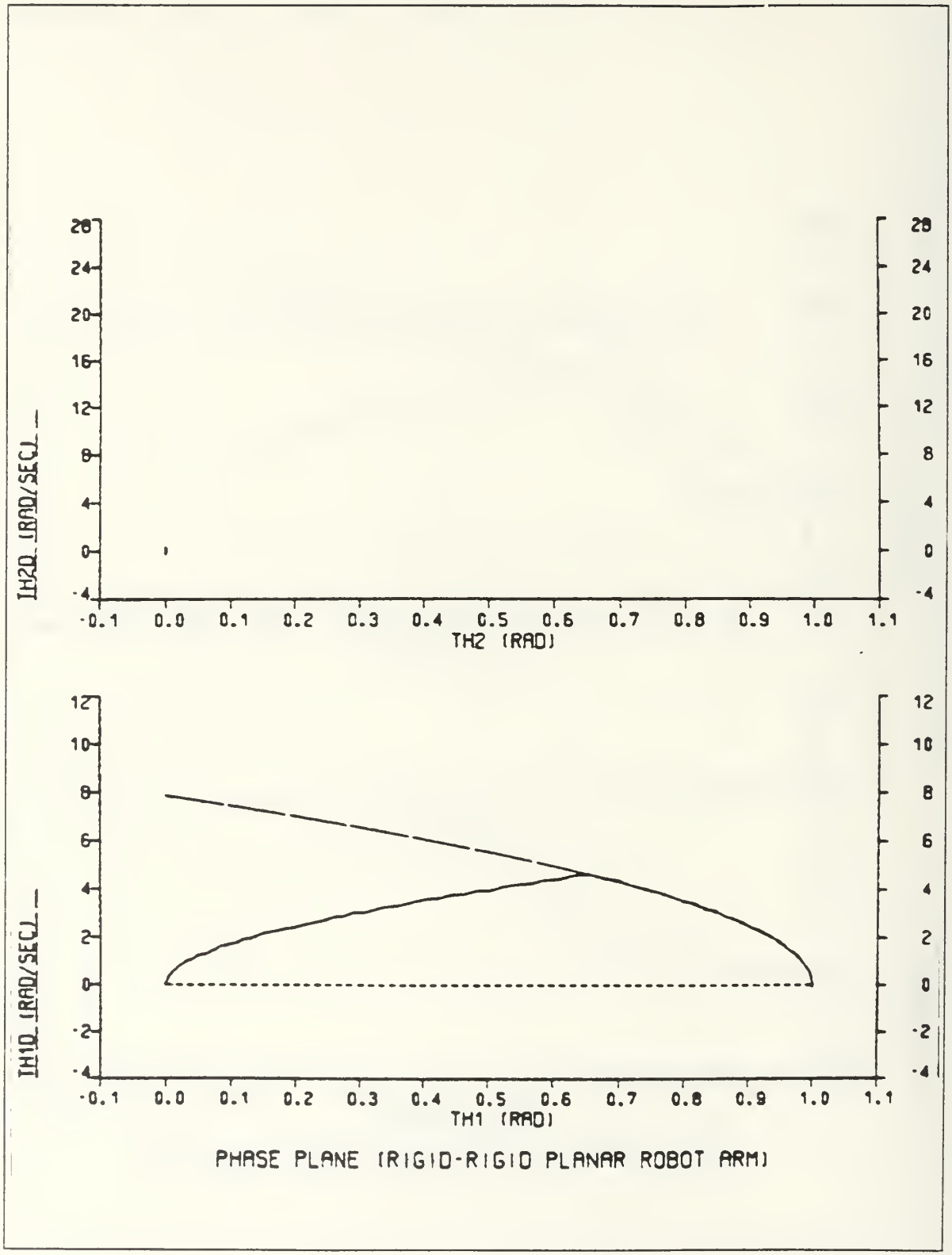

Figure 6.6 Rigid-rigid planar robot arm, Phase plane when moving only LINK1 (arm loaded).

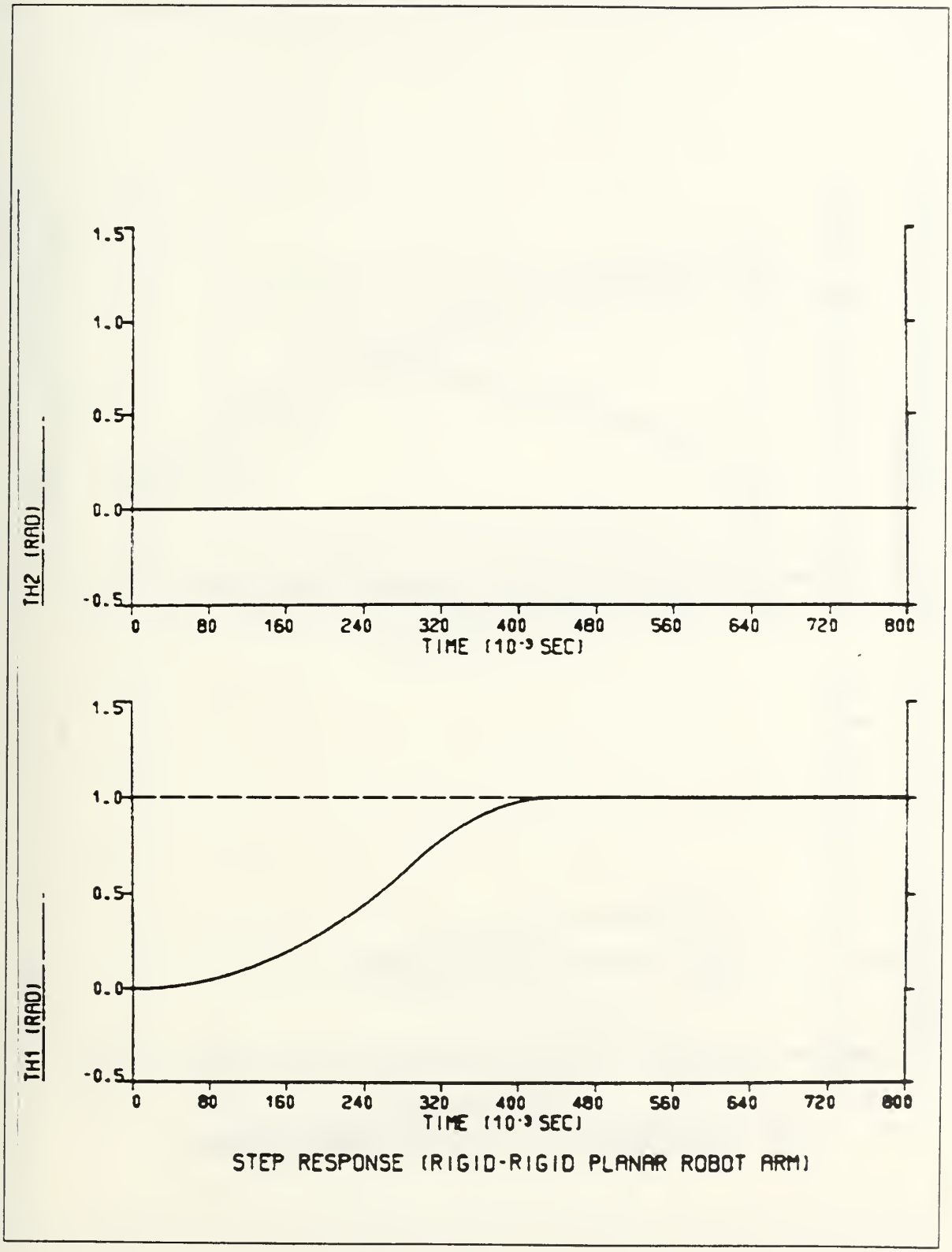

Figure 6.7 Rigid-rigid planar robot arm, Step response when moving only LINK1 (arm loaded).

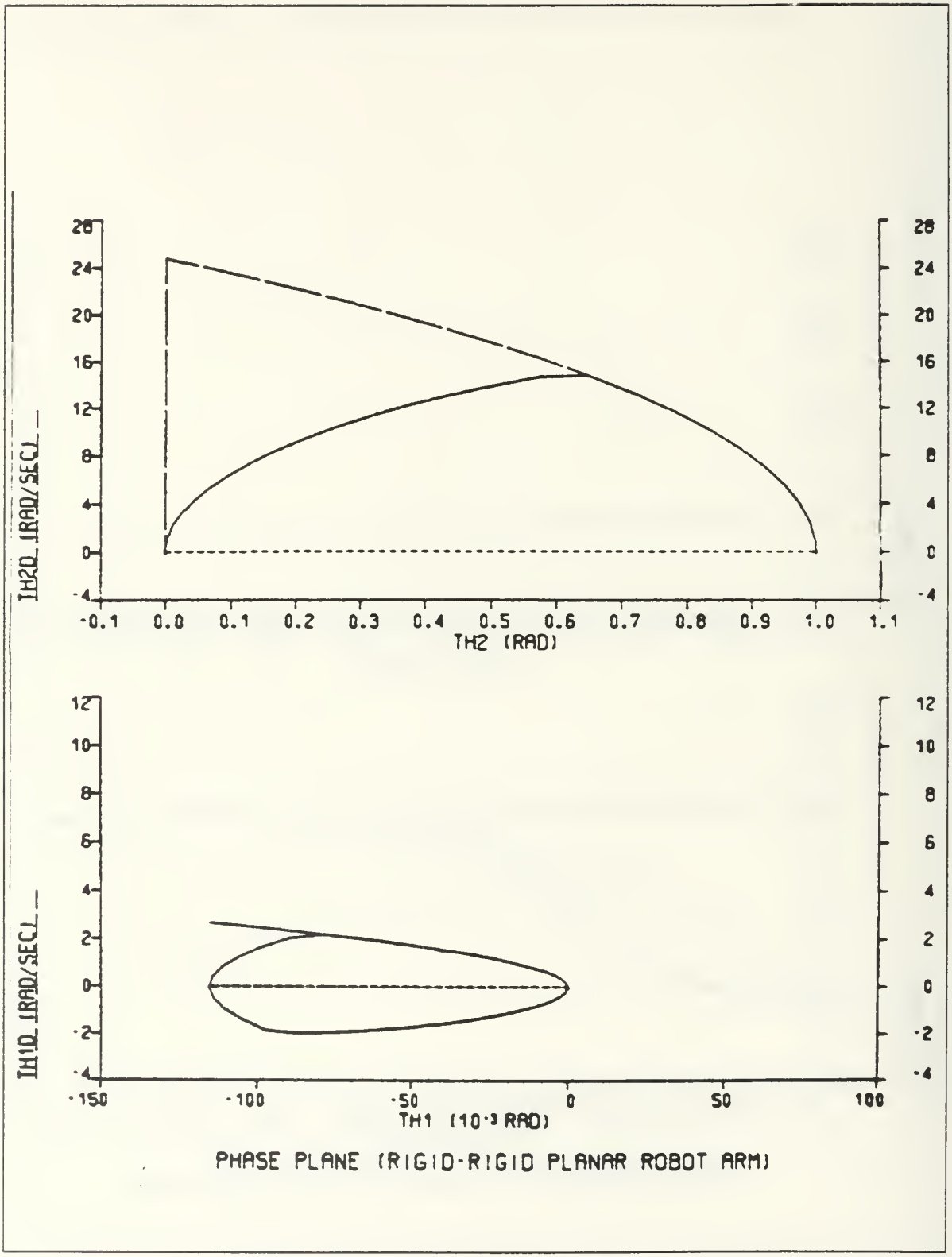

Figure 6.8 Rigid-rigid planar robot arm, Phase plane when moving only LINK2 (arm loaded).

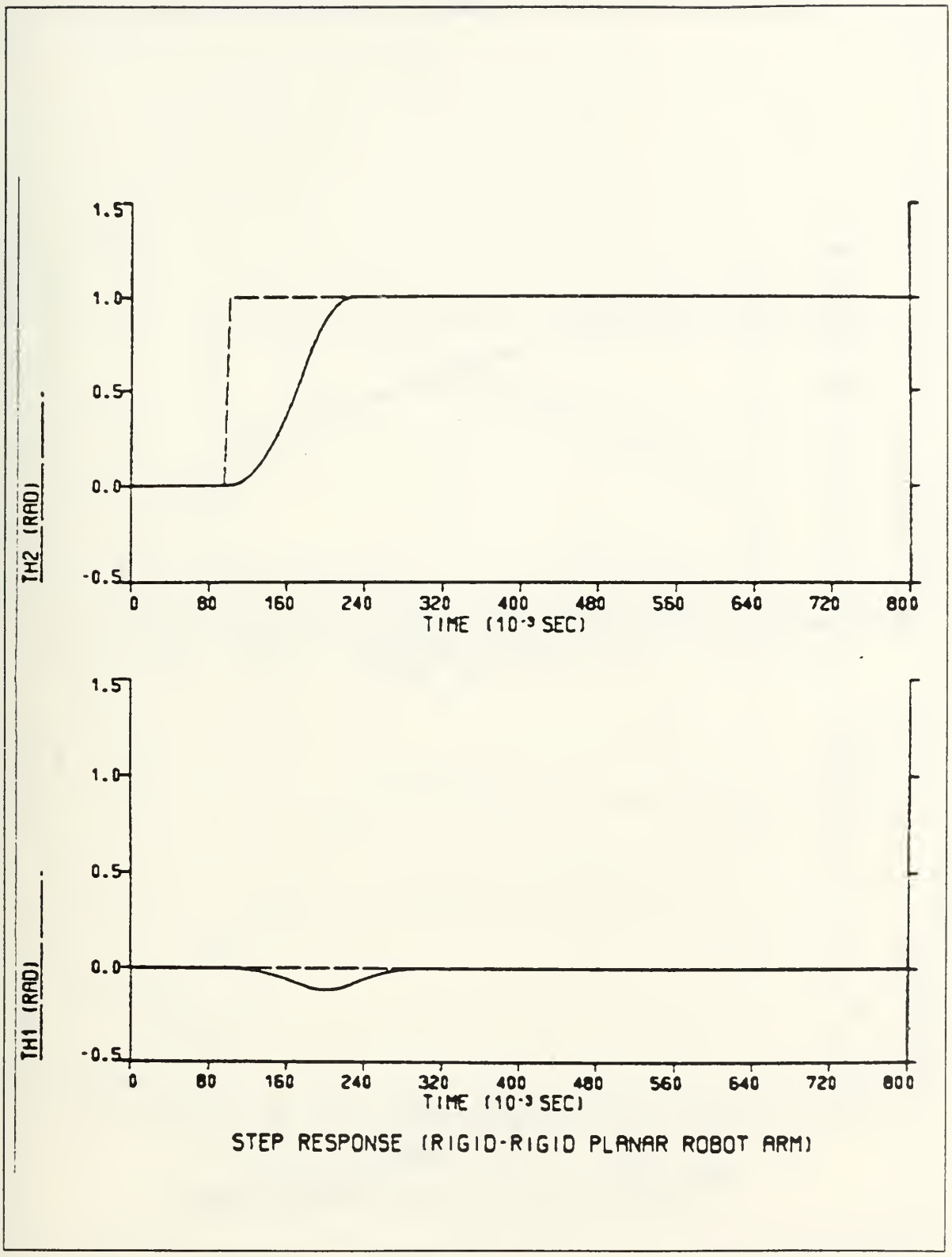

Figure 6.9 Rigid-rigid planar robot arm, Step response when moving only LINK2 (arm loaded).

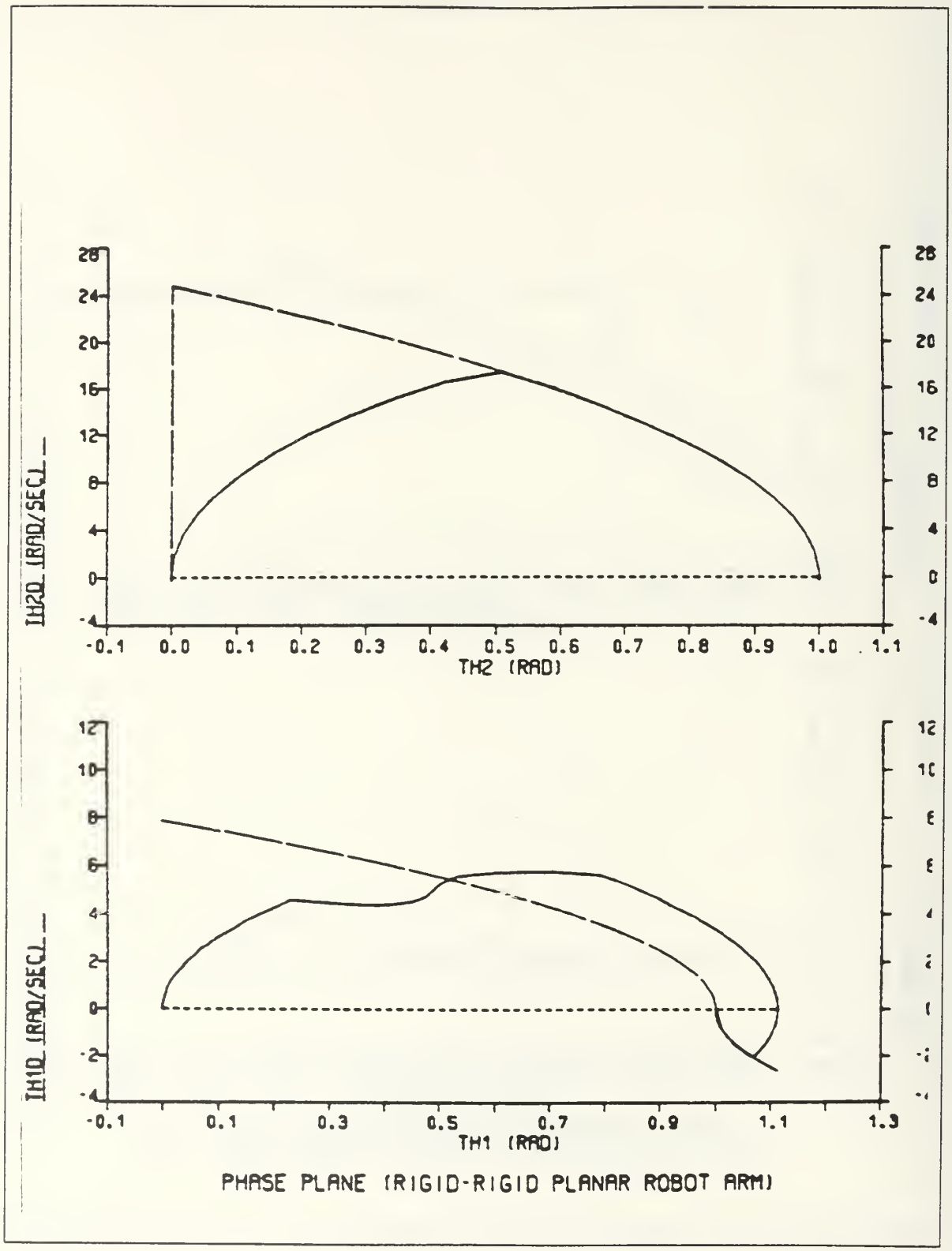

Figure 6.10 Rigid-rigid planar robot arm, Phase plane (gravitational-free environment).

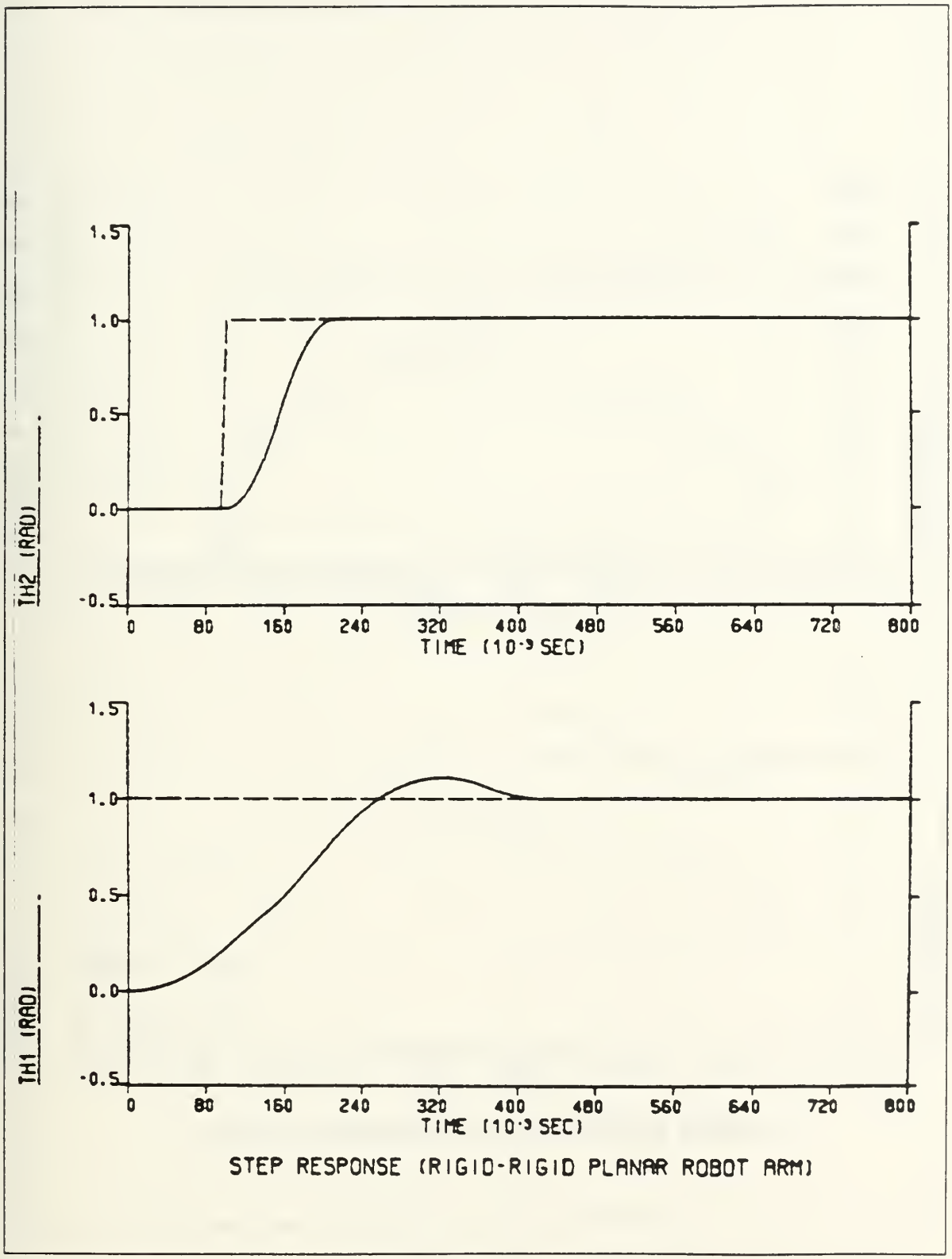

Figure 6.11 Rigid-rigid planar robot arm, Step response (gravitational-free environment).

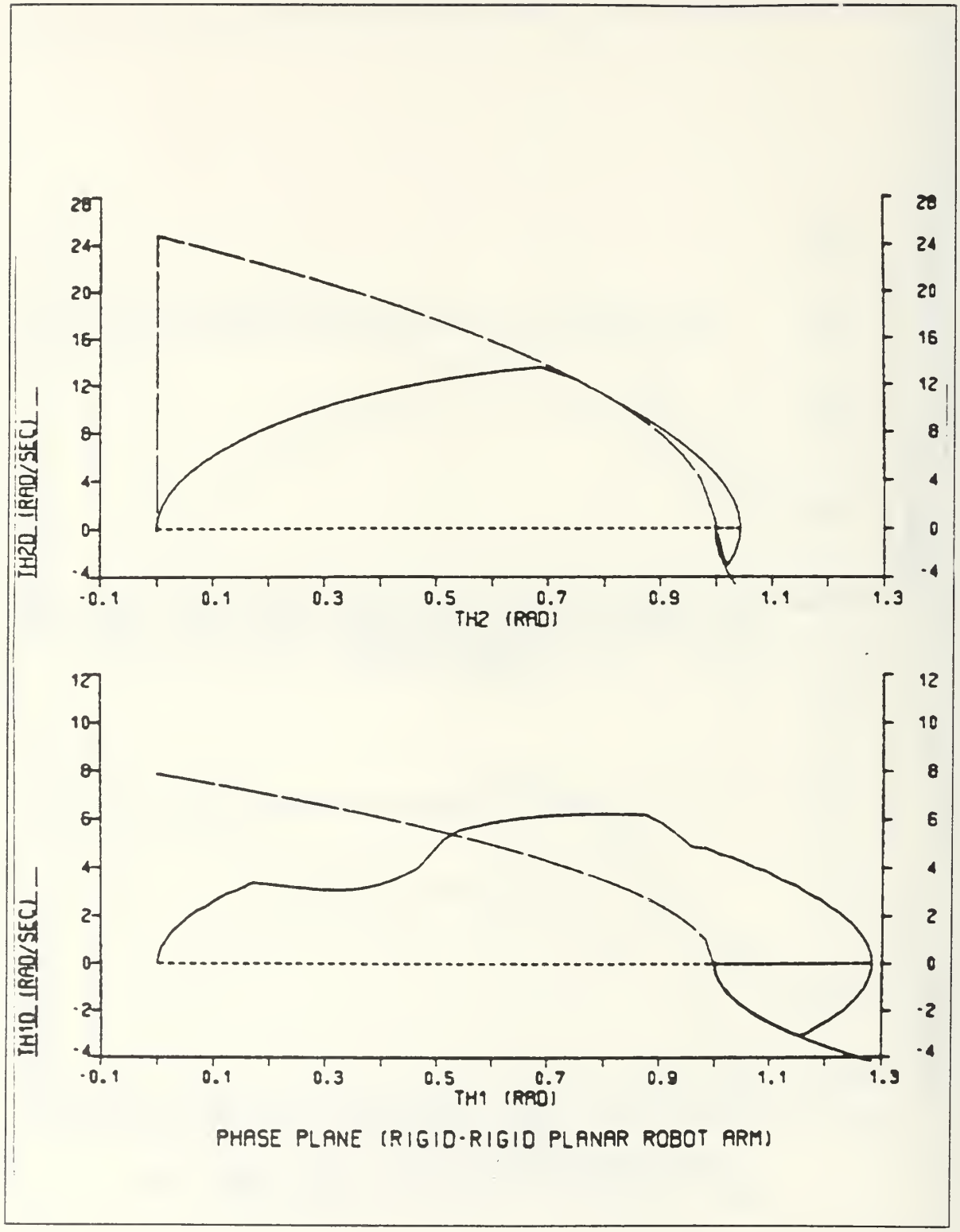

Figure 6.12 Rigid-rigid planar robot arm, Phase plane (arm loaded, not including the gravitational forces).

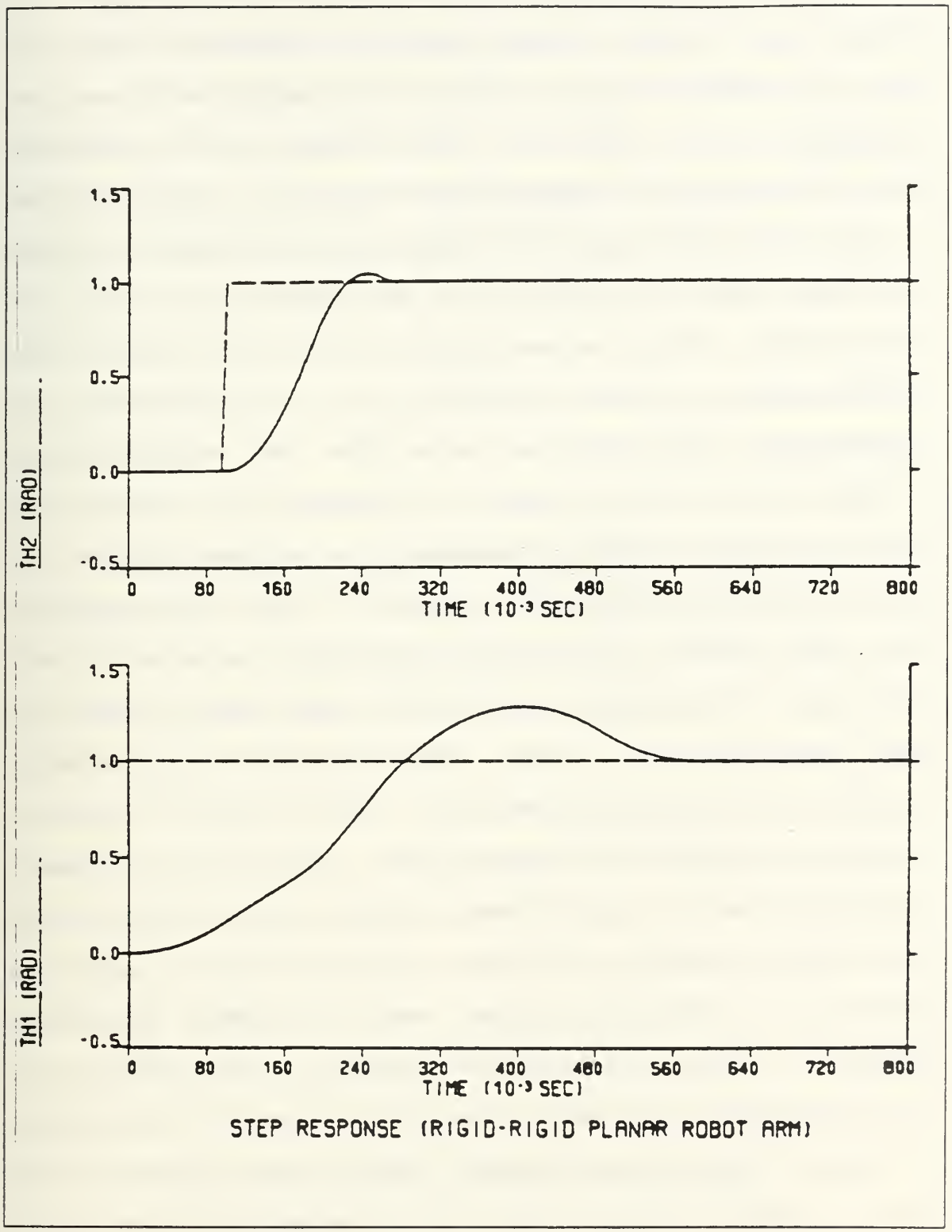

Figure 6.13 Rigid-rigid planar robot arm, Step response (arm loaded,not including the gravitational forces).

second arm, to be carried from the manipulator the resulting phase plane and step response plots are shown in Figures 6.4 and 6.5 respectively. To complete the sample motion in two successive steps, LINK1 is moved first with the resulting phase plane and step response plots shown in Figures 6.6 and 6.7 and then LINK2 is moved having the resulting phase plane and step response plots given in Figures 6.8 and 6.9, respectively. When the sample motion of the two rigid links planar robot arm is considered in a gravitational-free environment, the resulting plots when the manipulator is unloaded are given in Figures 6.10 and 6.11. Figures 6.12 and 6.13 are the plots corresponding to a loaded manipulator in a gravitational-free environment. In the gravitational-free environment cases small overshoots occured in the response of the angular position for both links, especially with the manipulator loaded. The reason for these effects is that the motors were selected with parametric values to satisfy a gravitational environment. Therefore the motors overdrive when no gravitational forces are included in the equations of motion. The two links accelerate past the deceleration curve which then cannot slow down the system enough to stop at the desired position. This causes the small overshoots to appear. The step response of the system for any of the above situations confirm that the use of the velocity curve follow as the control scheme of a two rigid links robot arm results to a near minimum time response.

E. SIMULATION OF THE RIGID-FLEXIBLE PLANAR ROBOT ARM.

The model of the rigid-flexible planar robot arm will be tested using the same sample motion. For the particular situation this sample motion represents the hypothetical rigid motion with the elastic motion superposed on this motion. For the case of the rigid-flexible planar robot arm in the simulation results the plots for the flexible motion of the end-point of the flexible beam will be also obtained.

Figures 6.14, 6.15 and 6.16 illustrate the phase plane, step response and elastic motion of the end-point respectively for the case of the rigid-flexible planar robot arm in a gravitational environment with the manipulator not carrying any load. The plots demonstrate that the proposed velocity curve follow control scheme is fully applicable with the system of a planar robot arm having a rigid first link and a flexible second link. The resulting plots indicate a good overall system performance with the hypothetical rigid motion being completed in near minimum time. The elastic motion of the flexible beam has no effect in the response of the first link, that actually is smoother due to a lighter second link as compared to the two rigid links case. The motion produces a very small overshoot, less then 2%, in the response of the flexible link. The response of the overall system is of course much slower due to the settling time required for the elastic motion of the flexible beam.

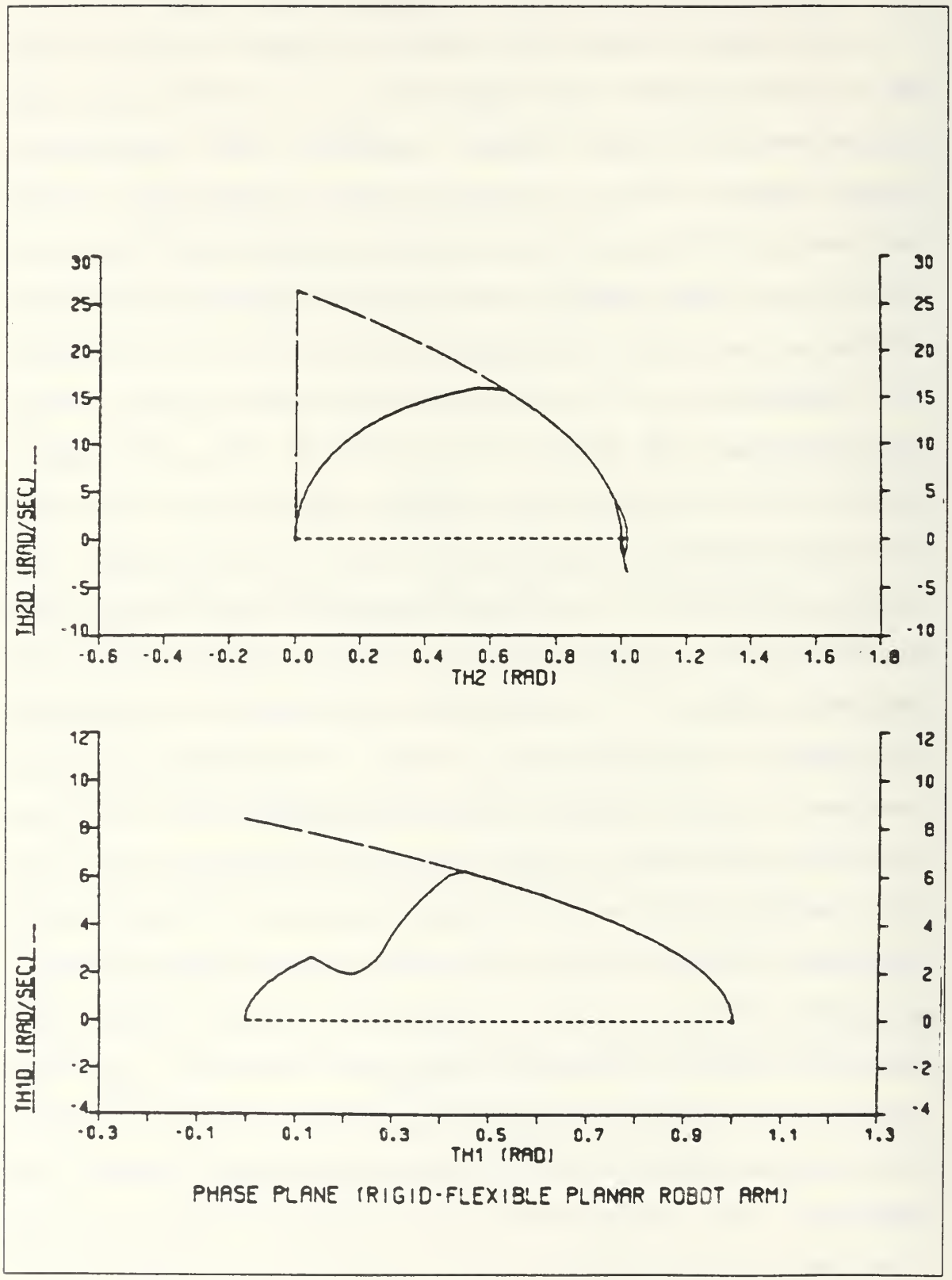

Figure 6.14 Rigid-flexible planar robot arm, Phase plane.

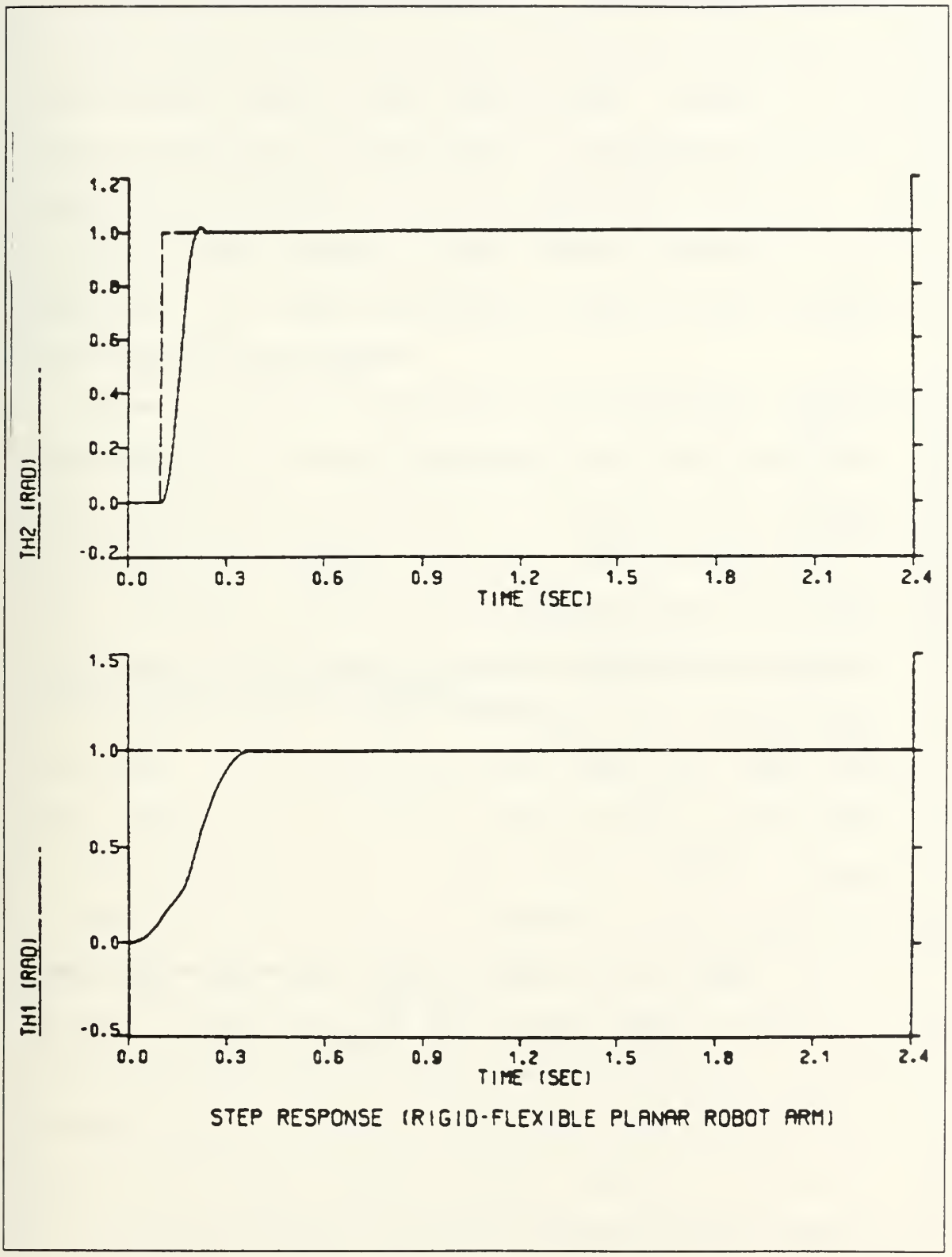

Figure 6.15 Rigid-flexible planar robot arm, Step response.

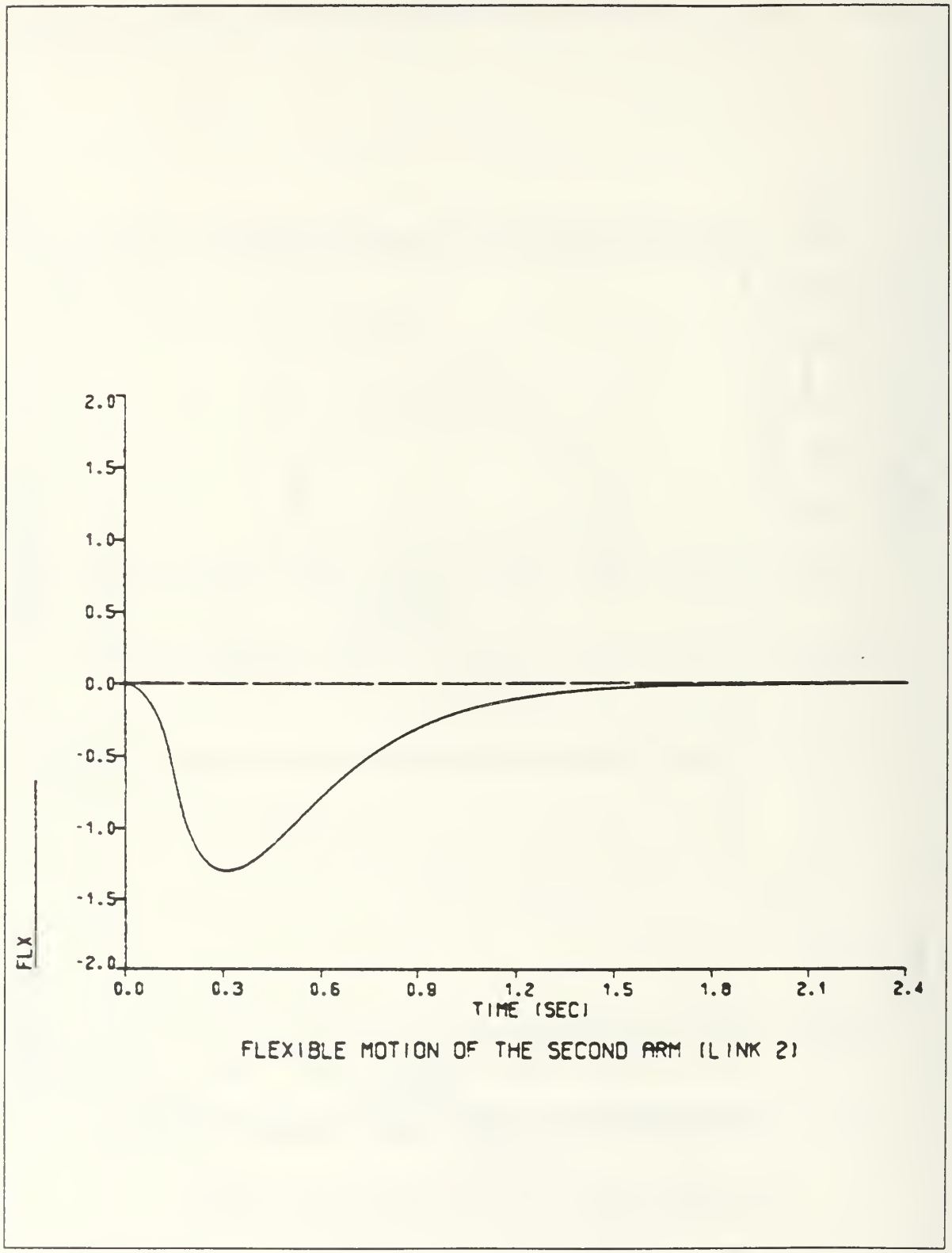

Figure 6.16 Rigid-flexible planar robot arm, Elastic motion of the end-point.

Due to the flexible motion of the end-point this time is approximately 1.5 sec, which is about 5 times more then the required time for the rigid motion. Figure 6.16 shows that the end-point is displayed in a negative direction with respect to the center line of an equivalent rigid arm. This is due to the bending of the flexible arm as it is accelerated. No other vibrations occur in the response of the flexible displacement.

When a load is carried by the manipulator the simulation results are given in Figures 6.16, 6.17 and 6.18. The load carried by the manipulator is equal to the load used in the simulation studies of the two rigid links planar robot arm, resulting a load that is approximately 50% more then the weight of the flexible link. Therefore in the case of the rigid-flexible planar robot arm the payload will be increased. The resulting phase plane and step response plots indicate some vibration modes acting on the system due to the increased weight of the flexible beam. The effects of these vibrations are more apparent in the response of the flexible beam where they cause some overshoots to occur. Because of the nature of the system, the overshoots in the response of the flexible beam are not constant in frequency and amplitude. The reason for this is the several vibration modes, due to the elastic motion, acting on the system and the coupling effects of the two arms during the hypothetical rigid motion of the system.

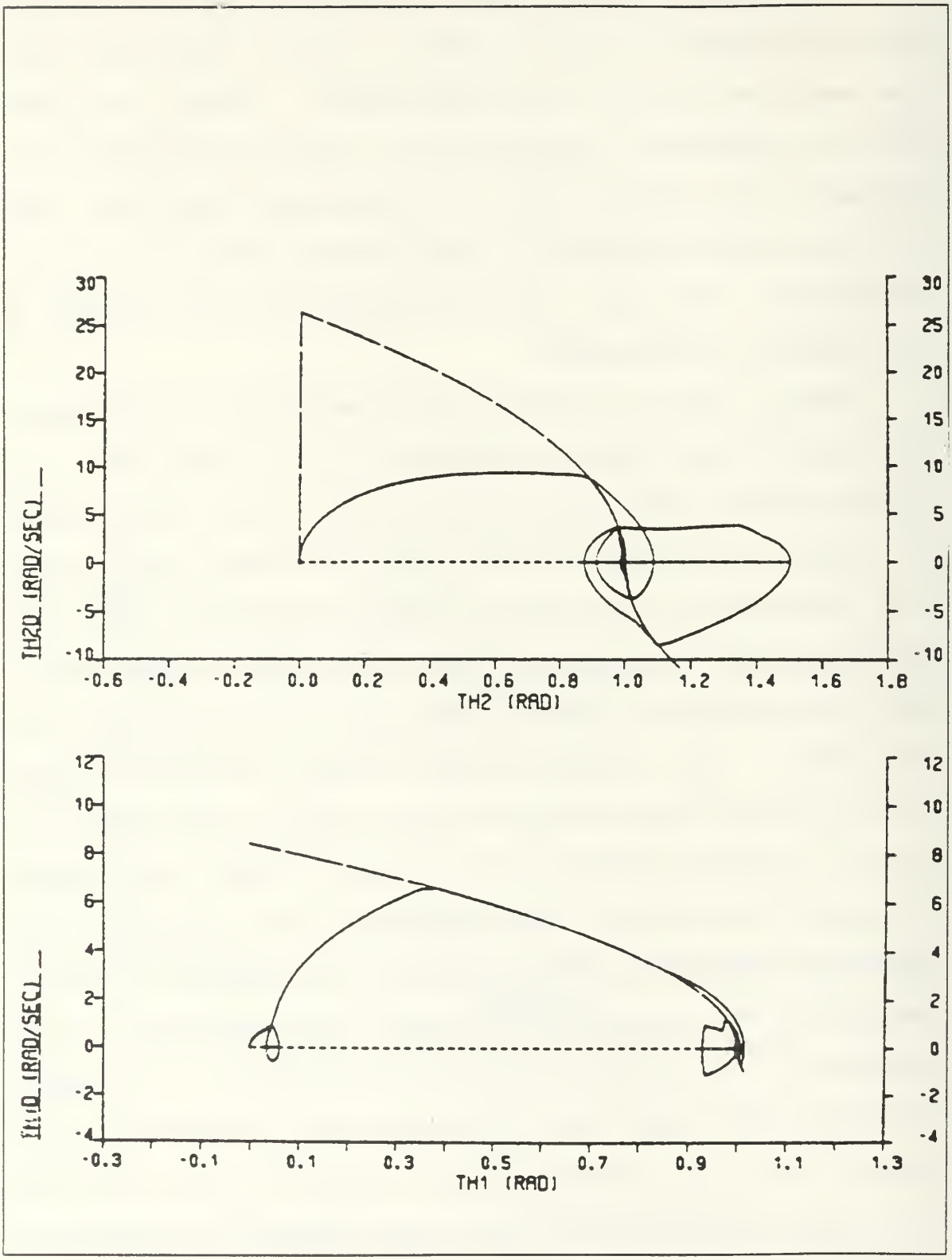

Figure 6.17 Rigid-flexible planar robot arm, Phase plane (arm loaded).

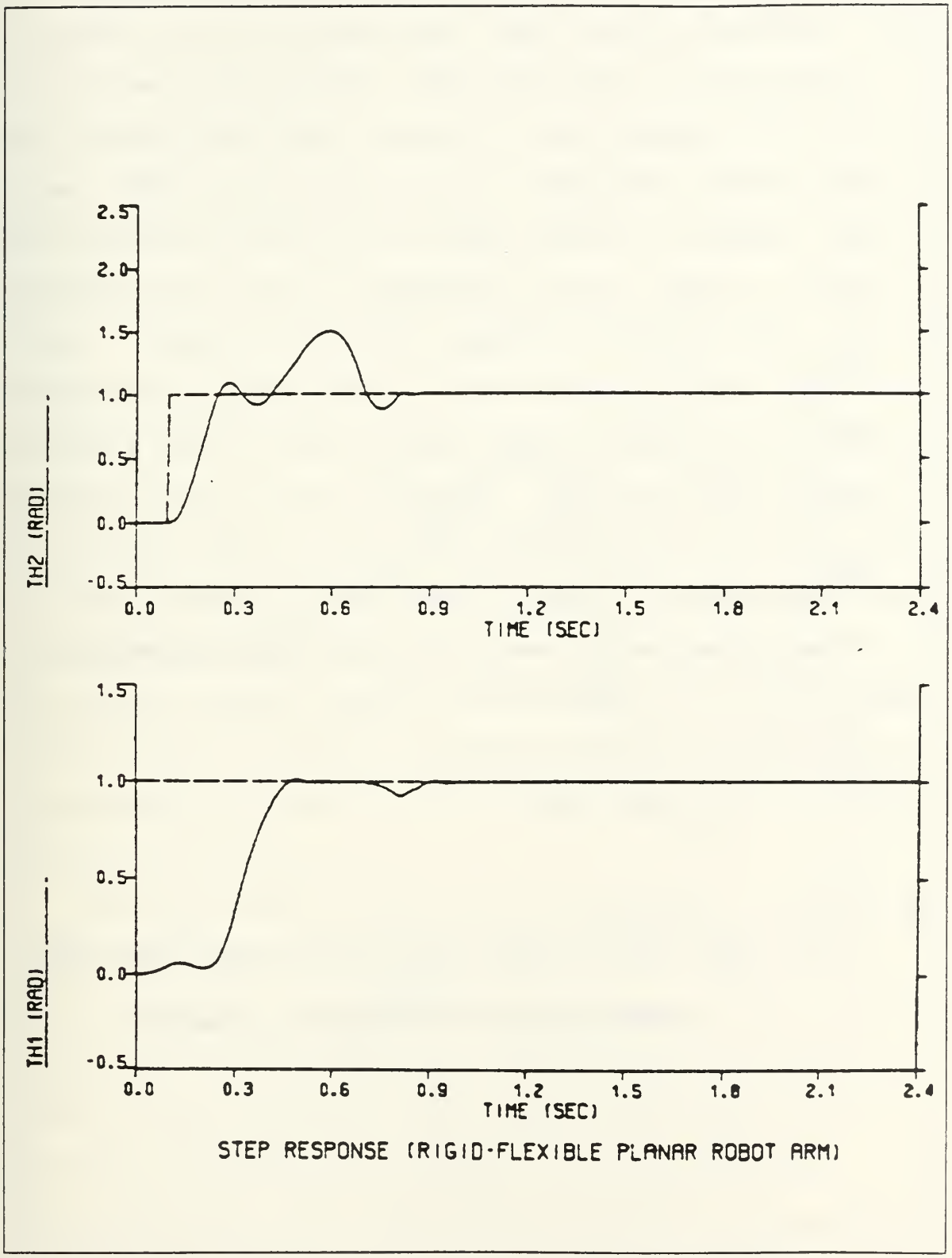

Figure 6.18 Rigid-flexible planar robot arm, Step response (arm loaded).

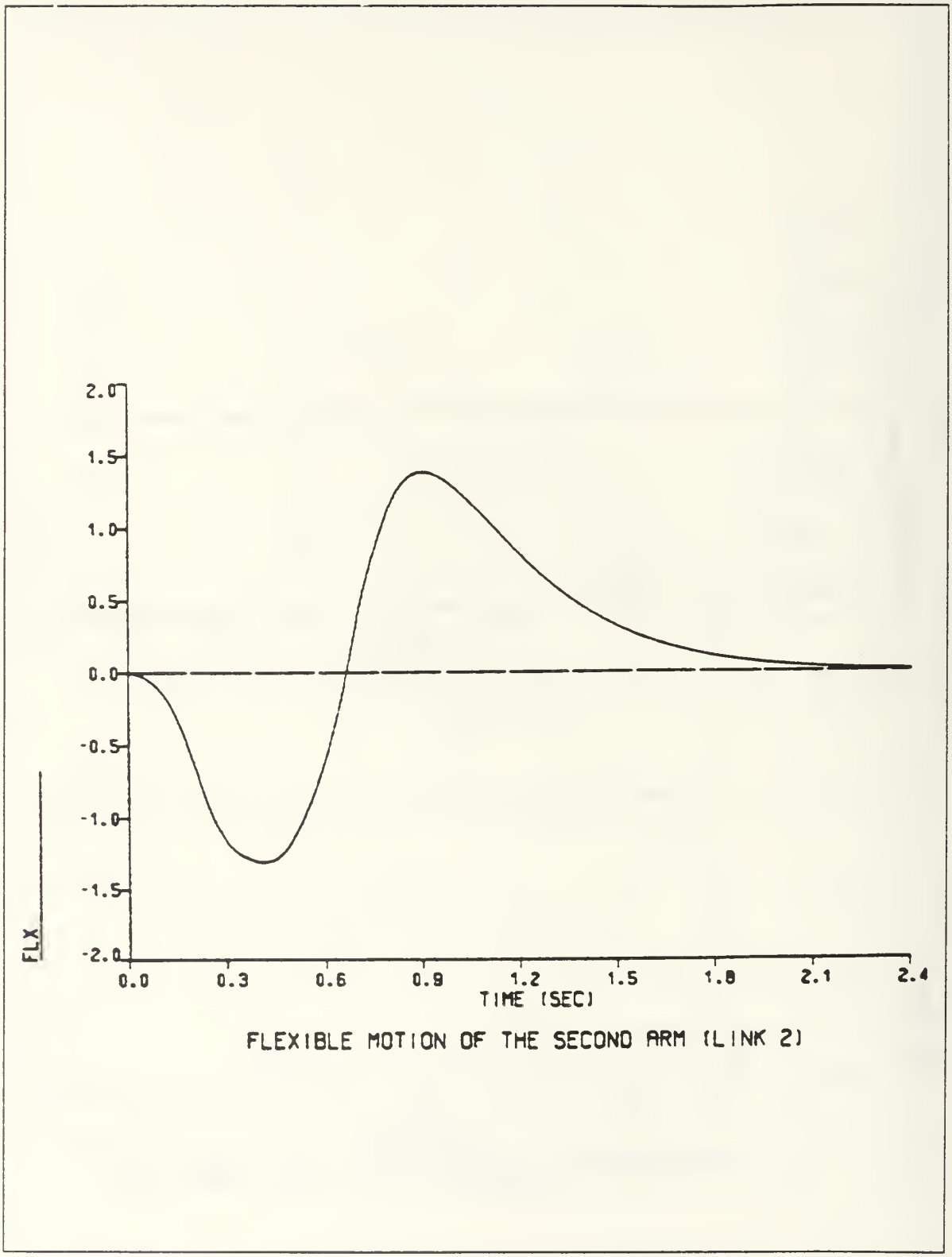

Figure 6.19 Rigid-flexible planar robot arm, Elastic motion of the end-point (arm loaded).

These coupling effects are also indicated in the response of the rigid arm, where some vibrations exist having small amplitudes. The vibrations of the flexible arm are coupled into the rigid arm and increase its settling time. When the flexible arm is loaded the settling time of the rigid arm is about 1.0 sec, which is greater then the settling time for an unloaded arm by about a factor of three. This is also the required settling time for the hypothetical rigid motion of the flexible link. The actual settling time of the flexible link is given by the required settling time of the end-point. Thus the settling time of the flexible arm is also increased by the load, which causes its oscillation to last about 2.1 sec. The load also tends to cause the end-point to overshoot the desired position. The total response time of the end-point is 0.6 sec longer when the arm is loaded. The additional time requirement may be acceptable related to the incresed weight of the flexible arm due to the load.

For the sample motion to be completed in successive steps the requested motion for only the rigid arm will be first completed, followed by the movement of the flexible beam. The same results will be obtained by reversing the order of the successive steps, first moving the flexible arm and when its motion is completed moving the rigid arm. The resulting plots are illustrated in Figures 6.20, 6.21 and 6.22 for the phase plane, the step response and the flexible

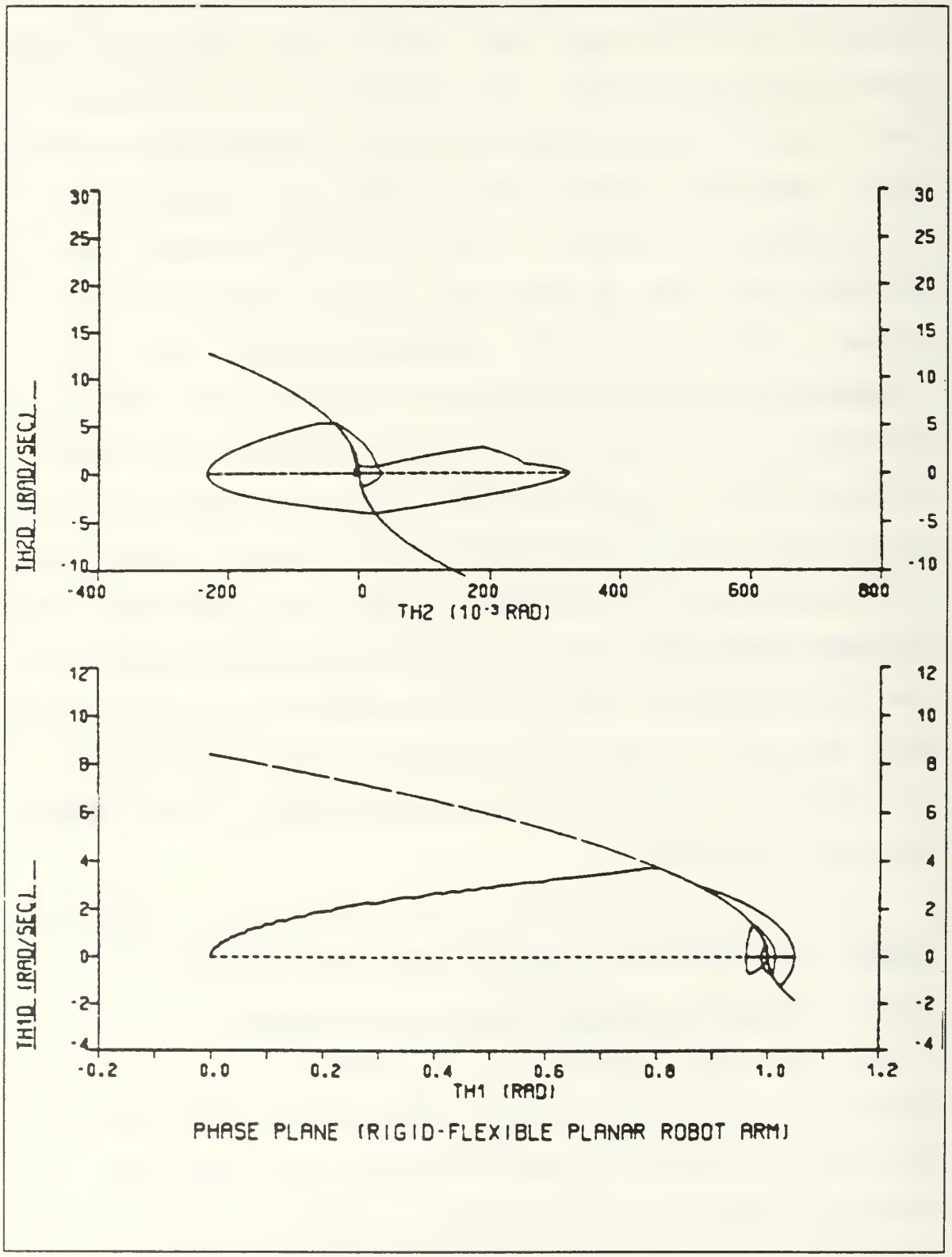

Figure 6.20 Rigid-flexible planar robot arm, Phase plane moving only the rigid link (arm loaded).

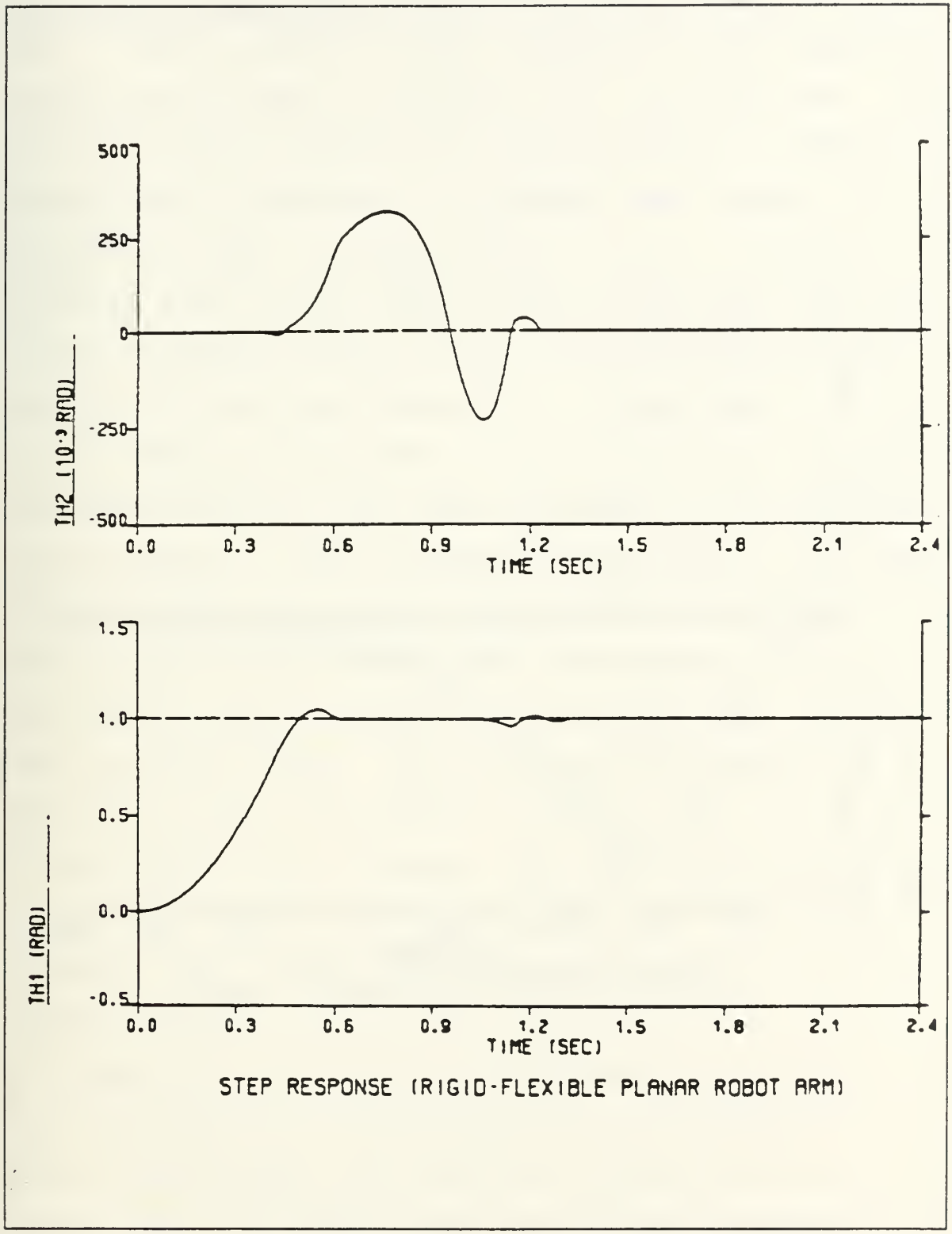

Figure 6.21 Rigid-flexible planar robot arm, Step response moving only the rigid link (arm loaded).

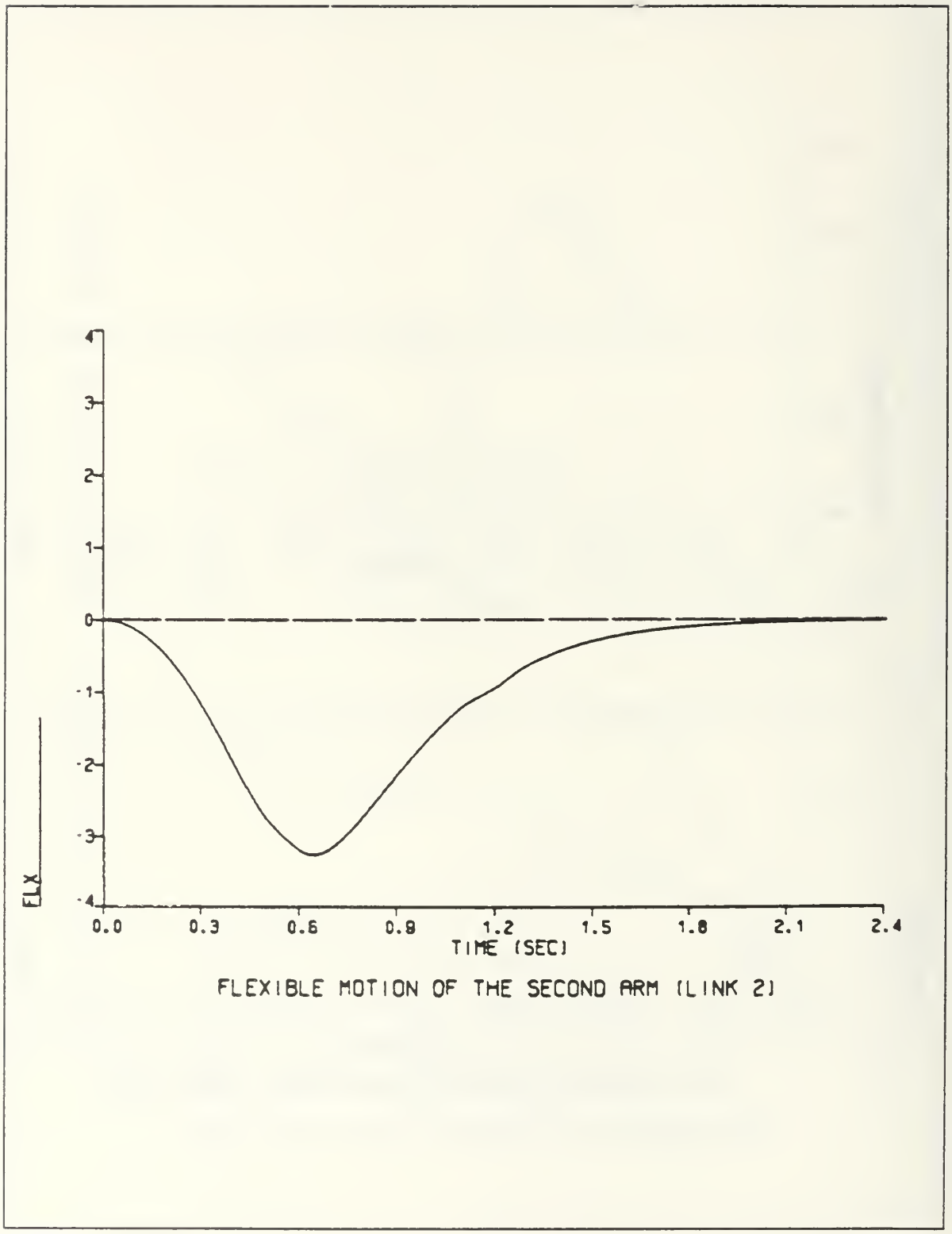

Figure 6.22 Rigid-flexible planar robot arm, End-point displacement, moving the rigid link (arm loaded).

end-point displacement respectively when moving the rigid arm. For the motion of the flexible arm the respective plots will be shown in Figures 6.23, 6.24 and 6.25. The required time to complete the sample motion, by adding the time that is required to complete each motion of the successive steps, is approximately 4.0 sec. Therefore the settling time for the sample motion, when using the method of the successive steps, will be twice the required settling time of the previous simulations. If the time is not the only important requirement, then the use of the method described above will give some advantages in the performance of the system. These advantages can be shown in the phase plane and the step response plots of the two motions. From these plots one can observe that the responses of the rigid arm and the flexible arm have less vibration and insignificant coupling effects. Thus, the resulting response for the flexible arm has much smaller overshoot and is close to a linear system type response. That was expected from the simulation results for a planar robot arm having only one flexible link, as was illustrated at Figures 3.5 and 3.6 in Chapter III.

When the rigid-flexible planar robot arm motion is to be performed in a gravitational-free environment (i.e., space applications) the simulation results giving the phase plane, the step response and the flexible displacement of the end-point will be illustrated for the unloaded planar

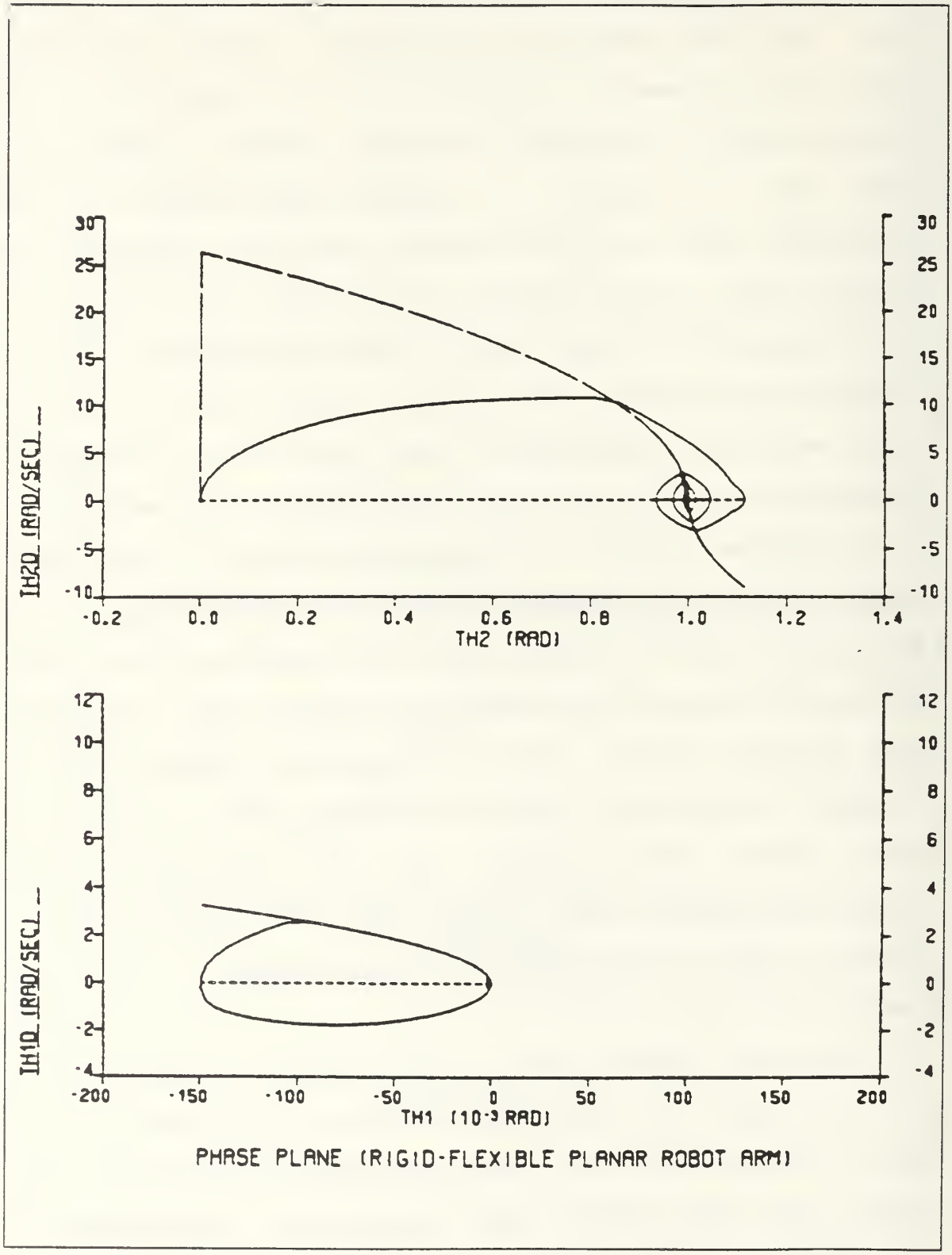

Figure 6.23 Rigid-flexible planar robot arm, Phase plane moving only the flexible link (arm loaded).

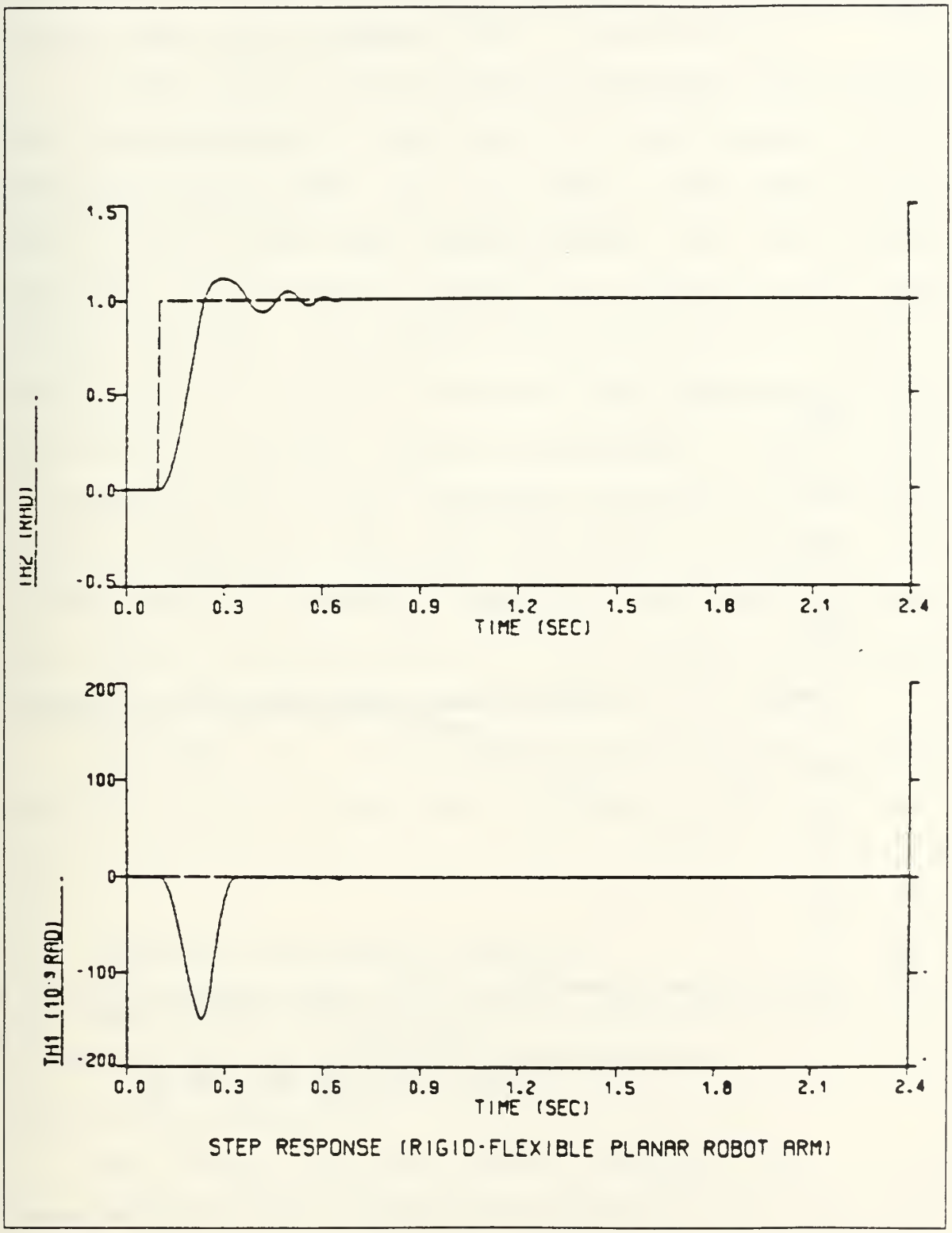

Figure 6.24 Rigid-flexible planar robot arm, Step response, moving only the flexible link (arm loaded).

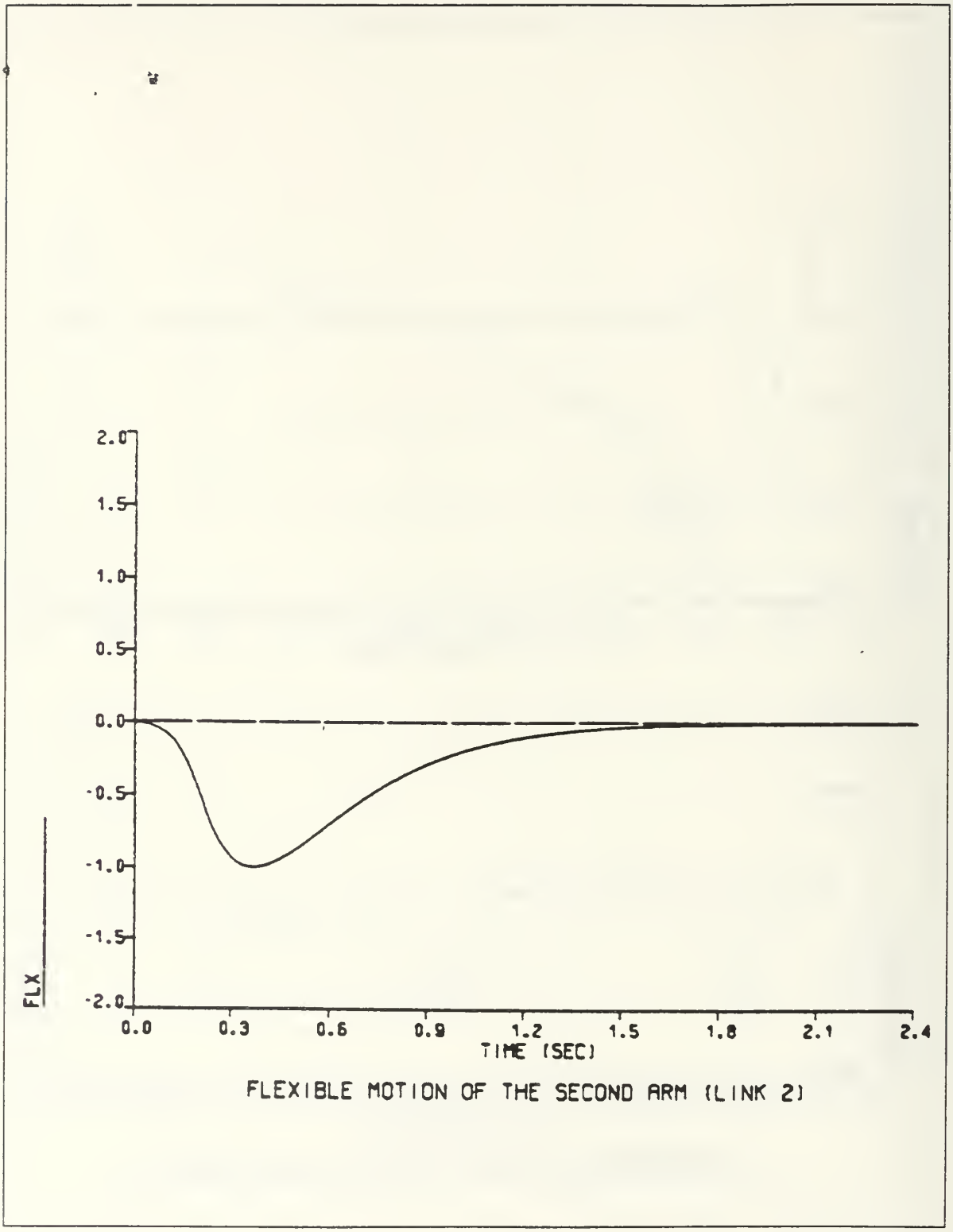

Figure 6.25 Rigid-flexible planar robot arm, End-point displacement, moving the loaded flexible link.

robor arm in Figures 6.26, 6.27 and 6.28 and for the loaded planar robot arm in Figures 6.29, 6.31 and 6.31.

In the case of a gravity-free environment the response for the hypothetical rigid motion of the unloaded rigid-flexible planar robot arm, as shown at the phase plane (Fig. 6.26) and the step response (Fig. 6.27), are almost identical to the results obtained for the two rigid links planar robot arm. The required settling time of the overall motion will be about 0.8 sec due to the required settling time for the end-point flexible displacement. When the arm is loaded the size of the overshoots occurring in the system becomes larger and the required settling time for the overall motion increases to about 1.9 sec, (that is about the required settling time of the unloaded manipulator moving in a gravitational environment).

Therefore in a gravity-free environment the rigid-flexible two links planar robot arm gave very good performance.

F. COMPARING THE SIMULATION RESULTS

Many observations can be made by comparing the obtained simulation results for the rigid-flexible and the two rigid links planar robot arms.

The results for the required settling time of the hypothetical rigid motion of the rigid-flexible robot arm are very close to the near minimum time positioning of the

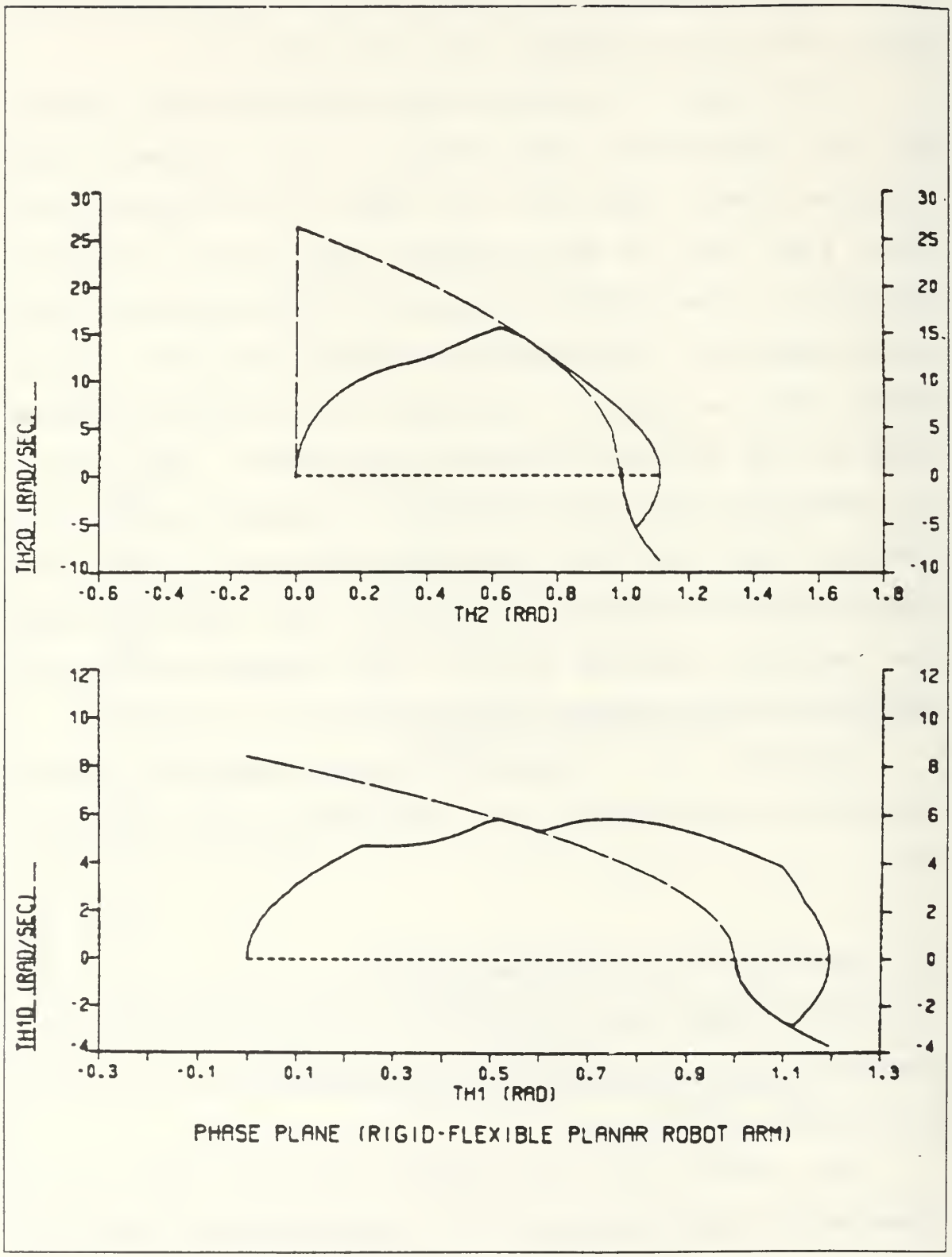

Figure 6.26 Rigid-flexible planar robot arm, Phase plane (gravitational-free environment).

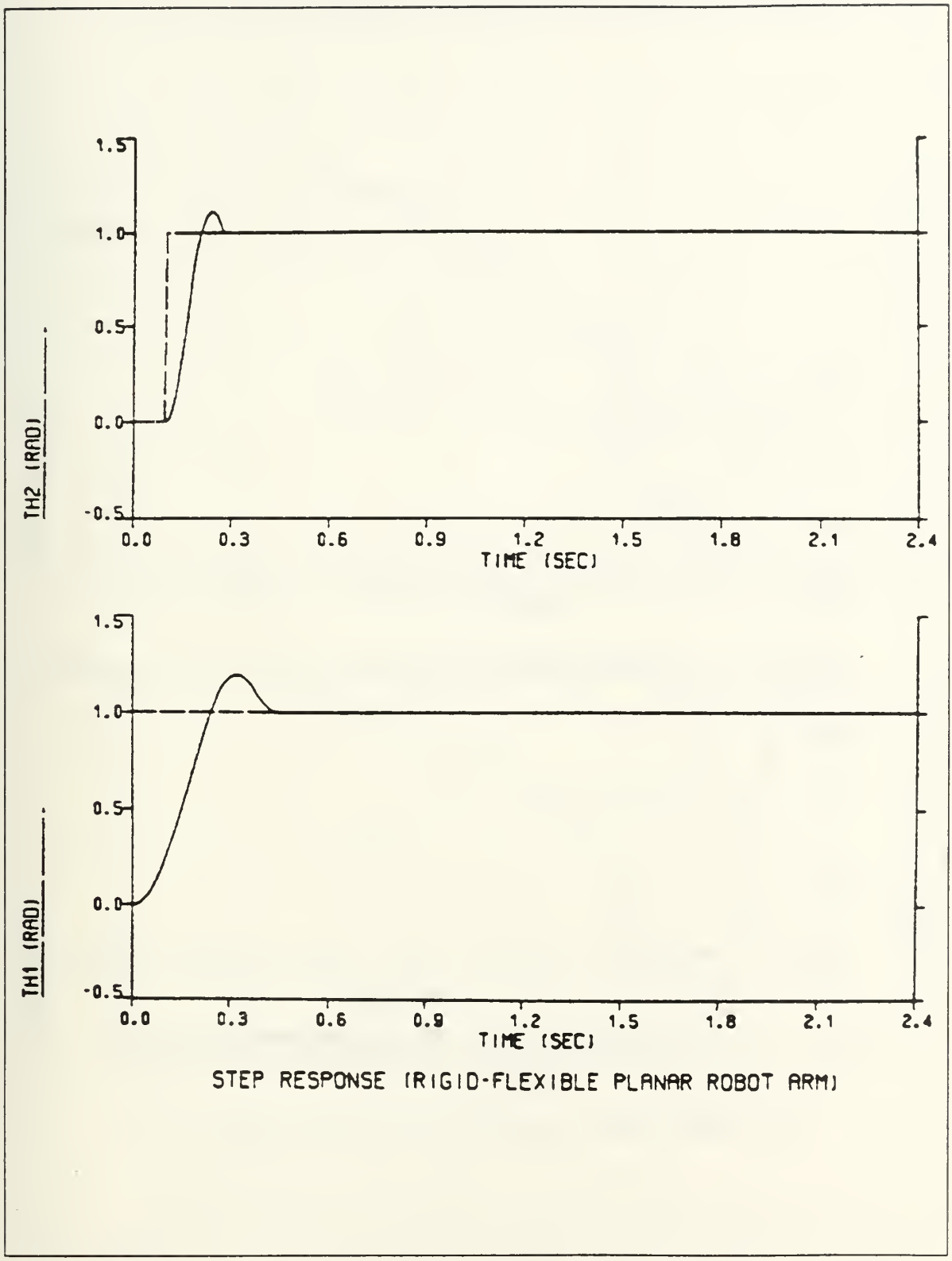

Figure 6.27 Rigid-flexible planar robot arm, Step response (gravitational-free environment).

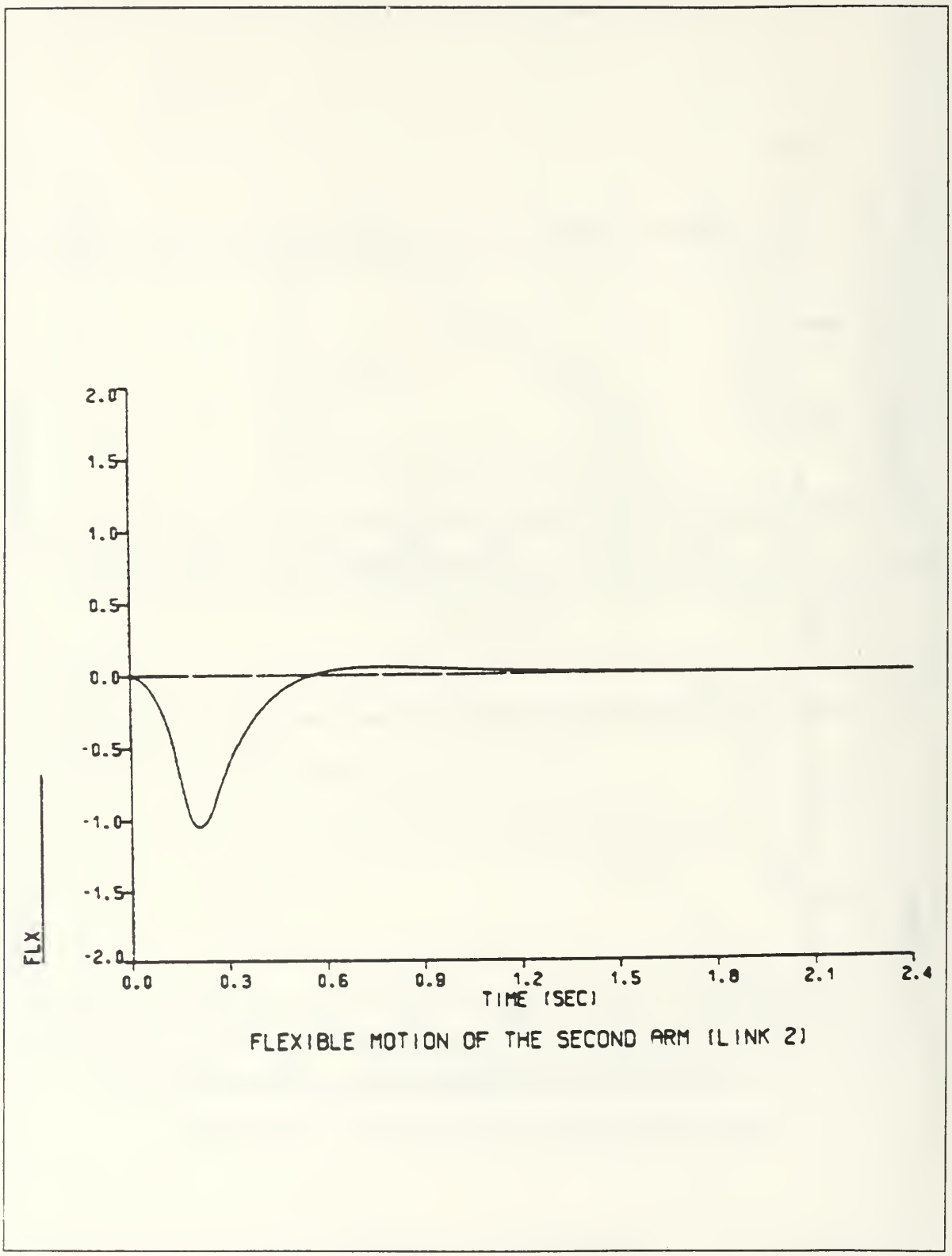

Figure 6.28 Rigid-flexible planar robot arm, End-point displacement (gravity-free environment).

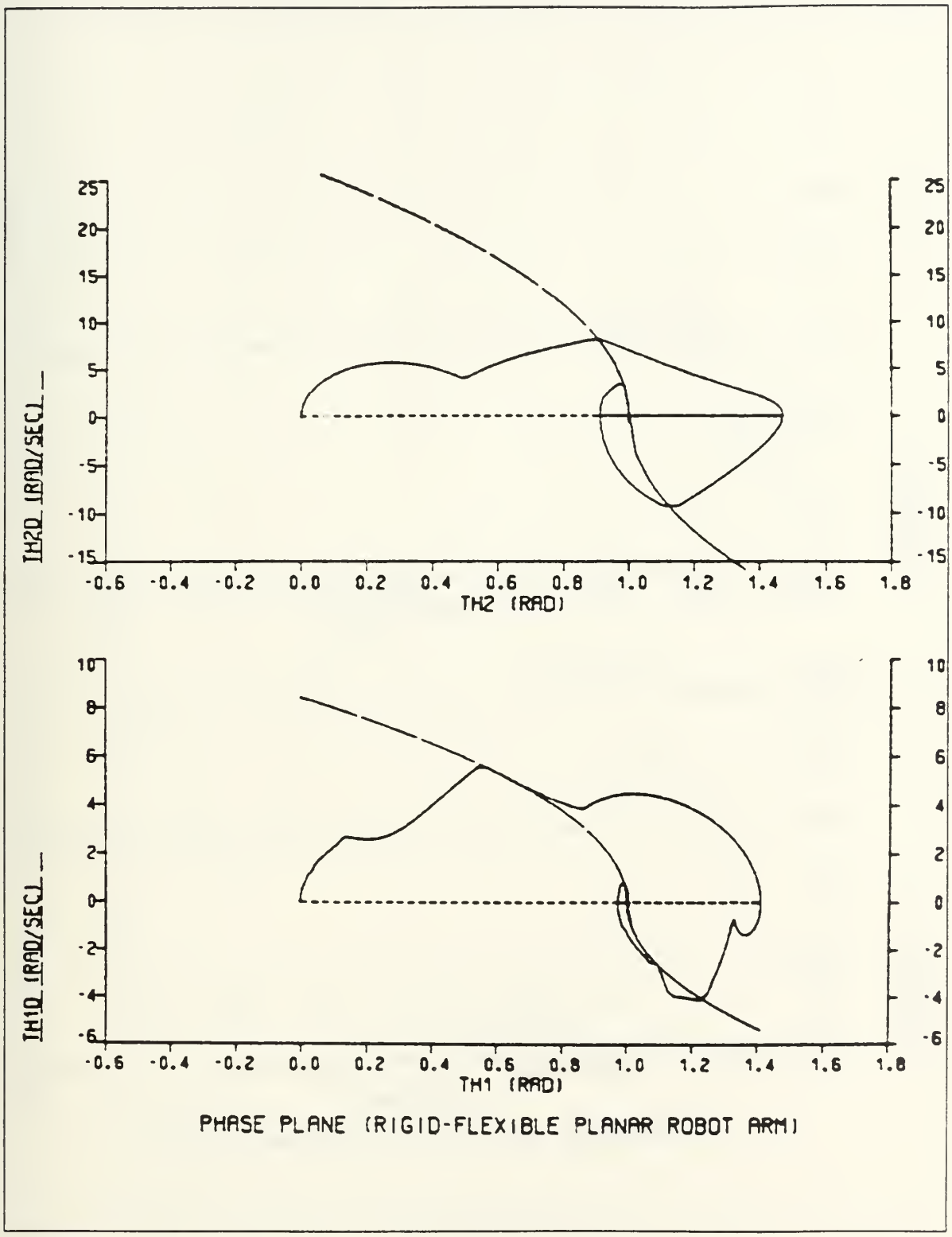

Figure 6.29 Rigid-flexible planar robot arm, Phase plane (arm loaded-not including gravitational forces).

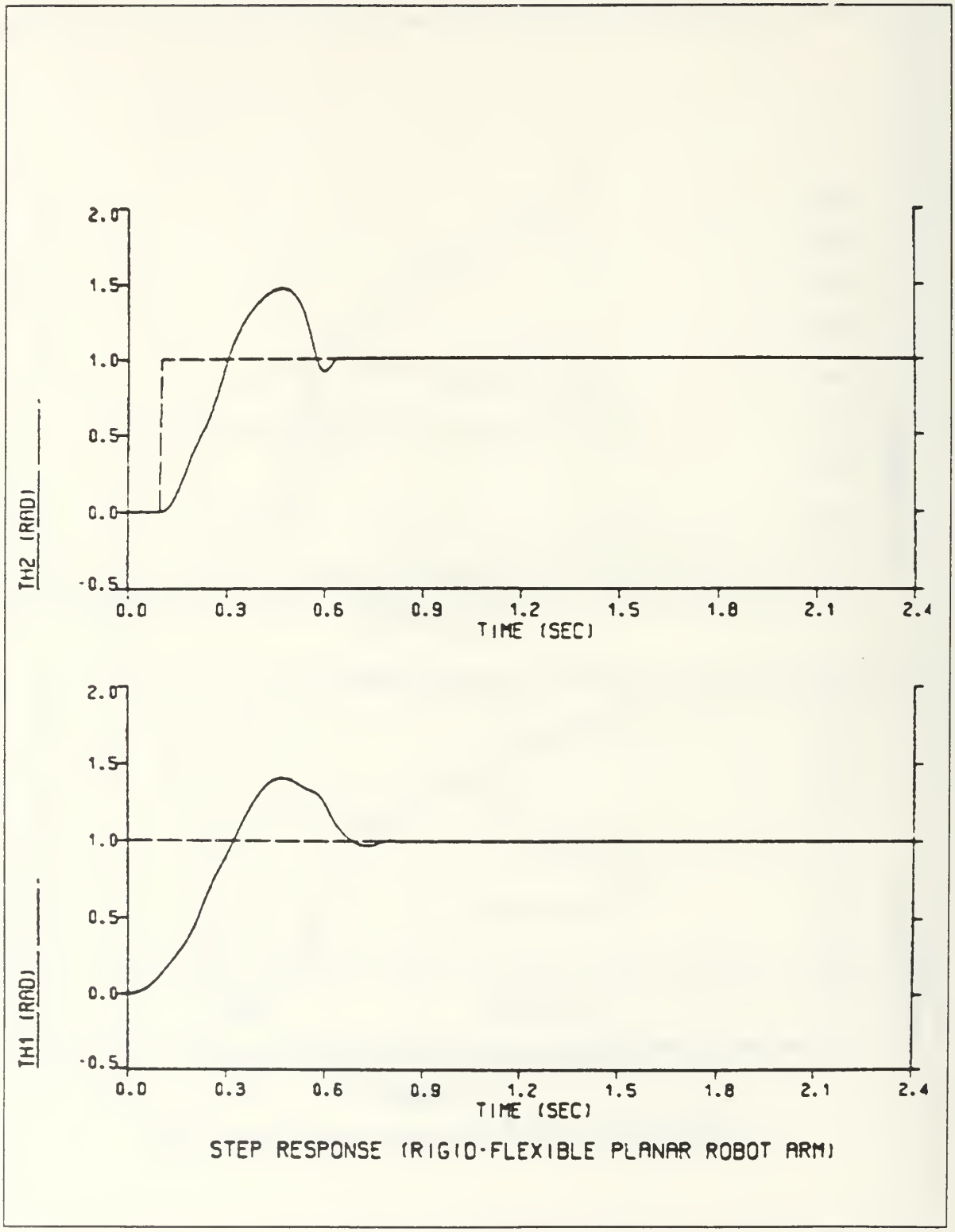

Figure 6.30 Rigid-flexible planar robot arm, Step response (arm loaded - no gravitational forces included).

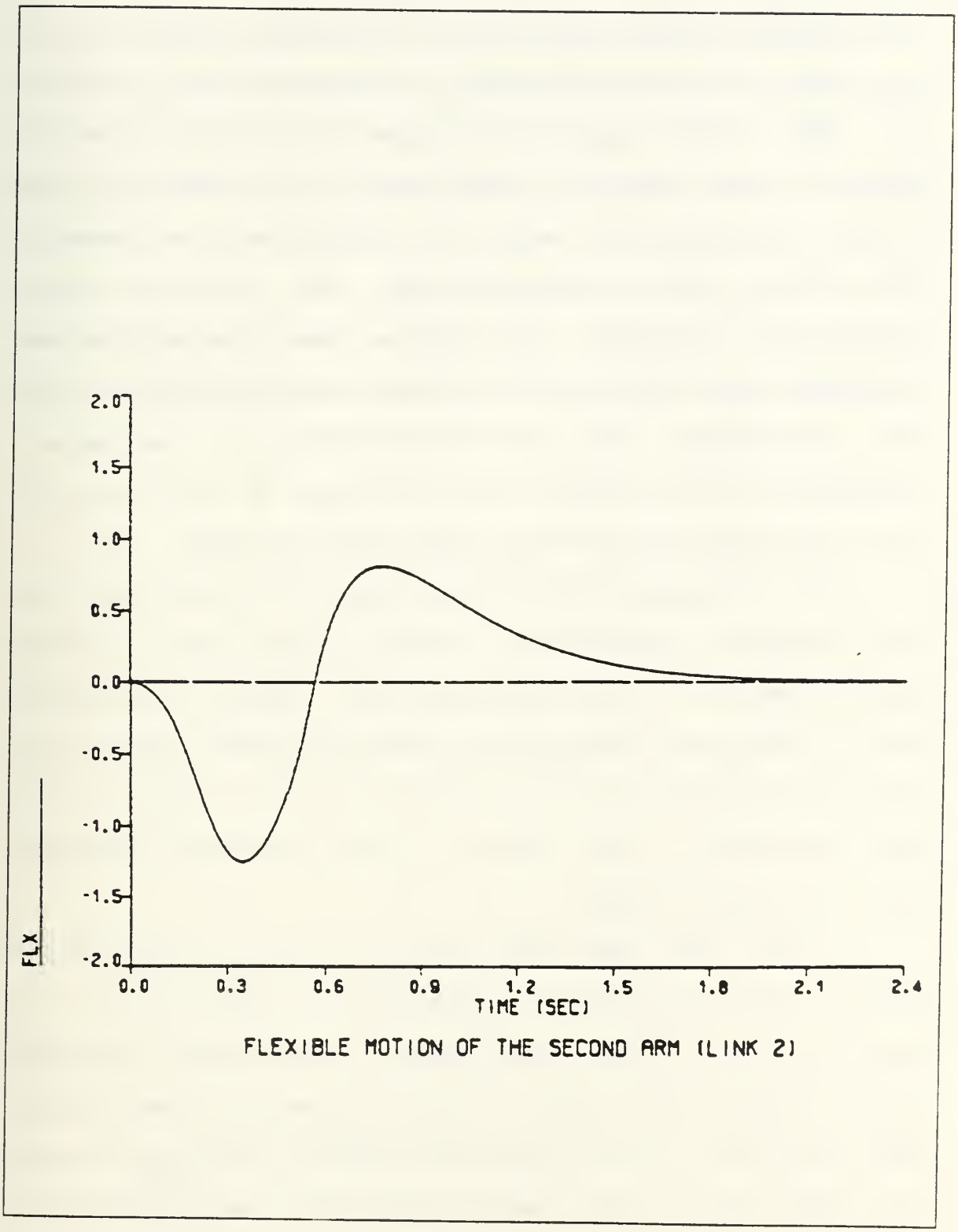

Figure 6.31 Rigid-flexible planar robot arm, End-point displacement (arm loaded - no gravitational forces included).

two rigid links. The hypothetical rigid motion of the rigid-flexible robot arm resulted in overshoots and vibrations, that are highly nonlinear in amplitude and in frequency. The reason for the overshoots is that the system presents four natural frequencies, two rigid and two flexible as the model takes into account only two modes of the flexible beam, combined with the coupling effects between the two links. By lowering these frequencies when increasing the load of the flexible link these effects are more pronounced. The stated nonlinearity in the system's response can be observed from the shapes of the curves for both the phase plane and the step response plots.

From the plots of the elastic motion of the system, for the end-point displacement, it can be seen that accurate results require a long settling time. Another interesting point is that the end-point of the manipulator bounces back and forth from its final position slowly but not many times. That indicates a good control of the flexible components from the adaptive model.

In the case where the sample motion, or any desired motion, will be completed in successive steps by moving the links one at a time, the system's performance indicates better results with respect to the accuracy and the introduced vibrations. In this case the required settling time for the completion of the sample motion will be approximately twice the time required when the two links are moving

simultaneously. Therefore once more a decision must be made based on the requirements of the specific application.

For the case where no gravitational forces are included in the environment, the rigid-flexible robot arm has a better performance, not very different from the one obtained for the two rigid links. Because the performances are not very different, the other advantages of the flexible manipulator make its use more advantageous for applications in a gravity-free environment, such as space applications.

VII. CONCLUSION / AREAS FOR FURTHER STUDY

As a result of the research conducted in this thesis, the control of the rigid-flexible, two links planar robot arm, using the curve following system, appears not only possible but resulted in a relatively good predicted performance of the system.

The sample motion used in testing the adaptive system introduced relatively large inputs for both links of the manipulator in order to examine the system under large parameter variations.

The simulation plots indicate that the system provided very good steady-state accuracy (of the order 10E-3) for the elastic motion of the flexible link under all tested conditions. The steady-state accuracy was independent of the load of the flexible link, but not the settling time of the elastic motion. The required settling time of the elastic motion for all cases was many times greater than the required settling time of the hypothetical rigid motion. Which was approximately equal to the near minimum time positioning of the two rigid links planar robot arm.

In the case of a loaded arm increased overshoots with more vibration modes were introduced in the angular position of the arm. This problem was partially alleviated by completing the motion in successive steps, i.e., by moving the rigid and the flexible links sequentially. This

solution results in an overall increase of the required settling time and the whole situation is a trade-off between time and the amount of oscillation.

It was also observed that for the case of the direct drive arm that was used as the model, the effects of the disturbance torques caused by the elastic motion and the coupling inertia between the two links as well as the centripetal, coriolis and gravitational forces acting on the robot arm, are larger. Therefore the servo motor must apply larger torques which implies high torque constant and high armature current capabilities. Due to the lighter structure of the flexible link the torque requirements (for both motors) are smaller than the requirements in the case of a two rigid links planar robot arm. Therefore the lighter rigid-flexible planar robot arm results in less power consumption, that also means use of smaller actuators.

Combining the above stated main advantage with the resulting end-point accuracy (from the simulation of the adaptive model) the rigid-flexible manipulator may be an attractive solution for many applications.

Compared with a two rigid links planar robot arm, the rigid-flexible planar robot arm may be preferable in many applications especially when time is not the main requirement and also in gravity-free environment applications, such as space applications.

An area for further study arises when the feasibility of controlling two flexible links with the proposed adaptive computer simulation model is to be investigated.

Modelling the manipulator both links were assumed to be massless. Another area for further study arises when two links having their masses distributed along their lengths are used to build a robot arm.

Finally a very interesting area for further study will be the use of the same curve following method as the adaptive control scheme but with curve reshaping through the adaptive algorithm in order to obtain better system performance.

APPENDIX A

DERIVATION OF THE LAGRANGIAN EOUATIONS FOR THE TWO RIGID LINKS PLANAR ROBOT ARM

For the sake of the analysis the configuration of the system for the two rigid links planar robot arm will be repeated as Figure A.1.

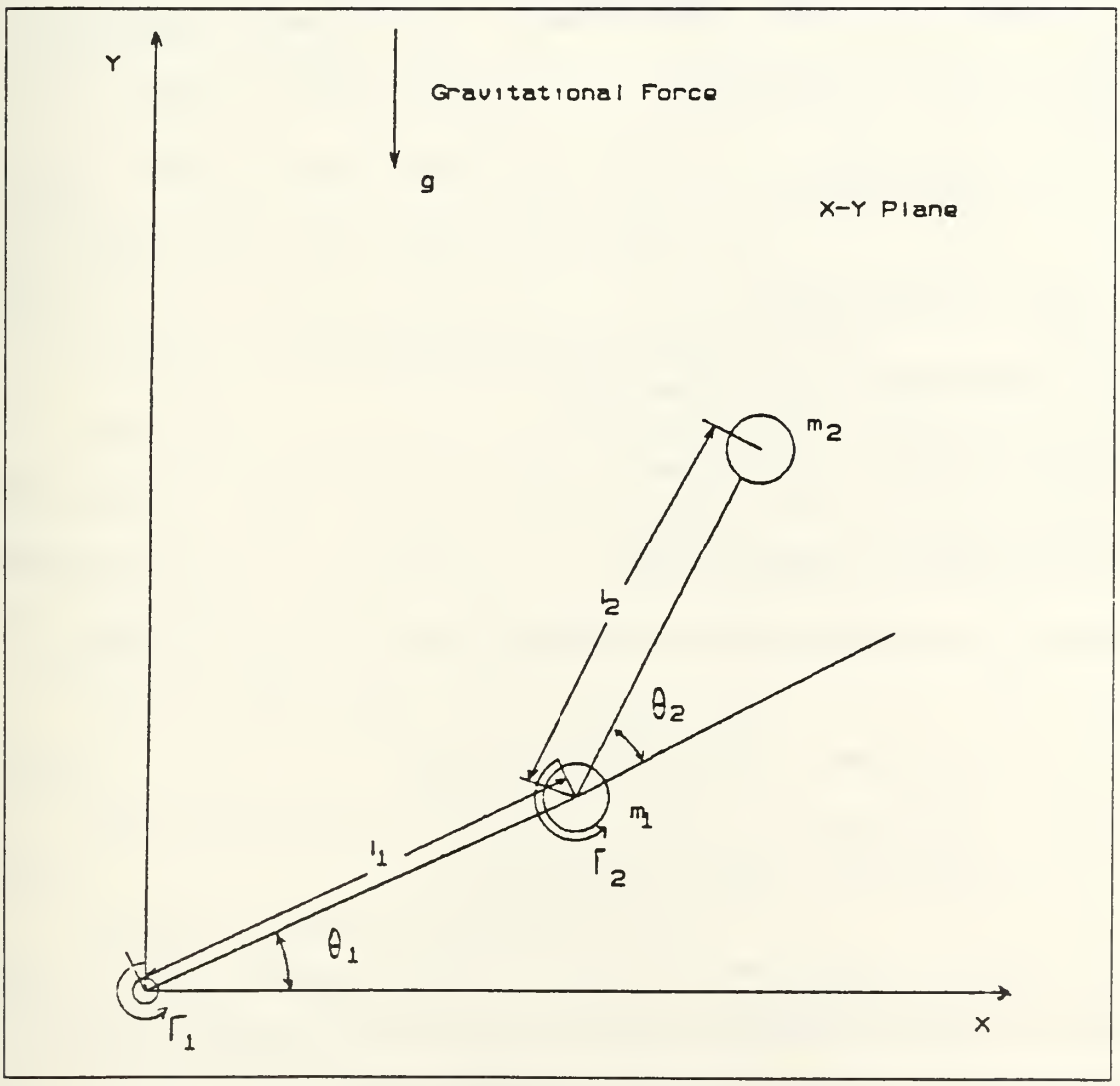

Figure A.1 Planar robot arm with two rigid links.

For this particular system the generalized coordinates are Θ_1 and Θ_2, and the generalized forces Γ_1 and Γ_2 as defined in Chapter II. To form the Lagrangian function L, the kinetic and potential energies of the system must derived in terms of the generalized coordinates. The kinetic energy of any multi-link robot arm system can be obtained from the kinetic energies of the individual links, therefore, for the two links robot arm system, the kinetic energy T will be the sum of the kinetic energies T_1 and T_2 of LINK1 and LINK2 respectively. The kinetic energies, T_1 and T_2, will be given as:

$$T_1 = \frac{1}{2} m_1 l_1^2 \dot{\Theta}_1^2 \qquad (A.1)$$

$$T_2 = \frac{1}{2} m_2 (\dot{x}_2^2 + \dot{y}_2^2) \qquad (A.2)$$

By coordinates transformation:

$$x_2 = l_1 \cos\Theta_1 + l_2 \cos(\Theta_1 + \Theta_2) \qquad (A.3)$$

$$y_2 = l_1 \sin\Theta_1 + l_2 \sin(\Theta_1 + \Theta_2) \qquad (A.4)$$

Taking the derivatives of the Equations A.3 and A.4 then:

$$\dot{x}_2 = -l_1 \dot{\Theta}_1 \sin\Theta_1 - l_2 (\dot{\Theta}_1 + \dot{\Theta}_2) \sin(\Theta_1 + \Theta_2) \qquad (A.5)$$

$$\dot{y}_2 = l_1 \dot{\Theta}_1 \cos\Theta_1 + l_2 (\dot{\Theta}_1 + \dot{\Theta}_2) \cos(\Theta_1 + \Theta_2) \qquad (A.6)$$

Substituting Equations A.5 and A.6 into Equation A.2, after simple algebraic manipulations, the kinetic energy for the second link is given by the following equation:

$$T_2 = \frac{1}{2} m_2[l_1^2\dot{\theta}_1^2+l_2^2(\dot{\theta}_1^2+2\dot{\theta}_1\dot{\theta}_2+\dot{\theta}_2^2)+2l_1l_2(\dot{\theta}_1^2+\dot{\theta}_1\dot{\theta}_2)\cos\theta_2] \quad (A.7)$$

Therefore the kinetic energy of the system will be given as:

$$T = \frac{1}{2}[(m_1+m_2)l_1^2\dot{\theta}_1^2+m_2l_2(\dot{\theta}_1^2+2\dot{\theta}_1\dot{\theta}_2+\dot{\theta}_2^2)] + m_2l_1l_2(\dot{\theta}_1^2+\dot{\theta}_1\dot{\theta}_2)\cos\theta_2 \quad (A.8)$$

The total potential energy of the system can be computed by following the same procedure from the potential energies of the individual links, given as:

$$V_1 = m_1gy_1 = m_1gl_1\sin\theta_1 \quad (A.9)$$

$$V_2 = m_2gy_2 = m_2g[l_1\sin\theta_1+l_2\sin(\theta_1+\theta_2)] \quad (A.10)$$

Therefore the total potential energy is:

$$V = V_1+V_2 = (m_1+m_2)gl_1\sin\theta_1+m_2gl_2\sin(\theta_1+\theta_2) \quad (A.11)$$

Thus the Lagrangian function, L = T - V, for the system of the two rigid links planar robot arm will be obtained from Equations A.8 and A.11. After algebraic manipulations the Lagrangian function obtains the final form:

$$L = \frac{1}{2}(m_1l_1^2+J_1)\dot{\theta}_1^2 + \frac{1}{2}(m_2l_2^2+J_2)\dot{\theta}_2^2 + \frac{1}{2}m_2(l_1^2+l_2^2+2l_1l_2\cos\theta_2)\dot{\theta}_1+m_2(l_2^2+l_1l_2\cos\theta_2)\dot{\theta}_1\dot{\theta}_2 - [(m_1+m_2)l_1\sin\theta_1+m_2l_2\sin(\theta_1+\theta_2)]g \quad (A.12)$$

From the above derived Lagrangian function L, the partial derivatives of L with respect the generalized coordinates θ_1

and θ_2 and their rate of change θ_1 and θ_2 will give the following results:

$$\frac{\delta L}{\delta \theta_1} = -(m_1+m_2)gl_1\cos\theta_1 - m_2gl_2\cos(\theta_1+\theta_2) \tag{A.13}$$

$$\frac{\delta L}{\delta \dot{\theta}_1} = (m_1l_1^2+J_1)\dot{\theta}_1 + m_2(l_1^2+l_2^2+2l_1l_2\cos\theta_2)\dot{\theta}_1 + m_2(l_2^2+l_1l_2\cos\theta_2)\dot{\theta}_2 \tag{A.14}$$

$$\frac{d}{dt}\left(\frac{\delta L}{\delta \dot{\theta}_1}\right) = (m_1l_1^2+J_1+m_2l_1^2+m_2l_2^2+2m_2l_1l_2\cos\theta_2)\ddot{\theta}_1 + (m_2l_2^2+m_2l_1l_2\cos\theta_2)\ddot{\theta}_2 - (2m_2l_1l_2\sin\theta_2)\dot{\theta}_1\dot{\theta}_2 - (m_2l_1l_2\sin\theta_2)\dot{\theta}_2^2 \tag{A.15}$$

$$\frac{\delta L}{\delta \theta_2} = -(m_2l_1l_2\sin\theta_2)\dot{\theta}_1^2 - (m_2l_1l_2\sin\theta_2)\dot{\theta}_1\dot{\theta}_2 - m_2gl_2\cos(\theta_1+\theta_2) \tag{A.16}$$

$$\frac{\delta L}{\delta \dot{\theta}_2} = (m_2l_2^2+J_2)\dot{\theta}_2 + m_2(l_1^2+l_1l_2\cos\theta_2)\dot{\theta}_1 \tag{A.17}$$

$$\frac{d}{dt}\left(\frac{\delta L}{\delta \dot{\theta}_2}\right) = (m_2l_2^2+J_2)\ddot{\theta}_2 + (m_2l_2^2+m_2l_1l_2\cos\theta_2)\ddot{\theta}_1 - m_2l_1l_2\sin\theta_2\,\dot{\theta}_1\dot{\theta}_2 \tag{A.18}$$

A set of two nonlinear second order differential equations will then be obtained by direct substitution of

the Equations A.13, A.15, A.16 and A.18 into the formula for the Lagrange's equations:

$$\frac{d}{dt}\left(\frac{\delta L}{\delta \dot{q}_i}\right) - \frac{\delta L}{\delta q_i} = Q_i \qquad i=1,2 \qquad \text{(A.19)}$$

with the generalized forces to be, in this particular case, $Q_1=\Gamma_1$ and $Q_2=\Gamma_2$. The derived pair of the nonlinear second order differential equations was given in Chapter II of this thesis, as a result of this analysis.

APPENDIX B

DERIVATION OF THE MODEL FOR A PLANAR ROBOT ARM HAVING ONE FLEXIBLE LINK USING THE ASSUMED-MODES METHOD

B1. GENERAL REMARKS

In this Appendix, the derivation of the mathematical models for a planar robot arm having one flexible link will be given, with the flexibility being approximated using the assumed-modes method. The set of the second order differential equations of motion that describe that system will be derived using the Lagrangian dynamics approach.

The Lagrangian function can be computed as L=T-V, where T and V are the kinetic and the potential energies of the system respectively. Therefore the Lagrangian function will be derived similar to the method followed in the case of the flexible second link of the planar robot arm, as will be given in Appendix D. Expressing the Lagrangian function in terms of the flexible displacement u_E the following equation are obtained:

$$L = \frac{1}{2}\left[ml^2\dot{\Theta}^2 + m\dot{\Theta}^2 u_E^2 + m\dot{u}_E^2\right] + ml\ddot{\Theta}u_E$$
$$- g[ml\sin\Theta + mu\cos\Theta] - \frac{1}{2}\sum_{i=1}^{n}(KW_i g_i^2) \qquad (B.1)$$

where n = 1, 2 or 3.

With the above derived Lagrangian function L, the set of the differential equations that describe that system can be

obtained by forming the Lagrange's equation with respect the generalized coordinates. For this system the generalized coordinates are defined to be Θ and g_i (i=1, 2 or 3). Thus sets of two, three and four nonlinear second order differential equations will be obtained when the numbers of the assumed modes used to approximate the flexibility are n=1,2 or 3, respectively. The differential equations will be obtained by forming the Lagrangian equation, as is given below:

$$\frac{d}{dt}\left(\frac{\delta L}{\delta \dot{q}_i}\right) - \frac{\delta L}{\delta q_i} = Q_i \qquad i=1,2,... \qquad (B.2)$$

B2. EXPRESSING THE FLEXIBILITY WITH ONE ASSUMED-MODE

For the case in which the flexible displacement will be expressed using one assumed mode then:

$$u_E = f_{1E} g_1 \qquad (B.3)$$

Replacing the above expression for the flexible displacement the Lagrangian function will obtain the form:

$$\begin{aligned} L = {} & \frac{1}{2}\left[ml^2\dot{\Theta}^2 + m\dot{\Theta}^2 (f_{1E}g_1)^2 + m(f_{1E}\dot{g}_1)^2\right] \\ & + ml\dot{\Theta}(f_{1E}\dot{g}_1) - \frac{1}{2} KW_1 g_1^2 \\ & - g\left[ml\sin\Theta + m(f_{1E}g_1)\cos\Theta\right] \end{aligned} \qquad (B.4)$$

Forming the Lagrangian equation of the above given Lagrangian function with respect the generalized coordinate Θ, then:

$$\frac{\delta L}{\delta \theta} = -g\,[ml\theta\cos\theta - m\sin\theta f_{1E} g_1] \tag{B.5}$$

$$\frac{\delta L}{\delta \dot{\theta}} = ml^2\dot{\theta} + mlf_{1E}\dot{g}_1 + m\dot{\theta}(f_{1E}g_1)^2 \tag{B.6}$$

$$\frac{d}{dt}\left(\frac{\delta L}{\delta \dot{\theta}}\right) = ml^2\ddot{\theta} + mlf_{1E}\ddot{g}_1 + m\ddot{\theta}(f_{1E}g_1)^2 + 2m\dot{\theta}\,\dot{g}_1(f_{1E}^2 g_1) \tag{B.7}$$

The same approach with respect the generalized coordinate g_1 results in:

$$\frac{\delta L}{\delta g_1} = m\dot{\theta}^2 f_{1E}^2 g_1 - KW_1 g_1 - gmf_{1E}\cos\theta \tag{B.8}$$

$$\frac{\delta L}{\delta \dot{q}_1} = mf_{1E}^2\dot{g}_1 + ml\dot{\theta}f_{1E} \tag{B.9}$$

$$\frac{d}{dt}\left(\frac{\delta L}{\delta \dot{q}_1}\right) = mf_{1E}^2\ddot{g}_1 + mlf_{1E}\ddot{\theta} \tag{B.10}$$

Combining Equations B.5 and B.7 the first nonlinear second order differential equation can be produced. The second nonlinear differential equation will be derived from the Equations B.8 and B.10. The final form of the differential equations that describe the system when one assumed mode is to be used to describe the flexibility of the arm will be given as follows:

$$\Gamma = D_{111}\ddot{\theta} + D_{122}\ddot{g}_1 + D_{112}\dot{\theta}\,\dot{g}_1 + D_1 \tag{B.11}$$

$$0 = D_{211}\ddot{\theta} + D_{222}\ddot{g}_1 + D_{2111}\dot{\theta}^2 + D_2 \tag{B.12}$$

where

$$D_{111} = ml^2 + mf_{1E}^2 g_1^2$$

$$D_{122} = mlf_{1E}$$

$$D_{112} = 2mf_{1E}^2 g_1$$

$$D_1 = g[ml\theta \cos\theta - mf_{1E} g_1 \sin\theta]$$

$$D_{211} = mlf_{1E}$$

$$D_{222} = mf_{1E}^2$$

$$D_{2111} = -mf_{1E}^2 g_1$$

$$D_2 = gmf_{1E}\cos\theta + KW_1 g_1$$

$$KW_1 = EI \int_0^{l_2} \ddot{f}_1(x)\, \ddot{f}_1(x)\, dx$$

Equations B.11 and B.12 are the mathematical model used in the analysis of the flexible arm, in Chapter III, when the flexible displacement is to be expressed with one assumed-mode.

B3. EXPRESSING THE FLEXIBILITY WITH TWO ASSUMED-MODES

Having the flexible displacement, u_E, being expressed with two assumed-modes then:

$$u_E = f_{1E} g_1 + f_{2E} g_2 \qquad (B.13)$$

By replacing the derived expression for the flexible displacement the Lagrangian function will achieve the form:

$$L = \frac{1}{2} [ml^2\dot{\theta}^2 + m\dot{\theta}^2 (f_{1E} g_1 + f_{2E} g_2)^2 + m(f_{1E}\dot{g}_1 + f_{2E}\dot{g}_2)^2]$$

$$+ ml\dot{\Theta}(f_{1E}\dot{g}_1+f_{2E}\dot{g}_2) - \frac{1}{2}(KW_1g_1^2+KW_2g_2^2) \qquad (B.14)$$

$$- g[ml\sin\Theta + m(f_{1E}g_1+f_{2E}g_2)\cos\Theta]$$

In these case the generalized coordinates are Θ, g_1 and g_2. Therefore a set of three second order differential equations will be obtained by following the same procedure as was illustrated in the case of the one assumed-mode. By taking partial derivatives of the Lagrangian function with respect each generalized coordinate and their corresponding velocities and differentiate with respect the time the following equations will be obtained:

$$\Gamma = D_{111}\ddot{\Theta} + D_{122}\ddot{g}_1 + D_{133}\ddot{g}_2 + D_{112}\dot{\Theta}\dot{g}_1 + D_{113}\dot{\Theta}\dot{g}_2 + D_1 \qquad (B.15)$$

$$0 = D_{211}\ddot{\Theta} + D_{222}\ddot{g}_1 + D_{233}\ddot{g}_2 + D_{2111}\dot{\Theta}^2 + D_2 \qquad (B.16)$$

$$0 = D_{311}\ddot{\Theta} + D_{322}\ddot{g}_1 + D_{333}\ddot{g}_2 + D_{3111}\dot{\Theta}^2 + D_3 \qquad (B.17)$$

where

$$D_{111} = ml^2 + mf_{1E}^2g_1^2 + mf_{2E}^2g_2^2 + 2mf_{1E}f_{2E}g_1g_2$$

$$D_{122} = mlf_{1E}$$

$$D_{133} = mlf_{2E}$$

$$D_{112} = 2mf_{1E}^2g_1 + 2mf_{1E}f_{2E}g_2$$

$$D_{133} = 2mf_{2E}^2g_2 + 2mf_{1E}f_{2E}g_1$$

$$D_1 = gml\Theta\cos\Theta - gm(f_{1E}g_1+f_{2E}g_2)\sin\Theta$$

$$D_{211} = mlf_{1E}$$

$$D_{222} = mf_{1E}^2$$

$$D_{233} = mf_{1E}f_{2E}$$

$$D_{2111} = -mf_{1E}(f_{1E}g_1+f_{2E}g_2)$$

$$D_2 = gmf_{1E}\cos\theta + KW_1g_1$$

$$D_{311} = mlf_{2E}$$

$$D_{322} = D_{233}$$

$$D_{333} = mf_{2E}^2$$

$$D_{3111} = -mf_{2E}(f_{1E}g_1+f_{2E}g_2)$$

$$D_3 = gmf_{2E}\cos\theta + KW_2g_2$$

$$KW_1 = El \int_0^{l_2} \ddot{f}_1(x)\, \ddot{f}_1(x)\, dx$$

$$KW_2 = El \int_0^{l_2} \ddot{f}_2(x)\, \ddot{f}_2(x)\, dx$$

The derived Equations B.15, B.16 and B.17 will become the mathematical model of the flexible arm, for the analysis presented in Chapter III, when two assumed-modes are to be used to express the flexible displacement of the arm.

B4. EXPRESSING THE FLEXIBILITY WITH THREE ASSUMED-MODES

By expressing the flexible displacement, u_E, with three assumed-modes then:

$$u_E = f_{1E}g_1 + f_{2E}g_2 + f_{3E}g_3 \qquad (B.18)$$

Replacing into the Lagrangian function the approximation of

the flexible displacement, given by Equation B.18, the following equation is obtained:

$$L = \frac{1}{2}\,[ml^2\dot{\Theta}^2 + m\dot{\Theta}^2(f_{1E}g_1+f_{2E}g_2+f_{3E}g_3)^2$$
$$+m(f_{1E}\dot{g}_1+f_{2E}\dot{g}_2+f_{3E}\dot{g}_3)^2]+ml\dot{\Theta}(f_{1E}\dot{g}_1+f_{2E}\dot{g}_2+f_{3E}\dot{g}_3)$$
$$-g[ml\sin\Theta+m(f_{1E}g_1+f_{2E}g_2+f_{3E}g_3)\cos\Theta] \qquad \text{(B.19)}$$
$$-\frac{1}{2}\,(KW_1g_1^2 +KW_2g_2^2 +KW_3g_3^2)$$

For this model the generalized coordinates are Θ, g_1, g_2 and g_3. Therefore a set of four nonlinear second order differential equations will be obtained by taking partial derivatives of the Lagrangian function, with respect to each generalized coordinate as well as with respect to the rate of change of these generalized coordinates and differentiating the resulted equations with respect the time. This set of the second order differential equations is given as:

$$\Gamma = D_{111}\ddot{\Theta} +D_{122}\ddot{g}_1 +D_{133}\ddot{g}_2 +D_{144}\ddot{g}_3 +D_{112}\dot{\Theta}\,\dot{g}_1$$
$$+ D_{113}\dot{\Theta}\,\dot{g}_2 +D_{114}\dot{\Theta}\,\dot{g}_3 +D_1 \qquad \text{(B.20)}$$

$$0 = D_{211}\ddot{\Theta} +D_{222}\ddot{g}_1 +D_{233}\ddot{g}_2 +D_{244}\ddot{g}_3 +D_{2111}\dot{\Theta}^2 +D_2 \qquad \text{(B.21)}$$

$$0 = D_{311}\ddot{\Theta} +D_{322}\ddot{g}_1 +D_{333}\ddot{g}_2 +D_{344}\ddot{g}_3 +D_{3111}\dot{\Theta}^2 +D_3 \qquad \text{(B.22)}$$

$$0 = D_{411}\ddot{\Theta} +D_{422}\ddot{g}_1 +D_{433}\ddot{g}_2 +D_{444}\ddot{g}_3 +D_{4111}\dot{\Theta}^2 +D_4 \qquad \text{(B.23)}$$

where

$$D_{111} = ml^2 + m(f_{1E}g_1+f_{2E}g_2+f_{3E}g_3)^2$$

$$D_{122} = mlf_{1E}$$

$$D_{133} = mlf_{2E}$$

$$D_{144} = mlf_{3E}$$

$$D_{112} = 2mf_{1E}^2 g_1 + 2mf_{1E}f_{2E}g_2 + 2mf_{1E}f_{3E}g_3$$

$$D_{113} = 2mf_{2E}^2 g_2 + 2mf_{1E}f_{2E}g_1 + 2mf_{2E}f_{3E}g_3$$

$$D_{114} = 2mf_{3E}^2 g_3 + 2mf_{1E}f_{3E}g_1 + 2mf_{2E}f_{3E}g_2$$

$$D_1 = gml\Theta\cos\Theta - gm(f_{1E}g_1 + f_{2E}g_2 + f_{3E}g_3)\sin\Theta$$

$$D_{211} = mlf_{1E}$$

$$D_{222} = mf_{1E}^2$$

$$D_{233} = mf_{1E}f_{2E}$$

$$D_{244} = mf_{1E}f_{3E}$$

$$D_{2111} = -mf_{1E}(f_{1E}g_1 + f_{2E}g_2 + f_{3E}g_3)$$

$$D_2 = gmf_{1E}\cos\Theta + KW_1 g_1$$

$$D_{311} = mlf_{2E}$$

$$D_{322} = D_{233}$$

$$D_{333} = mf_{2E}^2$$

$$D_{344} = mf_{2E}f_{3E}$$

$$D_{3111} = -mf_{2E}(f_{1E}g_1 + f_{2E}g_2 + f_{3E}g_3)$$

$$D_3 = gmf_{2E}\cos\Theta + KW_2 g_2$$

$$D_{411} = mlf_{3E}$$

$$D_{422} = D_{244}$$

$$D_{433} = D_{344}$$

$$D_{444} = mf_{3E}^2$$

$$D_{4111} = -mf_{3E}(f_{1E}g_1+f_{2E}g_2+f_{3E}g_3)$$

$$D_4 = gmf_{3E}\cos\Theta + KW_3g_3$$

$$KW_1 = EI \int_0^{l_2} \ddot{f}_1(x)\, \ddot{f}_1(x)\, dx$$

$$KW_2 = EI \int_0^{l_2} \ddot{f}_2(x)\, \ddot{f}_2(x)\, dx$$

$$KW_3 = EI \int_0^{l_2} \ddot{f}_3(x)\, \ddot{f}_3(x)\, dx$$

The derived Equations B.20 - B.23 will represent the mathematical model of the flexible arm, when the flexible displacement will approximated using three assumed-modes.

B5. THE MODELS FOR THE FLEXIBLE ARM

A planar robot having one flexible rigid arm will have a mathematical model that can be represented by the models derived previously. All these models are very similar because they were based on the same idea with the difference that the flexible end-point displacement was expressed with one, two and three assumed-modes. These models will be used with an adaptive control scheme, the velocity curve follow, that will be derived in Chapter V. The three different models that will be resulted will be simulated in order to investigate the performance of the flexible arm.

APPENDIX C

SIMULATION PROGRAMS OF THE ADAPTIVE MODEL HAVING A FLEXIBLE ARM TO INVESTIGATE THE EFFECTS OF THE ASSUMED MODES

C1. APPROXIMATION USING ONE ASSUMED MODE (N=1)

```
TITLE     SIMULATION PROGRAM FOR THE ADAPTIVE MODEL OF A
TITLE     PLANAR ROBOT ARM HAVING ONE FLEXIBLE LINK.
TITLE     THE FLEXIBILITY WAS APPROXIMATED USING ONE ASSUMED
TITLE     MODE (N=1).
*
CONST     G=981.4
*
PARAM     K=1.0,K1=1.0,K2=10000.0,KM=2.341
PARAM     KT=1036.93
PARAM     VSAT=150.0
PARAM     J=2.38
PARAM     KV=0.1012
PARAM     BM=3.094,LL=0.0001,R=0.91
PARAM     KW1=0.57
PARAM     M=1.0
PARAM     L=32.0
PARAM     E1=1.8751
PARAM     REF=1.0
PARAM     DT=0.00025
*
INTGER    N,N1,FLAG,NCHK
*
INITIAL
           N=0
           N1=0
           FLAG=0
           Q1=0.0
           Q1D=0.0
           Q1DD=0.0
           TH=0.0
           THD=0.0
           THDD=0.0
           TH1=0.0
           SIG1=(SINH(E1)-SIN(E1))/(COSH(E1)+COS(E1))
           F1=COSH(E1)-COS(E1)-SIG1*(SINH(E1)-SIN(E1))
           A=SQRT(2.0*KM*VSAT)
*
DERIVATIVE
           RR=REF*STEP(0.0)
           ER=RR-P
NOSORT
```

```
*************************************************************
*******    PARAMETERS FOR THE EQUATIONS OF MOTION    ******
*************************************************************
          UE=F1*Q1
          D111=M*(L**2+UE**2)
          D112=2*M*F1*UE
          D122=M*L*F1
          D1=G*M*(L*COS(TH)-UE*SIN(TH))
          D211=M*L*F1
          D222=M*F1**2
          D2111=-M*F1*UE
          D2=G*M*F1*COS(TH)-KW1*Q1
*************************************************************
******    THE LAGRANGE'S EQUATIONS OF THE SYSTEM    *******
*************************************************************
          TL=D122*Q1DD+D112*THD*Q1D+D2
          Q1DD=(D21I*THDD+D2111*THD**2+D2)/D222
*************************************************************
***********          THE ADAPTIVE MODEL          ************
*************************************************************
          JTOT=J+D111
          IF (ER.LT.0.0) THEN
            XDOT=-A*K1*SQRT(ABS(ER))
          ELSE
            XDOT=A*K1*SQRT(ER)
          END IF
*************************************************************
************            FLEXIBLE LINK            ************
*************************************************************
SORT
          XD=XDOT-K*PD
          V=LIMIT(-VSAT,VSAT,K2*XD)
NOSORT
          IF (FLAG.EQ.1) GO TO 20
          IF (V.LT.VSAT.AND.TIME.GT.0.0005) FLAG=1
          NCHK=N1
 20       CONTINUE
SORT
          PDD=KM*V
          PD=INTGRL(0.0,PDD)
          P=INTGRL(0.0,PD)
          VP=V-(KV*THD)
          IM=REALPL(0.0,LL/R,VP/R)
          TM=KT*IM
          TNET=TM-THD*BM-TL
          THDD=(1./JTOT)*TNET
          THD=INTGRL(0.0,THDD)
          THD=INTGRL(0.0,THD)
*************************************************************
************            ASSUMED MODES            ************
*************************************************************
          Q1D=INTGRL(0.0,Q1DD)
```

```
          Q1=INTGRL(0.0,Q1D)
************************************************************
***********          SAMPLING THE SYSTEM          ***********
************************************************************
SAMPLE
*
NOSORT
          IF (N.EQ.0) GO TO 30
          P=TH
          IF (N.GE.2) THEN
          TH1D=(TH-TH2)/(2.*DT)
          ELSE
          TH1D=PD
          END IF
          IF (FLAG.EQ.0) THEN
            PD=(2.*((TH-TH1)/DT))-TH1D
            IF (N.GE.2) THEN
              KM=DABS(2.*TH/(V*((N1*DT)**2)))
            END IF
          END IF
          IF (N1.NE.NCHK) THEN
            PD=(2.*((TH-TH1)/DT))-TH1D
          END IF
 30       N=N+1
          N1=N1+1
          TH2=TH1
          TH1=TH
*
TERMINAL
METHOD   RKSFX
*
CONTRL   FINTIM=2.0,DELT=0.00005,DELS=0.00025
SAVE (S1) 0.005,XDOT,THD,TH
*
GRAPH (L1/S1,DE=TEK618)
             TH(LO=0.0,SC=.2,LE=10,NI=10,UN='RAD'),...
             THD(LO=-8,SC=4.0,LE=8,NI=8),...
             XDOT(LO=-8,SC=4,LE=8,NI=8,PO=10)
*
GRAPH (L2/S1,DE=TEK618) TIME(UN='SEC'), TH(UN='RAD')
*
LABEL (L1) PHASE PLANE OF THE FLEXIBLE BEAM (USING 1-MODE)
LABEL (L2) STEP RESPONSE OF THE FLEXIBLE BEAM (USING 1-MODE)
*
END
STOP
```

C2. APPROXIMATION USING TWO ASSUMED MODES (N=2)

```
TITLE    SIMULATION PROGRAM FOR THE ADAPTIVE MODEL OF A
TITLE    PLANAR ROBOT ARM HAVING A FLEXIBLE LINK.
TITLE    THE FLEXIBILITY IS APPROXIMATED USING TWO ASSUMED
TITLE    MODES (N=2).
*
CONST    G=981.4
*
PARAM    K=1.0, K1=1.0, K2=10000.0, KM=2.341
PARAM    KT=1036.93
PARAM    VSAT=150.0
PARAM    J=2.38
PARAM    KV=0.1012
PARAM    BM=3.094, LL=0.0001,R=0.91
PARAM    M=1.0
PARAM    L=32.0
PARAM    E1=1.8751, E2=4.6941
PARAM    KW1=0.00124, KW2=0.0433
PARAM    REF=1.0
PARAM    DT=0.00025
*
INTGER   N, N1, FLAG, NCHK
*
INITIAL
          N=0
          N1=0
          FLAG=0
          QD=0.0
          Q1=0.0
          Q1D=0.0
          Q2=0.0
          Q2D=0.0
          Q2DD=0.0
          TH=0.0
          THD=0.0
          THDD=0.0
          TH1=0.0
          SIG1=(SINH(E1)-SIN(E1))/(COSH(E1)+COS(E1))
          SIG2=(SINH(E2)-SIN(E2))/(COSH(E2)+COS(E2))
          F1=COSH(E1)-COS(E1)-SIG1*(SINH(E1)-SIN(E1))
          F2=COSH(E2)-COS(E2)-SIG2*(SINH(E2)-SIN(E2))
          A=SQRT(2.0*KM*VSAT)
*
DERIVATIVE
          RR=REF*STEP(0.0)
          ER=RR-P
NOSORT
**********************************************************
******    PARAMETERS FOR THE EQUATIONS OF MOTION     ******
**********************************************************
          UE=F1*Q1+F2*Q2
```

```
          D111=M*(L**2+UE**2)
          D112=2*M*F1*UE
          D113=2*M*F2*UE
          D122=M*L*F1
          D133=M*L*F2
          D1=G*M*(L*COS(TH)-UE*SIN(TH))
          D211=M*L*F1
          D222=M*F1**2
          D233=M*F1*F2
          D2111=-M*F1*UE
          D2=G*M*F1*COS(TH)+KW1*Q1
          D311=M*L*F2
          D322=D233
          D333=M*F2**2
          D3111=-M*F2*UE
          D3=G*M*F2*COS(TH)+KW2*Q2
**********************************************************
******    THE LAGRANGE'S EQUATIONS OF THE SYSTEM     ******
**********************************************************
          TL=D122*QD+D133*Q2DD+D112*THD*Q1D+D113*THD*Q2D+D1
          Q1DD=(D211*THDD+D233*Q2DD+D2111*THD**2+D2)/D222
          Q2DD=(D311*THDD+D322*QD+D3111*THD**2+D3)/D333
          QD=Q1DD
**********************************************************
***********          THE ADAPTIVE MODEL          ***********
**********************************************************
          JTOT=J+D111
          IF (ER.LT.0.0) THEN
            XDOT=-A*K1*SQRT(ABS(ER))
          ELSE
            XDOT=A*K1*SQRT(ER)
          END IF
**********************************************************
************            FLEXIBLE LINK            ************
**********************************************************
SORT
          XD=XDOT-K*PD
          V=LIMIT(-VSAT,VSAT,K2*XD)
NOSORT
          IF (FLAG.EQ.1) GO TO 20
          IF (V.LT.VSAT.AND.TIME.GT.0.0005) FLAG=1
          NCHK=N1
 20       CONTINUE
SORT
          PDD=KM*V
          PD=INTGRL(0.0,PDD)
          P=INTGRL(0.0,PD)
          VP=V-(KV*THD)
          IM=REALPL(0.0,LL/R,VP/R)
          TM=KT*IM
          TNET=TM-THD*BM-TL
          THDD=(1./JTOT)*TNET
```

```
          THD=INTGRL(0.0,THDD)
          TH=INTGRL(0.0,THD)
************************************************************
************           ASSUMED MODES          *************
************************************************************
          Q1D=INTGRL(0.0,Q1DD)
          Q2D=INTGRL(0.0,Q2DD)
          Q1=INTGRL(0.0,Q1D)
          Q2=INTGRL(0.0,Q2D)
************************************************************
***********          SAMPLING THE SYSTEM          ***********
************************************************************
SAMPLE
NOSORT
          IF (N.EQ.0) GO TO 30
          P=TH
          IF (N.GE.2) THEN
          TH1D=(TH-TH2)/(2.*DT)
          ELSE
          TH1D=PD
          END IF
          IF (FLAG.EQ.0) THEN
            PD=(2.*((TH-TH1)/DT))-TH1D
            IF (N.GE.2) THEN
              KM=DABS(2.*TH/(V*((N1*DT)**2)))
            END IF
          END IF
          IF (N1.NE.NCHK) THEN
            PD=(2.*((TH-TH1)/DT))-TH1D
          END IF
 30       N=N+1
          N1=N1+1
          TH2=TH1
          TH1=TH
*
TERMINAL
METHOD    RKSFX
*
CONTRL    FINTIM=2.0, DELT=0.00005, DELS=0.00025
SAVE (S1)  0.005,XDOT,THD,TH
*
GRAPH (L1/S1,DE=TEK618)
             TH(LO=0.0,SC=.2,LE=10,NI=10,UN='RAD'),...
          THD(LO=-8,SC=4.0,LE=8,NI=8),...
             XDOT(LO=-8,SC=4,LE=8,NI=8,PO=10)
GRAPH (L2/S1,DE=TEK618) TIME(UN='SEC'), TH(UN='RAD')
*
LABEL (L1) PHASE PLANE OF THE FLEXIBLE ARM (USING 2-MODES)
LABEL (L2) STEP RESPONSE OF THE FLEXIBLE ARM (USING 2-MODES)
*
END
STOP
```

C3. APPROXIMATION USING THREE ASSUMED MODES (N=3)

```
TITLE    SIMULATION PROGRAM FOR THE ADAPTIVE MODEL OF A
TITLE    PLANAR ROBOT ARM HAVING A FLEXIBLE LINK.
TITLE    THE FLEXIBILITY IS APPROXIMATED USING THREE ASSUMED
TITLE    MODES (N=3).
*
CONST    G=981.4
*
PARAM    K=1.0, K1=1.0, K2=10000.0, KM=2.341
PARAM    KT=1036.93
PARAM    VSAT=150.0
PARAM    J=2.38
PARAM    KV=0.1012
PARAM    BM=3.094, LL=0.0001,R=0.91
PARAM    M=1.0
PARAM    L=32.0
PARAM    E1=1.8751, E2=4.6941, E3=7.85467
PARAM    KW1=0.00124, KW2=0.0433, KW3=0.357
PARAM    REF=1.0
PARAM    DT=0.00025
*
INTGER   N, N1, FLAG, NCHK
*
INITIAL
          N=0
          N1=0
          FLAG=0
          QD1=0.0
          QD2=0.0
          Q1=0.0
          Q1D=0.0
          Q2=0.0
          Q2D=0.0
          Q3=0.0
          Q3D=0.0
          Q3DD=0.0
          TH=0.0
          THD=0.0
          THDD=0.0
          TH1=0.0
          SIG1=(SINH(E1)-SIN(E1))/(COSH(E1)+COS(E1))
          SIG2=(SINH(E2)-SIN(E2))/(COSH(E2)+COS(E2))
          SIG3=(SINH(E3)-SIN(E3))/(COSH(E3)+COS(E3))
          F1=COSH(E1)-COS(E1)-SIG1*(SINH(E1)-SIN(E1))
          F2=COSH(E2)-COS(E2)-SIG2*(SINH(E2)-SIN(E2))
          F3=COSH(E3)-COS(E3)-SIG3*(SINH(E3)-SIN(E3))
          A=SQRT(2.0*KM*VSAT)
*
DERIVATIVE
          RR=REF*STEP(0.0)
          ER=RR-P
```

```
NOSORT
*************************************************************
******    PARAMETERS FOR THE EQUATIONS OF MOTION     ******
*************************************************************
          UE=F1*Q1+F2*Q2+F3*Q3
          D111=M*(L**2+UE**2)
          D112=2*M*F1*UE
          D113=2*M*F2*UE
          D114=2*M*F3*UE
          D122=M*L*F1
          D133=M*L*F2
          D144=M*L*F3
          D1=G*M*(L*COS(TH)-UE*SIN(TH))
          D211=M*L*F1
          D222=M*F1**2
          D233=M*F1*F2
          D244=M*F1*F3
          D2111=-M*F1*UE
          D2=G*M*F1*COS(TH)+KW1*Q1
          D311=M*L*F2
          D322=D233
          D333=M*F2**2
          D344=M*F2*F3
          D3111=-M*F2*UE
          D3=G*M*F2*COS(TH)+KW2*Q2
          D411=M*L*F3
          D422=D244
          D433=D344
          D444=M*F3**2
          D4111=-M*F3*UE
          D4=G*M*F3*COS(TH)+KW3*Q3
*************************************************************
******    THE LAGRANGE'S EQUATIONS OF THE SYSTEM     ******
*************************************************************
          TL=D122*QD1+D133*QD2+D144*Q3DD...
              +D112*THD*Q1D+D113*THD*Q2D+D114*THD*Q3D+D1
          Q1DD=(D211*THDD+D233*QD2+D244*Q3DD...
              +D2111*THD**2+D2)/D222
          Q2DD=(D311*THDD+D322*QD1+D344*Q3DD...
              +D3111*THD**2+D3)/D333
          Q3DD=(D411*THDD+D422*QD1+D433*QD2...
              +D4111*THD**2+D4)/D444
          QD1=Q1DD
          QD2=Q2DD
*************************************************************
***********          THE ADAPTIVE MODEL          ************
*************************************************************
          JTOT=J+D111
          IF (ER.LT.0.0) THEN
            XDOT=-A*K1*SQRT(ABS(ER))
          ELSE
            XDOT=A*K1*SQRT(ER)
```

```
          END IF
*****************************************************
************          FLEXIBLE LINK          ************
*****************************************************
SORT
          XD=XDOT-K*PD
          V=LIMIT(-VSAT,VSAT,K2*XD)
NOSORT
          IF (FLAG.EQ.1) GO TO 20
          IF (V.LT.VSAT.AND.TIME.GT.0.0005) FLAG=1
          NCHK=N1
 20       CONTINUE
SORT
          PDD=KM*V
          PD=INTGRL(0.0,PDD)
          P=INTGRL(0.0,PD)
          VP=V-(KV*THD)
          IM=REALPL(0.0,LL/R,VP/R)
          TM=KT*IM
          TNET=TM-THD*BM-TL
          THDD=(1./JTOT)*TNET
          THD=INTGRL(0.0,THDD)
          TH=INTGRL(0.0,THD)
*****************************************************
************          ASSUMED MODES          ************
*****************************************************
          Q1D=INTGRL(0.0,Q1DD)
          Q2D=INTGRL(0.0,Q2DD)
          Q3D=INTGRL(0.0,Q3DD)
          Q1=INTGRL(0.0,Q1D)
          Q2=INTGRL(0.0,Q2D)
          Q3=INTGRL(0.0,Q3D)
*****************************************************
***********          SAMPLING THE SYSTEM          ***********
*****************************************************
SAMPLE
*
NOSORT
          IF (N.EQ.0) GO TO 30
          P=TH
          IF (N.GE.2) THEN
            TH1D=(TH-TH2)/(2.*DT)
          ELSE
            TH1D=PD
          END IF
          IF (FLAG.EQ.0) THEN
            PD=(2.*((TH-TH1)/DT))-TH1D
            IF (N.GE.2) THEN
              KM=DABS(2.*TH/(V*((N1*DT)**2)))
            END IF
          END IF
          IF (N1.NE.NCHK) THEN
```

```
            PD=(2.*((TH-TH1)/DT))-TH1D
          END IF
 30       N=N+1
          N1=N1+1
          TH2=TH1
          TH1=TH
*
TERMINAL
METHOD    RKSFX
*
CONTRL   FINTIM=3.0, DELT=0.00005, DELS=0.00025
SAVE (S1) 0.005,XDOT,THD,TH
*
GRAPH (L1/S1,DE=TEK618)
             TH(LO=0.0,SC=.2,LE=10,NI=10,UN='RAD'),...
             THD(LO=-8,SC=4.0,LE=8,NI=8),...
             XDOT(LO=-8,SC=4.0,LE=8,NI=8,PO=10)
*
GRAPH (L2/S1,DE=TEK618)  TIME(UN='SEC'), TH(UN='RAD')
*
LABEL (L1) PHASE PLANE OF THE FLEXIBLE ARM (USING 3-MODES)
LABEL (L2) STEP RESPONSE OF THE FLEXIBLE ARM (USING 3-MODES)
*
END
STOP
```

APPENDIX D

DERIVATION OF THE MODEL FOR A TWO LINKS PLANAR ROBOT ARM HAVING ONE RIGID AND ONE FLEXIBLE LINKS

In this Appendix, a complete derivation will be given for the mathematical model of the proposed two links planar robot arm having the first link rigid and the second link flexible. The set of the second order differential equations of motion that describe the proposed system will be derived using the Lagrangian dynamics approach. For the sake of the analysis Figure 3.2 given in Chapter III, illustrating the coordinates of the system for both the rigid and the flexible links will be repeated as Figure D.1, in order to give a better understanding in the derivation of the kinetic and the potential energies.

The Lagrangian function will again be given as L=T-V, where T and V are the kinetic and the potential energies of the system respectively. The kinetic and potential energies will derived from the kinetic and potential energies of the individual links. Therefore $T=T_1+T_2$ and $V=V_1+V_2$, where T_1,V_1 and T_2,V_2 are the kinetic and potential energies of the rigid and the flexible link respectively.

The kinetic energy for the rigid link will be given as:

$$T_1 = \frac{1}{2} m_1 l_1^2 \dot{\theta}_1^2 \qquad (D.1)$$

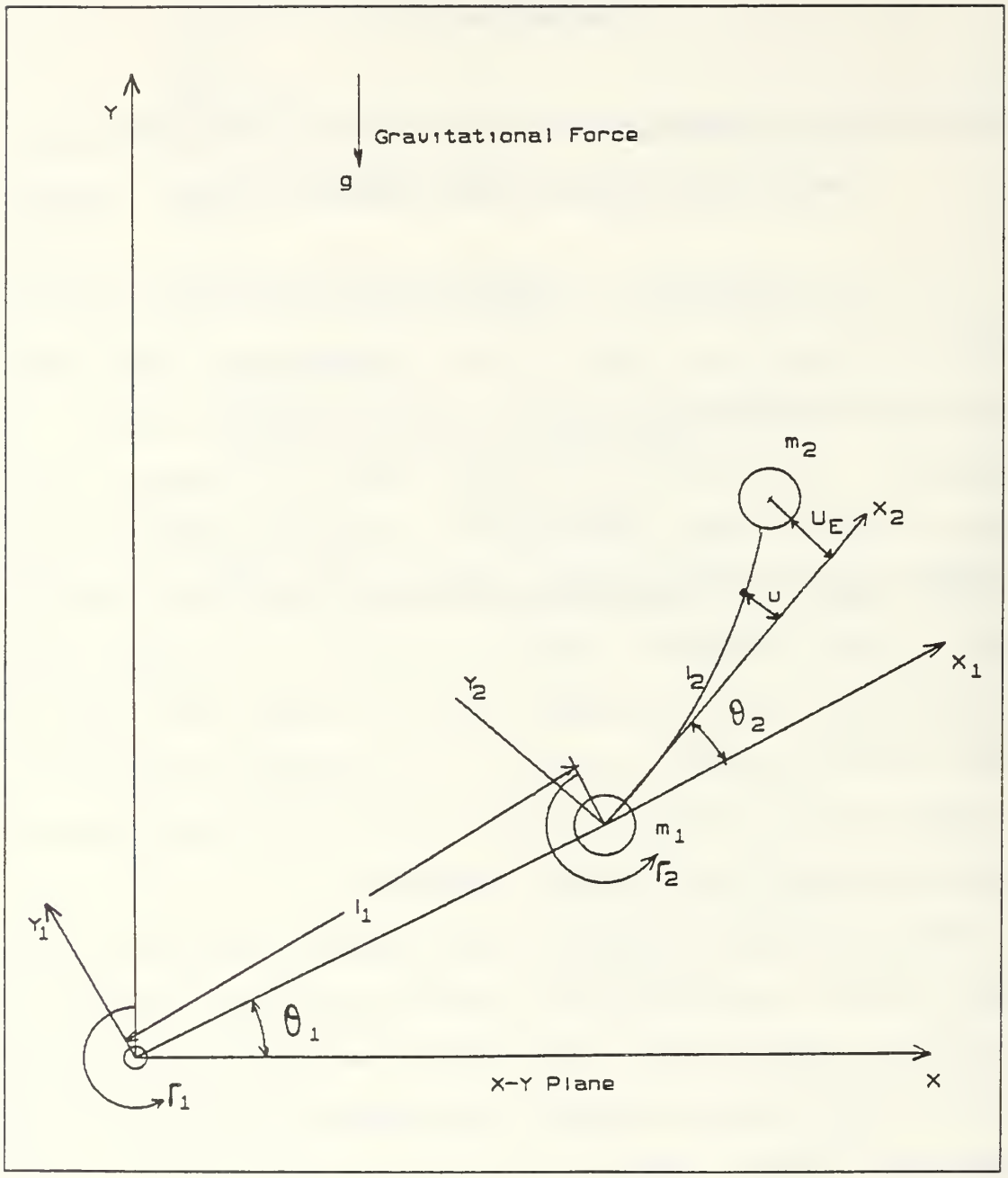

Figure D.1 Coordinates configuration of the (rigid-flexible) two links planar robot system.

The kinetic energy of the flexible link will be:

$$T = \frac{1}{2} m_2 (\dot{x}_2^2 + \dot{y}_2^2) \qquad (D.2)$$

where x_2 and y_2 are the end-point Cartesian coordinates of

the flexible beam. The transformation to the generalized coordinates, that were selected to describe that system, was given in Chapter III, with equations 3.2 and 3.3. Taking the derivatives of these equations the velocity components will be represented as:

$$\dot{x}_2 = -l_1\dot{\theta}_1\sin\theta_1 - l_2(\dot{\theta}_1+\dot{\theta}_2)\sin(\theta_1+\theta_2) - \dot{u}_E\sin(\theta_1+\theta_2) - u_E(\dot{\theta}_1+\dot{\theta}_2)\sin(\theta_1+\theta_2) \tag{D.3}$$

$$\dot{y}_2 = l_1\dot{\theta}_1\cos\theta_1 + l_2(\dot{\theta}_1+\dot{\theta}_2)\cos(\theta_1+\theta_2) - \dot{u}_E\cos(\theta_1+\theta_2) - u_E(\dot{\theta}_1+\dot{\theta}_2)\sin(\theta_1+\theta_2) \tag{D.4}$$

Taking the squares of the above equations then:

$$\begin{aligned}\dot{x}_2^2 = {} & l_1^2\dot{\theta}_1^2\sin^2\theta_1 + l_2^2(\dot{\theta}_1+\dot{\theta}_2)^2\sin^2(\theta_1+\theta_2) + \dot{u}^2\sin^2(\theta_1+\theta_2) \\ & + u_E(\dot{\theta}_1+\dot{\theta}_2)^2\cos^2(\theta_1+\theta_2) + l_1l_2\dot{\theta}_1(\dot{\theta}_1+\dot{\theta}_2)\sin\theta_1\sin(\theta_1+\theta_2) \\ & + \dot{u}_E\sin(\theta_1+\theta_2)[l_1\dot{\theta}_1\sin\theta_1 + l_2(\dot{\theta}_1+\dot{\theta}_2)\sin(\theta_1+\theta_2)] \\ & + l_1u_E\dot{\theta}_1(\dot{\theta}_1+\dot{\theta}_2)\sin\theta_1\cos(\theta_1+\theta_2) \\ & + l_2\dot{u}_E(\dot{\theta}_1+\dot{\theta}_2)\sin^2(\theta_1+\theta_2) \\ & + l_2u_E(\dot{\theta}_1+\dot{\theta}_2)^2\sin(\theta_1+\theta_2)\cos(\theta_1+\theta_2) \\ & + u_E\dot{u}_E(\dot{\theta}_1+\dot{\theta}_2)\sin(\theta_1+\theta_2)\cos(\theta_1+\theta_2)\end{aligned} \tag{D.5}$$

$$\begin{aligned}\dot{y}_2^2 = {} & l_1^2\dot{\theta}_1^2\cos^2\theta_1 + l_2^2(\dot{\theta}_1+\dot{\theta}_2)^2\cos^2(\theta_1+\theta_2) + \dot{u}_E^2\cos^2(\theta_1+\theta_2) \\ & + u_E^2(\dot{\theta}_1+\dot{\theta}_2)^2\cos^2(\theta_1+\theta_2) + l_1l_2\dot{\theta}_1(\dot{\theta}_1+\dot{\theta}_2)\cos\theta_1\cos(\theta_1+\theta_2)\end{aligned}$$

$$+l_1\dot{u}_E\dot{\theta}_1\cos\theta_1\cos(\theta_1+\theta_2)+l_2\dot{u}_E(\dot{\theta}_1+\dot{\theta}_2)\cos^2(\theta_1+\theta_2)$$

$$-l_1u_E\dot{\theta}_1(\dot{\theta}_1+\dot{\theta}_2)\cos\theta_1\sin(\theta_1+\theta_2) \qquad (D.6)$$

$$-l_2u_E(\dot{\theta}_1+\dot{\theta}_2)\cos(\theta_1+\theta_2)\sin(\theta_1+\theta_2)$$

$$-\dot{u}_Eu_E(\dot{\theta}_1+\dot{\theta}_2)\cos(\theta_1+\theta_2)\sin(\theta_1+\theta_2)$$

Combining Equations D.5 and D.6 into Equation D.2, and using trigonometric identities to simplify the expression, the kinetic energy for the flexible link obtains the form:

$$T_2 = \frac{1}{2}\, m_2[l_1^2\dot{\theta}_1^2+l_2^2(\dot{\theta}_1+\dot{\theta}_2)^2+ \dot{u}_E^2+ u_E^2(\dot{\theta}_1+\dot{\theta}_2)^2$$

$$+2l_1l_2\dot{\theta}_1(\dot{\theta}_1+\dot{\theta}_2)\cos\theta_2+ 2l_1\dot{u}_E\dot{\theta}_1\cos\theta_2 \qquad (D.7)$$

$$+2l_2(\dot{\theta}_1+\dot{\theta}_2)u_E+ 2l_1u_E\dot{\theta}_1(\dot{\theta}_1+\dot{\theta}_2)\sin(-\theta_2)]$$

To obtain the final form of the kinetic energy for the flexible link, the flexible displacement u_E and velocity u_E can be substituted from the expressions derived in Chapter III as given by Equations 3.6 and 3.7 respectively. For motions of the flexible arm in the range $-90°\leq\theta_2\leq90°$ then $\sin(-\theta_2)= -\sin\theta_2$. Therefore the total kinetic energy of the system is:

$$T = \frac{1}{2}\,[m_1l_1^2\dot{\theta}_1^2+m_2l_1^2\dot{\theta}_1^2+m_2l_1^2(\dot{\theta}_1+\dot{\theta}_2)^2+m_2(f_{1E}\dot{g}_1+f_{2E}\dot{g}_2)^2]$$

$$+ \frac{1}{2}\, m_2(\dot{\theta}_1+\dot{\theta}_2)^2(f_{1E}g_1+f_{2E}g_2)^2+m_2l_1l_2\dot{\theta}_1(\dot{\theta}_1+\dot{\theta}_2)\cos\theta_2 \qquad (D.8)$$

$$+ m_2l_1\dot{\theta}_1(f_{1E}\dot{g}_1+f_{2E}\dot{g}_2)\cos\theta_2+m_2l_2(\dot{\theta}_1+\dot{\theta}_2)(f_{1E}\dot{g}_1+f_{2E}\dot{g}_2)$$

$$- m_2 l_1 \dot{\theta}_1 (\dot{\theta}_1+\dot{\theta}_2)(f_{1E}g_1+f_{2E}g_2)\sin\theta_2$$

The potential energy for the rigid link will be:

$$V_1 = gm_1 l_1 \sin\theta_1 \tag{D.9}$$

For the flexible link the potential energy will be composed of the energy associated with the rigid motion plus the elastic potential energy. Assuming the magnitude of the elastic motion small compared to the overall motion, meaning small amplitude of the flexible displacement u, the potential energy of the flexible link can be written as:

$$V_2 = gm_2[l_1\sin\theta_1+l_2\sin(\theta_1+\theta_2)+u_E\cos(\theta_1+\theta_2)] - \frac{1}{2}\int_0^{l_2} EI\left(\frac{\delta^2 u}{\delta x^2}\right) dx \tag{D.10}$$

where EI is the stiffness of the flexible link, assumed constant for the purpose of this model.

Substituting the flexible displacement u_E with the equivalent expression, derived in Chapter III, given by Equation 3.6, the integral involved in the potential energy of the flexible beam can be evaluated as follows:

$$\int_0^{l_2} EI\left(\frac{\delta^2 u}{\delta x^2}\right) dx = EI\int_0^{l_2} (\ddot{f}_1 g_1+\ddot{f}_2 g_2)^2 dx = KW_1 g_1^2+KW_2 g_2^2 \tag{D.11}$$

where

$$KW_1 = EI\int_0^{l_2} (\ddot{f}_1 \ddot{f}_1) dx$$

and

$$KW_2 = EI \int_0^{l_2} (f_2'' \; f_2'') \, dx$$

Therefore the total potential energy of the system becomes:

$$V = g[m_1 l_1 \sin\theta_1 + m_2 l_1 \sin\theta_1 + m_2 l_2 \sin(\theta_1+\theta_2) + m_2(f_{1E}g_1 + f_{2E}g_2)\cos(\theta_1+\theta_2)] - \frac{1}{2}(KW_1 g_1^2 + KW_2 g_2^2) \quad \text{(D.12)}$$

The Lagrangian function, L, will then can be computed from the Equations D.8 and D.12, as follows:

$$\begin{aligned} L = {} & \frac{1}{2}[(m_1+m_2)l_1^2\dot{\theta}_1^2 + m_2 l_2^2(\dot{\theta}_1+\dot{\theta}_2)^2 + m_2(\dot{\theta}_1+\dot{\theta}_2)^2(f_{1E}g_1+f_{2E}g_2)^2 \\ & + m_2(f_{1E}\dot{g}_1+f_{2E}\dot{g}_2)^2] + m_2 l_1 l_2 \dot{\theta}_1(\dot{\theta}_1+\dot{\theta}_2)\cos\theta_2 \\ & + m_2 l_1 \dot{\theta}_1(f_{1E}\dot{g}_1+f_{2E}\dot{g}_2)\cos\theta_2 + m_2 l_1(\dot{\theta}_1+\dot{\theta}_2)(f_{1E}\dot{g}_1+f_{2E}\dot{g}_2) \\ & - m_2 l_1 \dot{\theta}_1(\dot{\theta}_1+\dot{\theta}_2)(f_{1E}g_1+f_{2E}g_2)\sin\theta_2 - [(m_1+m_2)l_1\sin\theta_1 \\ & + m_2 l_2 \sin(\theta_1+\theta_2) + m_2(f_{1E}g_1+f_{2E}g_2)\cos(\theta_1+\theta_2)]g \\ & + \frac{1}{2}(KW_1 g_1^2 + KW_2 g_2^2) \end{aligned} \quad \text{(D.13)}$$

Having derived the Lagrangian function, the differential equations that describe this system can be obtained by forming the Lagrange's equations that have the general form given from Equation 3.8 in Chapter III. For this particular system the generalized coordinates are defined to be θ_1, θ_2, g_1 and g_2. Therefore a set of four nonlinear second order differential equations will be obtained by taking partial derivatives of the Lagrangian function with respect to each generalized coordinate and their corresponding velocities

and differentiated with respect to time. This approach with respect to Θ_1 gives:

$$\frac{\delta L}{\delta \Theta_1} = -[(m_1+m_2)l_1\cos\Theta_1 + m_2 l_2 \cos(\Theta_1+\Theta_2) + m_2(f_{1E}g_1+f_{2E}g_2)\sin(\Theta_1+\Theta_2)]g \tag{D.14}$$

$$\begin{aligned}\frac{\delta L}{\delta \dot{\Theta}_1} &= (m_1+m_2)l_1^2\dot{\Theta}_1 + m_2 l_2^2(\dot{\Theta}_1+\dot{\Theta}_2) + m_2(\dot{\Theta}_1+\dot{\Theta}_2)(f_{1E}g_1+f_{2E}g_2)^2 \\ &+ m_2 l_1 l_2 \dot{\Theta}_2 \cos\Theta_2 + 2m_2 l_1 l_2 \dot{\Theta}_1 \cos\Theta_2 + m_2 l_1 (f_{1E}\dot{g}_1+f_{2E}\dot{g}_2)\cos\Theta_2 \\ &+ m_2 l_2 (f_{1E}\dot{g}_1+f_{2E}\dot{g}_2) - m_2 l_1 \dot{\Theta}_2 (f_{1E}g_1+f_{2E}g_2)\sin\Theta_2 \\ &- 2m_2 l_1 \dot{\Theta}_1 (f_{1E}g_1+f_{2E}g_2)\sin\Theta_2\end{aligned} \tag{D.15}$$

$$\begin{aligned}\frac{d}{dt}\left(\frac{\delta L}{\delta \dot{\Theta}_1}\right) &= (m_1+m_2)l_1^2\ddot{\Theta}_1 + m_2 l_2^2\ddot{\Theta}_1 + m_2 l_2^2\ddot{\Theta}_2 + m_2\ddot{\Theta}_1 (f_{1E}g_1+f_{2E}g_2) \\ &+ 2m_2\dot{\Theta}_1 f_{1E}^2\dot{g}_1 g_1 + 2m_2\dot{\Theta}_1 f_{1E}f_{2E}\dot{g}_1 g_2 + 2m_2\dot{\Theta}_1 f_{1E}f_{2E}\dot{g}_2 g_1 \\ &+ 2m_2\dot{\Theta}_1 f_{2E}^2\dot{g}_2 g_2 + 2m_2\dot{\Theta}_2 f_{1E}^2\dot{g}_1 g_1 + 2m_2\dot{\Theta}_2 f_{1E}f_{2E}\dot{g}_1 g_2 \\ &+ 2m_2\dot{\Theta}_2 f_{1E}f_{2E}\dot{g}_2 g_1 + 2m_2\dot{\Theta}_2 f_{2E}^2\dot{g}_2 g_2 + m_2 l_1 l_2 \ddot{\Theta}_2 \cos\Theta_2 \\ &+ 2m_2 l_1 l_2 \ddot{\Theta}_1 \cos\Theta_2 - m_2 l_1 l_2 \ddot{\Theta}_2 \sin\Theta_2 - 2m_2 l_1 l_2 \dot{\Theta}_1\dot{\Theta}_2\sin\Theta_2 \\ &+ m_2 l_1 \cos\Theta_2 (f_{1E}\ddot{g}_1 + f_{2E}\ddot{g}_2) - m_2 l_1 \dot{\Theta}_2 (f_{1E}\dot{g}_1+f_{2E}\dot{g}_2)\sin\Theta_2 \\ &+ m_2 l_2 f_{1E}\ddot{g}_1 + m_2 l_2 f_{2E}\ddot{g}_2 - m_2 l_1 \dot{\Theta}_2 (f_{1E}\dot{g}_1+f_{2E}\dot{g}_2)\sin\Theta_2 \\ &- m_2 l_1 \dot{\Theta}_2^2 (f_{1E}g_1+f_{2E}g_2)\cos\Theta_2 - m_2 l_1 \dot{\Theta}_2 \sin\Theta_2 (f_{1E}\dot{g}_1+f_{2E}\dot{g}_2) \\ &- 2m_2 l_1 (f_{1E}g_1+f_{2E}g_2)(\ddot{\Theta}_1 \sin\Theta_2 + \dot{\Theta}_1\dot{\Theta}_2\cos\Theta_2)\end{aligned} \tag{D.16}$$

$$-2m_2l_1\dot{\theta}_1f_{1E}\dot{g}_1\sin\theta_2-2m_2l_1\dot{\theta}_1f_{2E}\dot{g}_2\sin\theta_2$$

Combining the above Equations D.14 and D.16 the first non-linear second order differential equation can be derived, as given in Chapter III by Equation 3.9. The same approach with respect to θ_2 gives:

$$\frac{\delta L}{\delta\theta_2} =-m_2l_1l_2\dot{\theta}_1(\dot{\theta}_1+\dot{\theta}_2)\sin\theta_2-m_2l_1\dot{\theta}_1(f_{1E}\dot{g}_1+f_{2E}\dot{g}_2)\sin\theta_2$$

$$-m_2l_1\dot{\theta}_1(\dot{\theta}_1+\dot{\theta}_2)(f_{1E}g_1+f_{2E}g_2)\cos\theta_2- g[m_2l_2\cos(\theta_1+\theta_2) \quad \text{(D.17)}$$

$$-m_2(f_{1E}g_1+f_{2E}g_2)\sin(\theta_1+\theta_2)]$$

$$\frac{\delta L}{\delta\dot{\theta}_2} = m_2l_2^2\dot{\theta}_2+m_2\dot{\theta}_1(f_{1E}g_1+f_{2E}g_2)^2+m_2\dot{\theta}_2(f_{1E}g_1+f_{2E}g_2)^2$$

$$+m_2l_2(f_{1E}\dot{g}_1+f_{2E}\dot{g}_2)-m_2l_1\dot{\theta}_1(f_{1E}g_1+f_{2E}g_2)\sin\theta_2 \quad \text{(D.18)}$$

$$+m_2l_2^2\dot{\theta}_1+m_2l_1l_2\dot{\theta}_1\cos\theta_2$$

$$\frac{d}{dt}\left(\frac{\delta L}{\delta\dot{\theta}_2}\right)=m_2l_2^2\ddot{\theta}_1 +m_2l_2^2\ddot{\theta}_2 +m_2(f_{1E}g_1+f_{2E}g_2)^2\ddot{\theta}_1 +2m_2f_{1E}^2g_1\dot{g}_1\dot{\theta}_1$$

$$+2m_2f_{1E}f_{2E}\dot{g}_1g_2\dot{\theta}_1+2m_2f_{1E}f_{2E}g_1\dot{g}_2\dot{\theta}_1+2m_2f_{2E}^2g_2\dot{g}_2\dot{\theta}_1$$

$$+m_2(f_{1E}g_1+f_{2E}g_2)^2\ddot{\theta}_2 +2m_2f_{1E}^2g_1\dot{g}_1\dot{\theta}_2+2m_2f_{1E}f_{2E}\dot{g}_1g_2\dot{\theta}_2$$

$$+2m_2f_{1E}f_{2E}g_1\dot{g}_2\dot{\theta}_2+2m_2f_{2E}^2g_2\dot{g}_2\dot{\theta}_2+m_2l_1l_2\ddot{\theta}_1\cos\theta_2 \quad \text{(D.19)}$$

$$-m_2l_1l_2\dot{\theta}_1\dot{\theta}_2\sin\theta_2+m_2l_2f_{1E}\ddot{g}_1 -m_2l_1f_{1E}\ddot{\theta}_1\dot{g}_1\sin\theta_2$$

$$-m_2l_1f_{2E}\dot{\theta}_1\dot{g}_2\sin\theta_2-m_2l_2(f_{1E}g_1+f_{2E}g_2)\ddot{\theta}_1\sin\theta_2$$

$$-m_2l_1(f_{1E}g_1+f_{2E}g_2)\dot{\theta}_1\dot{\theta}_2\cos\theta_2+m_2l_2f_{2E}\ddot{g}_2$$

The second nonlinear second-order differential equation that describes the system will result from the above Equations D.17 and D.19, having the final form given by the Equation 3.10 in Chapter III. With respect to the generalized coordinate g_1 this approach gives:

$$\frac{\delta L}{\delta g_1} = m_2(\dot{\theta}_1+\dot{\theta}_2)^2 f_{1E}^2 g_1 + m_2(\dot{\theta}_1+\dot{\theta}_2)^2 f_{1E} f_{2E} g_2 - m_2 l_1 \dot{\theta}_1 (\dot{\theta}_1+\dot{\theta}_2) f_{1E} \sin\theta_2 - g m_2 f_{1E} \cos(\theta_1+\theta_1) + KW_1 g_1 \tag{D.20}$$

$$\frac{\delta L}{\delta \dot{g}_1} = m_2[f_{1E}^2 \dot{g}_1 + f_{1E} f_{2E} \dot{g}_2 + l_1 \dot{\theta}_1 f_{1E} \cos\theta_2 + l_2(\dot{\theta}_1+\dot{\theta}_2) f_{1E}] \tag{D.21}$$

$$\frac{d}{dt}\left(\frac{\delta L}{\delta \dot{g}_1}\right) = m_2 f_{1E}^2 \ddot{g}_1 + m_2 f_{1E} f_{2E} \ddot{g}_2 + m_2 l_1 f_{1E} \ddot{\theta}_1 \cos\theta_2 - m_2 l_1 f_{1E} \dot{\theta}_1 \dot{\theta}_2 \sin\theta_2 + m_2 l_2 f_{1E} \ddot{\theta}_1 + m_2 l_2 f_{1E} \ddot{\theta}_2 \tag{D.22}$$

Combining Equations D.20 and D.22 the third nonlinear second order differential equation can be produced with its final form given in Chapter III by Equation 3.11. The last Equation 3.12 of the second order differential equations given in Chapter III, can be derived from the given below (Equations D.23 and D.25). These equations can be derived by following the same procedure with respect to the fourth generalized coordinate g_2.

$$\frac{\delta L}{\delta g_2} = m_2(\dot{\theta}_1+\dot{\theta}_2)^2 f_{2E}^2 g_2 + m_2(\dot{\theta}_1+\dot{\theta}_2)^2 f_{1E} f_{2E} g_1 - m_2 l_1 \dot{\theta}_1 (\dot{\theta}_1+\dot{\theta}_2) f_{2E} \sin\theta_2 - g m_2 f_{2E} \cos(\theta_1+\theta_2) + KW_2 g_2 \tag{D.23}$$

$$\frac{\delta L}{\delta \dot{g}_2} = m_2[f_{2E}^2 \dot{g}_2 + f_{1E} f_{2E} \dot{g}_1 + l_1 \dot{\theta}_1 f_{2E} \cos\theta_2 + l_2(\dot{\theta}_1 + \dot{\theta}_2) f_{2E}] \quad \text{(D.24)}$$

$$\frac{d}{dt}\left(\frac{\delta L}{\delta \dot{g}_2}\right) = m_2 f_{2E}^2 \ddot{g}_2 + m_2 f_{1E} f_{2E} \ddot{g}_1 + m_2 l_1 f_{2E} \ddot{\theta}_1 \cos\theta_2 + m_2 l_1 f_{2E} \ddot{\theta}_1 + m_2 l_2 f_{2E} \ddot{\theta}_2 - m_2 l_1 f_{2E} \dot{\theta}_1 \dot{\theta}_2 \sin\theta_2 \quad \text{(D.25)}$$

APPENDIX E

SIMULATION PROGRAM FOR THE BASIC MODEL OF THE VELOCITY CURVE FOLLOW CONTROL SCHEME

```
TITLE     ADAPTIVE VELOCITY CURVE FOLLOW CONTROL SCHEME
*
PARAM     K1=0.8, K2=10000., KM=0.185, VSAT=300.0, K=1.0
PARAM     INP=1.0
*
INITIAL
          A=SQRT(2.*KM*VSAT)
          VEL=0.0
*
DERIVATIVE
          R=INP*STEP(0.0)
          ER=R-C
NOSORT
          IF (ER.LT.0.0)  THEN
             VEL=-A*K1*SQRT(ABS(ER))
          ELSE
             VEL=A*K1*SQRT(ER)
          END IF
SORT
          DVEL=VEL-FBVEL
          FBVEL=K*CDOT
          AMP=LIMIT(-VSAT,VSAT,K2*DVEL)
          CDDOT=KM*AMP
          CDOT=INTGRL(0.0,CDDOT)
          C=INTGRL(0.0,CDOT)
*
METHOD RKSFX
CONTROL   FINTIM=0.4, DELT=0.0001
SAVE    (S1) 0.001, C, CDOT, VEL
SAVE    (S2) 0.001, C, R
*
GRAPH   (G1/S1,DE=TEK618,PO=0,0)
                C(LE=8,NI=10,SC=0.1,UN='RAD'),...
                VEL(LE=4,NI=4,LO=0,SC=$AR,UN='RAD/SEC'),...
                CDOT(LE=4,NI=4,LO=0,SC=$AR,UN='RAD/SEC',PO=8)
GRAPH   (G2/S2,DE=TEK618,OV,PO=0,5)
                TIME(LE=8,UN='SECOND'),...
                C(LE=4,NI=4,LO=0,UN='RAD',SC=0.5),...
                R(LE=4,NI=4,LO=0,SC=0.5,AX=OMIT)
LABEL   (G1) PHASE PLANE
LABEL   (G2) STEP RESPONSE
END
STOP
```

APPENDIX F

SIMULATION PROGRAM FOR THE TWO LINKS (RIGID-RIGID) PLANAR ROBOT ARM

```
TITLE    SIMULATION PROGRAM OF THE ADAPTIVE MODEL FOR THE
TITLE    PLANAR ROBOT ARM HAVING TWO RIGID LINKS.
*
TITLE    THIS PROGRAM WAS USED FOR THE SIMULATION RESULTS
TITLE    FOR THAT SYSTEM, WITH OR WITHOUT LOAD AS ALSO
TITLE    WITH OR WITHOUT THE GRAVITATIONAL FORCES.
*
CONST    G=981.4
CONST    ZL=0.0
*
PARAM    K1=0.8,K2=10000.,K3=1.0,KM1=0.162,KM2=2.045,K=1.0
PARAM    KT1=1036.93,KT2=1036.93
PARAM    VSAT1=300.0,VSAT2=150.0
PARAM    J1=2.38,J2=2.38
PARAM    KV1=0.1012,KV2=0.1012
PARAM    R1=0.91,R2=0.91,L=0.0001
PARAM    BM1=3.094,BM2=3.094
PARAM    L1=40.0,L2=32.0
PARAM    M1=3.0,M2=0.5
PARAM    REF1=1.0,REF2=1.0
PARAM    DT=0.00025
*
INTGER   N,N1,N2,NCHK1,NCHK2,FLAG1,FLAG2
*
INITIAL
         N=0
         N1=0
         N2=0
         FLAG1=0
         FLAG2=0
         P1=0.0
         P2=0.0
         P1D=0.0
         P2D=0.0
         TH1=0.0
         TH2=0.0
         TH11=0.0
         TH21=0.0
         TH1D=0.0
         TH2D=0.0
         TH1DD=0.0
         TH2DD=0.0
         A1=SQRT(2.*KM1*VSAT1)
         A2=SQRT(2.*KM2*VSAT2)
```

```
*
DERIVATIVE
          RR1=REF1*STEP(0.0)
          RR2=REF2*STEP(0.0)
          RRD2=TRANSP(200,0.0,0.1,RR2)
          E1=RR1-P1
          E2=RRD2-P2
NOSORT
**********************************************************
******     PARAMETERS FOR THE EQUATIONS OF MOTION      ******
**********************************************************
          TH=TH1+TH2
          D11=(M1+M2)*(L1**2)+M2*(L2**2)+2*M2*L1*L2*COS(TH2)
          D12=M2*(L2**2)+M2*L1*L2*COS(TH2)
          D22=M2*(L2**2)
          D122=-M2*L1*L2*SIN(TH2)
          D112=D122
          D211=-D112
          D1=(M1+M2)*G*L1*COS(TH1)+M2*G*L2*COS(TH)
          D2=M2*G*L2*COS(TH)
**********************************************************
**********         DIFFERENTIAL EQUATIONS          **********
**********************************************************
          TL1=D12*TH2DD+D122*TH2D**2+2*D112*TH1D*TH2D+D1
          TL2=D12*TH1DD+D211*TH1D**2+D2
*
          JTOT1=J1+D11
          JTOT2=J2+D22
          IF (E1.LT.0.0) THEN
            X1DOT=-A1*K1*SQRT(ABS(E1))
          ELSE
            X1DOT=A1*K1*SQRT(E1)
          END IF
          IF (E2.LT.0.0) THEN
            X2DOT=-A2*K3*SQRT(ABS(E2))
          ELSE
            X2DOT=A2*K3*SQRT(E2)
          END IF
SORT
**********************************************************
*************              LINK  1             *************
**********************************************************
          X1D=X1DOT-K*P1D
          V1=LIMIT(-VSAT1,VSAT1,K2*X1D)
NOSORT
          IF (FLAG1.EQ.1) GO TO 5
          IF (V1.LT.VSAT1.AND.TIME.GT.0.0005) FLAG1=1
          NCHK1=N1
 5        CONTINUE
SORT
          P1DD=KM1*V1
          P1D=INTGRL(0.0,P1DD)
```

```
          P1=INTGRL(0.0,P1D)
          VP1=V1-(KV1*TH1D)
          IM1=REALPL(0.0,L/R1,VP1/R1)
          TM1=KT1*IM1
          TNET1=TM1-TH1D*BM1-TL1
          TH1DD=(1./JTOT1)*TNET1
          TH1D=INTGRL(0.0,TH1DD)
          TH1=INTGRL(0.0,TH1D)
**********************************************************
**************              LINK  2             **************
**********************************************************
          X2D=X2DOT-K*P2D
          V2=LIMIT(-VSAT2,VSAT2,K2*X2D)
NOSORT
          IF (FLAG2.EQ.1) GO TO 7
          IF (V2.LT.VSAT2.AND.TIME.GT.0.0005) FLAG2=1
          NCHK2=N2
 7        CONTINUE
SORT
          P2DD=KM2*V2
          P2D=INTGRL(0.0,P2DD)
          P2=INTGRL(0.0,P2D)
          VP2=V2-(KV2*TH2D)
          IM2=REALPL(0.0,L/R2,VP2/R2)
          TM2=KT2*IM2
          TNET2=TM2-TH2D*BM2-TL2
          TH2DD=(1./JTOT2)*TNET2
          TH2D=INTGRL(0.0,TH2DD)
          TH2=INTGRL(0.0,TH2D)
**********************************************************
**********          SAMPLING THE SYSTEM          ***********
**********************************************************
SAMPLE
NOSORT
           IF (N.EQ.0) GO TO 20
           P2=TH2
           P1=TH1
           IF (N.GE.2) THEN
           TH21D=(TH2-TH22)/(2.*DT)
           TH11D=(TH1-TH12)/(2.*DT)
           ELSE
           TH21D=P2D
           TH11D=P1D
           END IF
           IF (FLAG2.EQ.0) THEN
             P2D=(2.*((TH2-TH21)/DT))-TH21D
             IF (N.GE.2) THEN
               KM2=DABS(2.0*TH2/(V2*((N2*DT)**2)))
             END IF
           END IF
           IF (N2.NE.NCHK2) THEN
           P2D=(2.*((TH2-TH21)/DT))-TH21D
```

```
            END IF
            IF (FLAG1.EQ.0) THEN
              P1D=(2.*((TH1-TH11)/DT))-TH11D
              KM1=DABS(2.*TH1/(V1*((N1*DT)**2)))
            END IF
            IF (N1.NE.NCHK1) THEN
              P1D=(2.*((TH1-TH11)/DT))-TH11D
            END IF
 20         N=N+1
            N2=N2+1
            N1=N1+1
            TH22=TH21
            TH12=TH11
            TH21=TH2
            TH11=TH1
*
TERMINAL
METHOD     RKSFX
*
CONTRL     FINTIM=0.8, DELT=0.00005, DELS=0.00025
SAVE (S1)   0.005,X1DOT,P1D,TH1D,X2DOT,P2D,TH2D,TH1,TH2,ZL
SAVE (S3)   0.005,P1,P2,TH1,TH2,RR1,RRD2
*
GRAPH (L1/S1,DE=TEK618)
      TH1(LE=8,UN='RAD',LO=-0.1,SC=0.1,NI=12),...
      PID(LE=4,NI=8,LO=-4.,UN='RAD/SEC',SC=2.,PO=8),...
      X1DOT(LE=4,NI=8,LO=-4.,SC=2.,UN='RAD/SEC',AX=OMIT),...
      TH1D(LE=4,NI=8,LO=-4.,UN='RAD/SEC',SC=2.),...
      ZL(LE=4,NI=8,LO=-4.,SC=2.,AX=OMIT)
*
GRAPH (L2/S1,DE=TEK618,OV,PO=0,5)
      TH2(LE=8,UN='RAD',LO=-.1,SC=.1,NI=12),...
      P2D(LE=4,NI=8,LO=-4.,UN='RAD/SEC',SC=4.,PO=8),...
      X2DOT(LE=4,NI=8,LO=-4.,UN='RAD/SEC',SC=4.,AX=OMIT),...
      TH2D(LE=4,NI=8,LO=-4.,UN='RAD/SEC',SC=4.),...
      ZL(LE=4,NI=8,LO=-4.,SC=4.,AX=OMIT)
*
GRAPH (L3/S3,DE=TEK618)   TIME(LE=8,UN='SEC'),...
       P1(LE=4,NI=4,LO=-.5,UN='RAD',SC=.5,PO=8),...
       TH1(LE=4,NI=4,LO=-.5,SC=.5,UN='RAD'),...
       RR1(LE=4,NI=4,LO=-.5,SC=.5,AX=OMIT)
*
GRAPH (L4/S3,DE=TEK618,OV,PO=0,5)    TIME(LE=8,UN='SEC'),...
       P2(LE=4,NI=4,LO=-.5,UN='RAD',SC=.5,PO=8),...
       TH2(LE=4,NI=4,LO=-.5,UN='RAD',SC=.5),...
       RRD2(LE=4,NI=4,LO=-.5,SC=.5,AX=OMIT)
*
LABEL   (L1) PHASE PLANE (RIGID-RIGID PLANAR ROBOT ARM)
LABEL   (L3) STEP RESPONSE (RIGID-RIGID PLANAR ROBOT ARM)
*
END
STOP
```

APPENDIX G

SIMULATION PROGRAM FOR THE TWO LINKS (RIGID-FLEXIBLE) PLANAR ROBOT ARM

```
TITLE     SIMULATION PROGRAM FOR THE ADAPTIVE MODEL, USING
TITLE     THE VELOCITY CURVE FOLLOW CONTROL SCHEME, OF A TWO
TITLE     LINKS PLANAR ROBOT ARM HAVING ONE RIGID AND ONE
TITLE     FLEXIBLE LINK, USING TWO ASSUMED MODES TO EXPRESS
TITLE     THE ELASTIC MOTION OF THE FLEXIBLE BEAM.
TITLE     THIS SAME PROGRAM WAS USED TO OBTAIN SIMULATION
TITLE     RESULTS WITH THE SYSTEM TREATED WITH OR WITHOUT
TITLE     LOAD, AS ALSO WITH OR WITHOUT GRAVITY FORCES.
*
CONST     G=981.4
CONST     ZL=0.0
*
PARAM     K=1.0,K1=0.8,K2=1.0,K3=10000.0,KM1=0.185,KM2=2.31
PARAM     KT1=1036.93,KT2=1036.93
PARAM     VSAT1=300.0,VSAT2=150.0
PARAM     J1=2.38,J2=2.38
PARAM     KV1=0.1012,KV2=0.1012
PARAM     BM1=3.094,BM2=3.094,L=0.0001,R=0.91
PARAM     M1=3.0,M2=1.0
PARAM     L1=40.0,L2=32.0
PARAM     E1=1.8751,E2=4.6941
PARAM     KW1=0.00124,KW2=0.0433
PARAM     REF1=1.0,REF2=1.0
PARAM     DT=0.00025
*
INTGER    N,N1,N2,FLAG1,FLAG2,NCHK1,NCHK2
*
INITIAL
          N=0
          N1=0
          N2=0
          FLAG1=0
          FLAG2=0
          Q1=0.0
          Q1D=0.0
          QD=0.0
          Q2=0.0
          Q2D=0.0
          Q2DD=0.0
          TH1=0.0
          TH1D=0.0
          TH1DD=0.0
          TH2=0.0
          TH2D=0.0
```

```
          TH2DD=0.0
          TH11=0.0
          TH21=0.0
          SIG1=(SINH(E1)-SIN(E1))/(COSH(E1)+COS(E1))
          SIG2=(SINH(E2)-SIN(E2))/(COSH(E2)+COS(E2))
          F1=COSH(E1)-COS(E1)-SIG1*(SINH(E1)-SIN(E1))
          F2=COSH(E2)-COS(E2)-SIG2*(SINH(E2)-SIN(E2))
          A1=SQRT(2.0*KM1*VSAT1)
          A2=SQRT(2.0*KM2*VSAT2)
*
DERIVATIVE
          RR1=REF1*STEP(0.0)
          RR2=REF2*STEP(0.0)
          RRD2=TRANSP(200,0.0,0.1,RR2)
          ER1=RR1-P1
          ER2=RRD2-P2
NOSORT
************************************************************
******    PARAMETERS FOR THE EQUATIONS OF MOTION      ******
************************************************************
          UE=F1*Q1+F2*Q2
          TH=TH1+TH2
          D122=M2*L2**2+M2*UE**2+M2*L1*L2*COS(TH2)...
              -M2*L1*SIN(TH2)*UE
          D111=D122+(M1+M2)*L1**2+M2*L1*L2*COS(TH2)...
              -M2*L1*SIN(TH2)*UE
          D133=M2*L1*COS(TH2)*F1+M2*L2*F1
          D144=M2*L1*COS(TH2)*F2+M2*L2*F2
          D112=-2*M2*L1*(UE*COS(TH2)+L2*SIN(TH2))
          D113=2*M2*F1*(UE-L1*SIN(TH2))
          D114=2*M2*F2*(UE-L1*SIN(TH2))
          D1222=-M2*L1*(L2*SIN(TH2)+UE*COS(TH2))
          D123=D113
          D124=D114
          D1=((M1+M2)*L1*COS(TH1)+M2*L2*COS(TH)...
            -M2*UE*SIN(TH))*G
          D211=D122
          D222=M2*L2**2+M2*UE**2
          D213=2*M2*F1*UE
          D223=D213
          D214=2*M2*F2*UE
          D224=D214
          D233=M2*L2*F1
          D244=M2*L2*F2
          D2111=M2*L1*(L2*SIN(TH2)+UE*COS(TH2))
          D2=G*M2*(L2*COS(TH)-UE*SIN(TH))
          D311=M2*L1*F1*COS(TH2)+M2*L2*F1
          D322=M2*L2*F1
          D333=M2*F1**2
          D344=M2*F1*F2
          D312=-2*M2*F1*UE
          D3222=-M2*F1*UE
```

```
          D3111=D3222+M2*L1*F1*SIN(TH2)
          D3=G*M2*F1*COS(TH)+KW1*Q1
          D422=M2*L2*F2
          D411=D422+M2*L1*F2*COS(TH2)
          D433=D344
          D444=M2*F2**2
          D412=-2*M2*F2*UE
          D4222=-M2*F2*UE
          D4111=D4222+M2*L1*F2*SIN(TH2)
***********************************************************
******     THE LAGRANGE'S EQUATIONS OF THE SYSTEM    ******
***********************************************************
          TL1=D122*TH2DD+D133*QD+D144*Q2DD+D112*TH1D*TH2D...
             +D113*TH1D*Q1D+D114*TH1D*Q2D+D123*TH2D*Q1D...
             +D124*TH2D*Q2D+D1222*TH2D**2+D1
          TL2=D211*TH1DD+D233*QD+D244*Q2DD+D213*TH1D*Q1D...
             +D214*TH1D*Q2D+D223*TH2D*Q1D+D224*TH2D*Q2D...
             +D2111*TH1D**2+D2
          Q1DD=(D311*TH1DD+D322*TH2DD+D344*Q2DD...
              +D312*TH1D*TH2D+D3111*TH1D**2...
              +D3222*TH2D**2+D3)/D333
          Q2DD=(D411*TH1DD+D422*TH2DD+D433*QD...
              +D412*TH1D*TH2D+D4111*TH1D**2...
              +D4222*TH2D**2+D4)/D444
***********************************************************
***********         THE ADAPTIVE MODEL          ************
***********************************************************
          JTOT1=J1+D111
          JTOT2=J2+D222
          IF (ER1.LT.0.0) THEN
            X1DOT=-A1*K1*SQRT(ABS(ER1))
          ELSE
            X1DOT=A1*K1*SQRT(ER1)
          END IF
          IF (ER2.LT.0.0) THEN
            X2DOT=-A2*K2*SQRT(ABS(ER2))
          ELSE
            X2DOT=A2*K2*SQRT(ER2)
          END IF
***********************************************************
*************            FIRST LINK             *************
***********************************************************
SORT
          X1D=X1DOT-K*P1D
          V1=LIMIT(-VSAT1,VSAT1,K3*X1D)
NOSORT
          IF (FLAG1.EQ.1) GO TO 10
          IF (V1.LT.VSAT1.AND.TIME.GT.0.0005) FLAG1=1
          NCHK1=N1
 10       CONTINUE
SORT
          P1DD=KM1*V1
```

```
          P1D=INTGRL(0.0,P1DD)
          P1=INTGRL(0.0,P1D)
          VP1=V1-(KV1*TH1D)
          IM1=REALPL(0.0,L/R,VP1/R)
          TM1=KT1*IM1
          TNET1=TM1-TH1D*BM1-TL1
          TH1DD=(1./JTOT1)*TNET1
          TH1D=INTGRL(0.0,TH1DD)
          TH1=INTGRL(0.0,TH1D)
**********************************************************
*************           SECOND LINK           *************
**********************************************************
          X2D=X2DOT-K*P2D
          V2=LIMIT(-VSAT2,VSAT2,K3*X2D)
NOSORT
          IF (FLAG2.EQ.1) GO TO 20
          IF (V2.LT.VSAT2.AND.TIME.GT.0.0005) FLAG2=1
          NCHK2=N2
 20       CONTINUE
SORT
          P2DD=KM2*V2
          P2D=INTGRL(0.0,P2DD)
          P2=INTGRL(0.0,P2D)
          VP2=V2-(KV2*TH2D)
          IM2=REALPL(0.0,L/R,VP2/R)
          TM2=KT2*IM2
          TNET2=TM2-TH2D*BM2-TL2
          TH2DD=(1./JTOT2)*TNET2
          TH2D=INTGRL(0.0,TH2DD)
          TH2=INTGRL(0.0,TH2D)
**********************************************************
********       ASSUMED MODES AND FLEXIBILITY       ********
**********************************************************
          Q1D=INTGRL(0.0,Q1DD)
          Q2D=INTGRL(0.0,Q2DD)
          Q1=INTGRL(0.0,Q1D)
          Q2=INTGRL(0.0,Q2D)
          FLX =-UE/L2
**********************************************************
***********         SAMPLING THE SYSTEM          ***********
**********************************************************
SAMPLE
*
NOSORT
          IF (N.EQ.0) GO TO 30
          P2=TH2
          P1=TH1
          IF (N.GE.2) THEN
            TH21D=(TH2-TH22)/(2.*DT)
            TH11D=(TH1-TH12)/(2.*DT)
          ELSE
            TH21D=P2D
```

```
            TH11D=P1D
          END IF
          IF (FLAG2.EQ.0) THEN
            P2D=(2.*((TH2-TH21)/DT))-TH21D
            IF (N.GE.2) THEN
              KM2=DABS(2.*TH2/(V2*((N2*DT)**2)))
            END IF
          END IF
          IF (N2.NE.NCHK2) THEN
            P2D=(2.*((TH2-TH21)/DT))-TH2ID
          END IF
          IF (FLAG1.EQ.0) THEN
            P1D=(2.*((TH1-TH11)/DT))-TH11D
            KM1=DABS(2.*TH1/(V1*((N1*DT)**2)))
          END IF
          IF (N1.NE.NCHK1) THEN
            P1D=(2.*((TH1-TH11)/DT))-TH11D
          END IF
30        N=N+1
          N2=N2+1
          N1=N1+1
          TH22=TH21
          TH12=TH11
          TH21=TH2
          TH11=TH1
*
TERMINAL
METHOD    RKSFX
*
CONTRL    FINTIM=2.4, DELT=0.00005, DELS=0.00025
SAVE (S1)  0.005,X1DOT,P1D,TH1D,X2DOT,P2D,TH2D,TH1,TH2,ZL
SAVE (S3)  0.005,P1,P2,TH1,TH2,RR1,RRD2
SAVE (S5)  0.005,FLX,ZL
*
GRAPH (L1/S1,DE=TEK618)
     TH1(LE=8,UN='RAD',LO=-.3,SC=.1,NI=16),...
     P1D(LE=4,NI=8,LO=-4.,SC=2.,UN='RAD/SEC',SC=2.,PO=8),...
     X1DOT(LE=4,NI=8,LO=-4.,SC=2.,UN='RAD/SEC',AX=OMIT),...
     TH1D(LE=4,NI=8,LO=-4.,UN='RAD/SEC',SC=2.),...
     ZL(LE=4,NI=8,LO=-4.,SC=2.,AX=OMIT)
*
GRAPH (L2/S1,DE=TEK618,OV,PO=0,5)
     TH2(LE=8,UN='RAD',LO=-.6,SC=.2,NI=12),...
     P2D(LE=4,NI=8,LO=-10.,UN='RAD/SEC',SC=5.,PO=8),...
     X2DOT(LE=4,NI=8,LO=-10.,UN='RAD/SEC',SC=5.,AX=OMIT),...
     TH2D(LE=4,NI=8,LO=-10.,UN='RAD/SEC',SC=5.),...
 ZL(LE=4,NI=8,LO=-10.,SC=5.,AX=OMIT)
*
GRAPH (L3/S3,DE=TEK618)  TIME(LE=8,NI=8,SC=.3,UN='SEC'),...
              P1(LE=4,NI=4,LO=-.5,UN='RAD',SC=.5 PO=8),...
              TH1(LE=4,NI=4,LO=-.5,SC=.5,UN='RAD'),...
              RRI(LE=4,NI=4,LO=-.5,SC=.5,AX=OMIT)
```

```
GRAPH (L4/S3,DE=TEK618,OV,PO=0,5)
             TIME(LE=8,NI=8,SC=.3,UN='SEC'),...
             P2(LE=4,NI=6,LO=-.5,UN='RAD',SC=.5,PO=8),...
             TH2(LE=4,NI=6,LO=-.5,UN='RAD',SC=.5),...
             RRD2(LE=4,NI=6,LO=-.5,SC=.5,AX=OMIT)
*
GRAPH (L9/S5,DE=TEK618) TIME(LE=8,UN='SEC',NI=8,SC=.3),...
                        FLX(LE=6,LO=-2.,NI=8,SC=.5),...
                        ZL(LE=6,LO=-2.,NI=8,SC=.5,AX=OMIT)
*
LABEL   (L1) PHASE PLANE (RIGID-FLEXIBLE PLANAR ROBOT ARM)
LABEL   (L3) STEP RESPONSE (RIGID-FLEXIBLE PLANAR ROBOT ARM)
LABEL   (L9) FLEXIBLE MOTION OF THE END-POINT
*
END
STOP
```

LIST OF REFERENCES

1. Zouzias, J., Control of a flexible one-link manipulator, Master's Thesis, Naval Postgraduate School, Monterey, California, June 1987.

2. Ozaslan, K., The near-minimum time control of a robot arm, Master's Thesis, Naval Postgraduate School, Monterey, California, December 1986.

3. Book, W.J., Modeling design and control of flexible manipulator arms, PhD Thesis, MIT Department of Mechanical Engineering, April 1974.

4. Book, W.J., Recursive Lagrangian dynamics of flexible manipulator arms, The International Journal of Robotics Research, MIT Press, Cambridge, Massachusetts, Vol. 3, No. 3.

5. Maiza-Neto, O., Modal analysis and control of flexible manipulator arms, PhD Thesis, MIT Department of Mechanical Engineering, September 1974.

6. Book, W.J., Maiza-Neto, O., and Whitney, D.E., Feedback control of two beam, two joint with distributed flexibility, ASME J. DYNAMIC SYSTEMS, MEASUREMENT AND CONTROL, Vol. 97, No. 4, pp. 424-431, December 1975.

7. Usoro, P.B., Nadira, R., Mahil, S.S, and Mehra, R.K., Advanced control of flexible manipulators, Phase I Final Report, NSF Award Number ECS-8260419, April 1893.

8. Mahil, S.S, On the application of Lagrange methods to the description of dynamic systems, IEEE Transactions on SYSTEMS MAN AND CYBERNETICS, Vol. SMC-12, No. 6, November/December 1982.

9. Schmitz, E., Experiments on the end-point position control of a very flexible one link manipulator, Ph.D Thesis, Stanford University, Stanford, California, June 1985.

10. Meirovitch, L., Analytical methods in vibrations, The McMillan Co., 1967.

11. Bishop, R.E.D, and Johnson, D.C, Mechanics of vibration, Cambridge at the University Press, 1960.

12. Thaler, G.J, and Stein, W.A., Transfer function and parameter evaluation for D-C servo motors, Applications and Industry, pp. 410-417, January 1956.

13. Luh, J.Y., Fisher, W.D, and Paul, R.C, Joint torque control by a direct feedback for industrial robots, IEEE Transactions on Automatic Control, V. AC-28, No. 2, pp. 153-161, February 1983.

14. Thaler, G.J., "Nonlinear feedback controls theory and methods for analysis and design", Unpublished Notes for ECE-4350, Nonlinear Controls, Naval Postgraduate School, Monterey, California, October 1986.

15. Wikstrom, R.K., An adaptive model based disk file head positioning servo system, Master's Thesis, Naval Postgraduate School, California, September 1985.

INITIAL DISTRIBUTION LIST

		No. Copies
1.	Defense Technical Information Center Cameron Station Alexandria, Virginia 22304-6145	2
2.	Library, Code 0412 Naval Postgraduate School Monterey California 93943-5002	2
3.	Chairman, Code 62 Department of Electrical & Computer Engineering Naval Postgraduate School Monterey, California, 93943	1
4.	Professor G. J. Thaler, Code 62Tr Department of Electrical & Computer Engineering Naval Postgraduate School Monterey, California, 93943	5
5.	Professor H. A. Titus, Code 62Ti Department of Electrical & Computer Engineering Naval Postgraduate School Monterey, California, 93943	1
6.	Russ Weneth, Code u25 Naval Surface Weapons Center White Oak, Maryland, 20910	1
7.	Paul Heckman, Code 943 Head, Undersea AI & Robotics Branch Naval Ocean System Center San Diego, California, 92152	1
8.	Dr. D. Milne, Code 1563 DTNSRDC, Carderock, Bethesda, Maryland 20084-5000	1
9.	RADM G. Curtis, USW PMS-350 Naval Sea Systems Command Washington, D.C., 20362-5101	1

10. LT Relle L. Lyman, Jr., USN Code 90G 1
Naval Sea Systems Command
Washington, D.C., 20362-5101

11. Mardas, Constantinos 8
Thiseos & Pleiadon 76
Kifissia, 14564
Athens, Greece

Thesis
M34175 Mardas
c.1 Adaptive control in positioning a rigid-flexible robot arm.